EG&G Idaho, Inc.

(LTR)

Report No. LO-00-79-108

Date: February 8, 1980

MASTER

RELEASED BY LOFT CDCS

USNRC-P-394

INTERNAL TECHNICAL REPORT

Title: AN EVALUATION OF THE PBF LOFT LEAD ROD TEST RESULTS CONCERNING SURFACE THERMOCOUPLE PERTURBATION EFFECTS

Organization: LOFT EXPERIMENTAL PROGRAM DIVISION

Author: M. L. Carboneau/E. L. Tolman

Checked By: S. A. Naff

Approved By: L. P. Leach

DISTRIBUTION OF THIS DOCUMENT IS UNLIMITED

EG&G Idaho, Inc.

LOFT TECHNICAL REPORT
LOFT PROGRAM

FORM EG&G-220
(Rev. 06-79)

TITLE	REPORT NO.
An Evaluation of the PBF LOFT Lead Rod Test Results Concerning Surface Thermocouple Perturbation Effects	LTR-LO-00-79-108
AUTHOR M. L. Carboneau/E. L. Tolman	Charge Number 52DFL0901
PERFORMING ORGANIZATION LOFT Experiment Program Division	DATE RELEASED BY LOFT CDCS February 8, 1980
LOFT APPROVAL L. P. Leach (SW) L P Leach LEPD Mgr.	

It is the purpose of the attached document to review and evaluate the data from the Power Burst Facility (PBF) Loss-of-Fluid Test (LOFT) Lead Rod (LLR) experiments concerning the existence or non-existence of surface thermocouple effects. Although the LLR experiments were not explicitly designed to evaluate cladding thermocouple perturbation phenomena, linear variable differential transformers (LVDTs) attached to the fuel rods provided an alternate means of evaluating the fuel rod behavior during blowdown and reflood events. In addition, several tests were performed with a rod equipped with a LVDT but no surface cladding thermocouples. This afforded an opportunity to compare the response of rods with and without cladding thermocouples by studying the LVDT data for each rod.

A systematic review is presented of the PBF LLR tests LLR-03, -05, -04, and -04A concerning possible thermocouple influences on the time-to-CHF and the time-to-quench behavior of the fuel rods. An interpretation of the data will be presented when feasible.

Furthermore, since an evaluation of the LVDT data is crucial to understanding the fuel cladding behavior and the corresponding response of the surface cladding thermocouples, appendices to this document review and analyze the LVDT data in detail.

DISPOSITION OF RECOMMENDATIONS

No disposition required.

ABSTRACT

The purpose of the PBF LOFT Lead Rod (LLR) Test program was to provide experimental data to characterize the mechanical behavior of LOFT type nuclear fuel rods under loss of coolant accident (LOCA) conditions, simulating the test conditions expected for the LOFT Power Ascension (L2) Test series.

Although the LLR tests were not explicitly designed to evaluate cladding surface thermocouple perturbation effects, comparison of the Linear Variable Differential Transformer (LVDT) data for rods instrumented with and without cladding thermocouples provided pertinent information concerning the effects of cladding thermocouples on the time to DNB and time to quench data. Documentation and review of this data is presented in the following report. It will be shown that most of the LLR data indicate that the cladding surface thermocouples did not enhance the rewetting characteristics of the rods they are attached to, even though other evidence shows that the surface clad thermocouples did quench early.

Finally, in order to accurately interpret and understand the limitations of the LVDT instrumentation, upon which thermocouple perturbation effects were evaluated, an analysis of the LVDT data as well as a review of the atypical response events that occurred during the LLR tests are presented in appendices to this document.

SUMMARY

The LOFT Lead Rod (LLR) tests have provided valuable information concerning nuclear fuel rod behavior during Loss-of-Coolant-Experiments (LOCEs) which were intended to simulate the first planned nuclear tests in the LOFT reactor complex. The data provides information on rods instrumented with and without cladding surface thermocouples (TCs), thereby furnishing a basis for evaluating the selective cooling effects of surface thermocouples and the influence of thermocouples on rod behavior.

Estimation of the cladding elongation for each test rod, based on the Linear Variable Differential Transformer (LVDT) data, is compared with the cladding thermocouple data. Observations regarding the selective cooling or quenching characteristics of rods instrumented with surface thermocouples are summarized as follows:

(1) The LLR test data show that surface thermocouples quench before large sections of the rod can quench. Differences between LVDT and TC quench times have varied from about 0.1, for high pressure high flooding rates, to approximately 3.8 seconds, corresponding to low pressure low flooding rates.

(2) Cladding elongation measurements on rods with and without external thermocouples are not identical; however, general trends are consistent. As a result, non-uniform rod conditions and/or non-uniform coolant conditions may exist among the LLR test rods. Nevertheless, the LVDT data for rods instrumented with and without external clad thermocouples indicates that the TCs have no significant effect on the overall cladding quench times.

(3) From the above observations it can be concluded that the cladding thermocouples do quench somewhat earilier than that indicated by the cladding elongation measurements; however, the overall mechanical response of the rod, as indicated by the LVDT, is not significantly affected.

Because of uncertainties in some of the LLR data, and the applicability of the LLR test configuration, the above observations and inferences are not conclusive with regard to the cooling effects the cladding thermocouples may have had on the LOFT experiments. Additional experimentation is ongoing to resolve these issues.

CONTENTS

FIGURES

TEST LLR-03

TEST LLR-05

TEST LLR-04

TEST LLR-4A

APPENDIX A FIGURES

APPENDIX B FIGURES

TABLES

I. INTRODUCTION

The fuel clad temperature is an essential indicator of the fuel rod response and the local thermal-hydraulic behavior in a nuclear reactor during off normal and accident conditions. The measurement of the cladding temperature during a Loss-of-Coolant-Experiment (LOCE) can be sensitive to the thermocouple rod attachment and geometry. For example, external surface clad thermocouples can influence the cladding temperature and possibly modify the thermal-hydraulic conditions surrounding the rod in such a way as to (a) selectively enchance the heat transfer characteristics from the rod (fin effect), (b) influence the rod critical heat flux (CHF), and (c) affect rod rewet and quench times. Any phenomenon that significantly influences rod behavior and can be attributed to the presence of surface clad thermocouples will be referred to as a thermocouple/rod perturbation effect.

A series of four tests, identified as LLR-03, -05, -04, and -4A (performed in this sequence), was recently completed at the Power Burst Facility (PBF). These tests were designed to investigate the thermal-mechanical behavior of LOFT type fuel rods during loss of coolant transients similar to those expected in the LOFT power ascension (L2) test series. Although the LLR tests were not explicitly designed to evaluate cladding surface thermocouple effects, linear variable differential transformers (LVDTs) attached to the fuel rods have provided an alternate means of evaluating the fuel rod behavior during blowdown and reflood events. In addition, several tests were performed with a rod equipped with a LVDT but no surface cladding thermocouples. This afforded an opportunity to compare the response of rods with and without cladding thermocouples by studying the LVDT data for each rod. It is the purpose of this report to review and evaluate the pertinent data from the LLR tests concerning the existence or nonexistence of thermocouple perturbation effects.

The next section of the report summarizes the LLR test sequence, test geometry, and initial test conditions. Section III describes the analysis methodology for evaluating the perturbation effects of surface cladding thermocouples. Section IV presents the test data and evaluates the DNB and quench characteristics for each of the LLR test rods in each experiment. In addition, a review of several instrument response anomalies observed during each test is addressed. Section V presents the conclusions of this report concerning the effects of thermocouples on rod behavior.

II. LLR TEST SEQUENCE, GEOMETRY, AND INITIAL TEST CONDITIONS

A detailed discussion of the design and function of the PBF LLR test train, test program, experimental equipment, test procedure, and test predictions is presented in references (1), (2), and (3). For convenience, however, a short outline of the major features relating to the LLR test sequence, test geometry, and initial test conditions is presented below.

The LLR test series consisted of four LOCE transients, preceded by a power ramping sequence to precondition the test rods. Each of the LLR tests was performed with four separately shrouded LOFT type fuel rods. The design of the LLR fuel rods is identical with the LOFT fuel rod design with only a few exceptions. For example, the active length of the LOFT rod is 1.68 m while the LLR fuel rod is only 0.914 m long. In order to provide individual flow channels for each test rod, the LLR fuel rods are separately enclosed within a circular flow shroud. The geometric design of the LLR test assembly provides similar but not necessarily identical thermal-hydraulic conditions for each test rod. Typical test configurations for these experiments appear in Figures 1A, 1B, and 1C. Table 1 lists the thermocouple location and flow shroud material data for each test; notice that for tests 5, 4, and 4A, rod #3452 did not have surface cladding thermocouples. Table 2 summarizes the LLR initial test conditions. The valve sequencing for the LLR tests was selected to closely simulate the expected LOFT system thermal hydraulic conditions that existed during the first few seconds of the blowdown transient.

Selected fuel rods were replaced after tests LLR-03 and LLR-04. A replacement rod in tests LLR-05, -04, and -4A was unique in that no cladding external thermocouples were utilized. Figure 2 shows the rod configuration and thermocouple location for each test. Also, the peak cladding temperature for each rod is identified in Figure 2. A schematic of the PBF LLR test train installed in the PBF reactor In-Pile Tube (IPT) is illustrated in Figure 3.

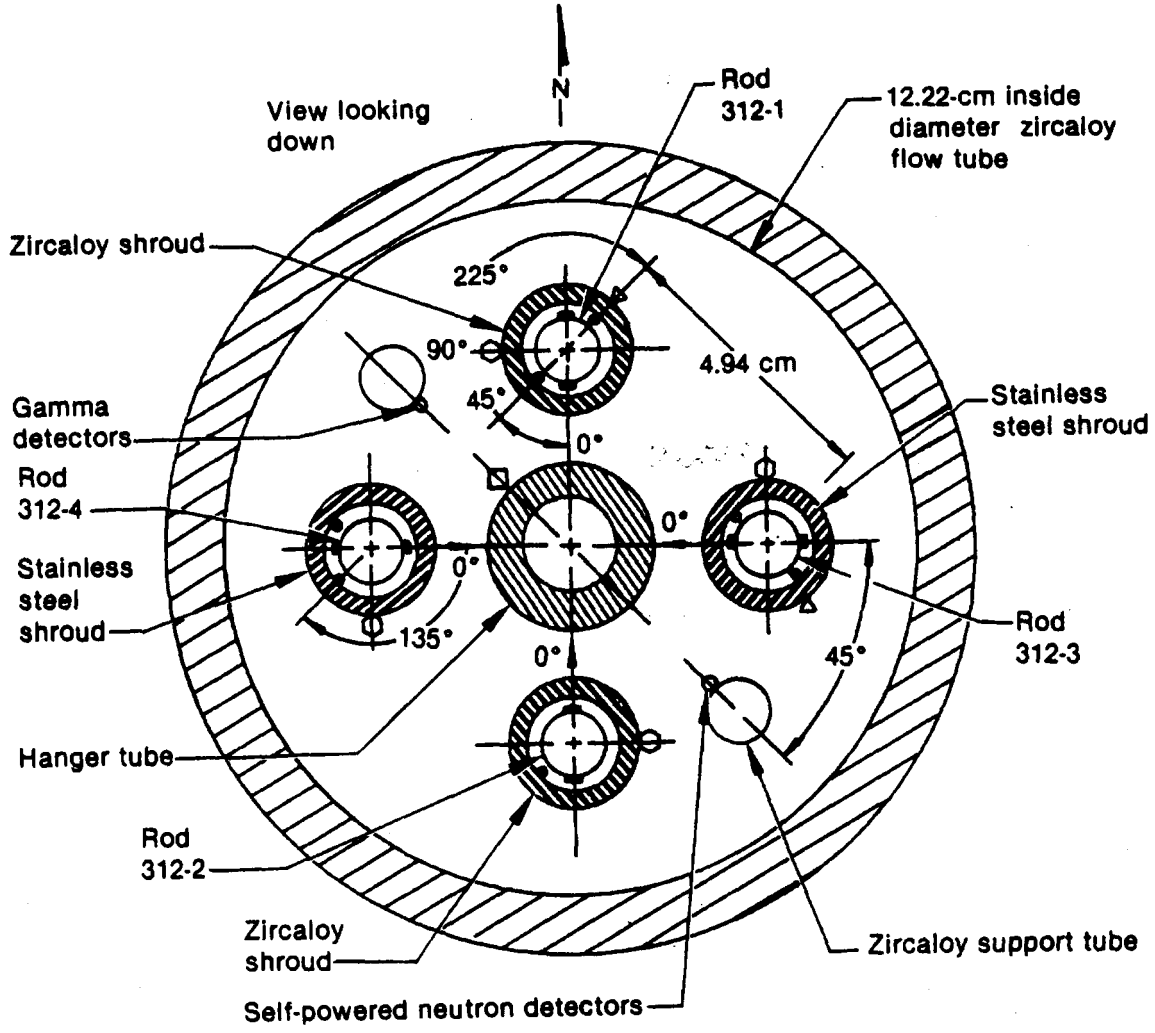

△ 3 Outer shroud thermocouples
○ 3 Midcoolant thermocouples
● Differential thermocouples
⬬ Cladding thermocouples
○ Flux wire
□ Test train flux wire

All rod shrouds have inlet and outlet thermocouples located at the 45° azimuthal location inside the shroud

INEL-A-12 785

Fig. 1A Test fuel rod instrumentation schematic. Test LLR-03.

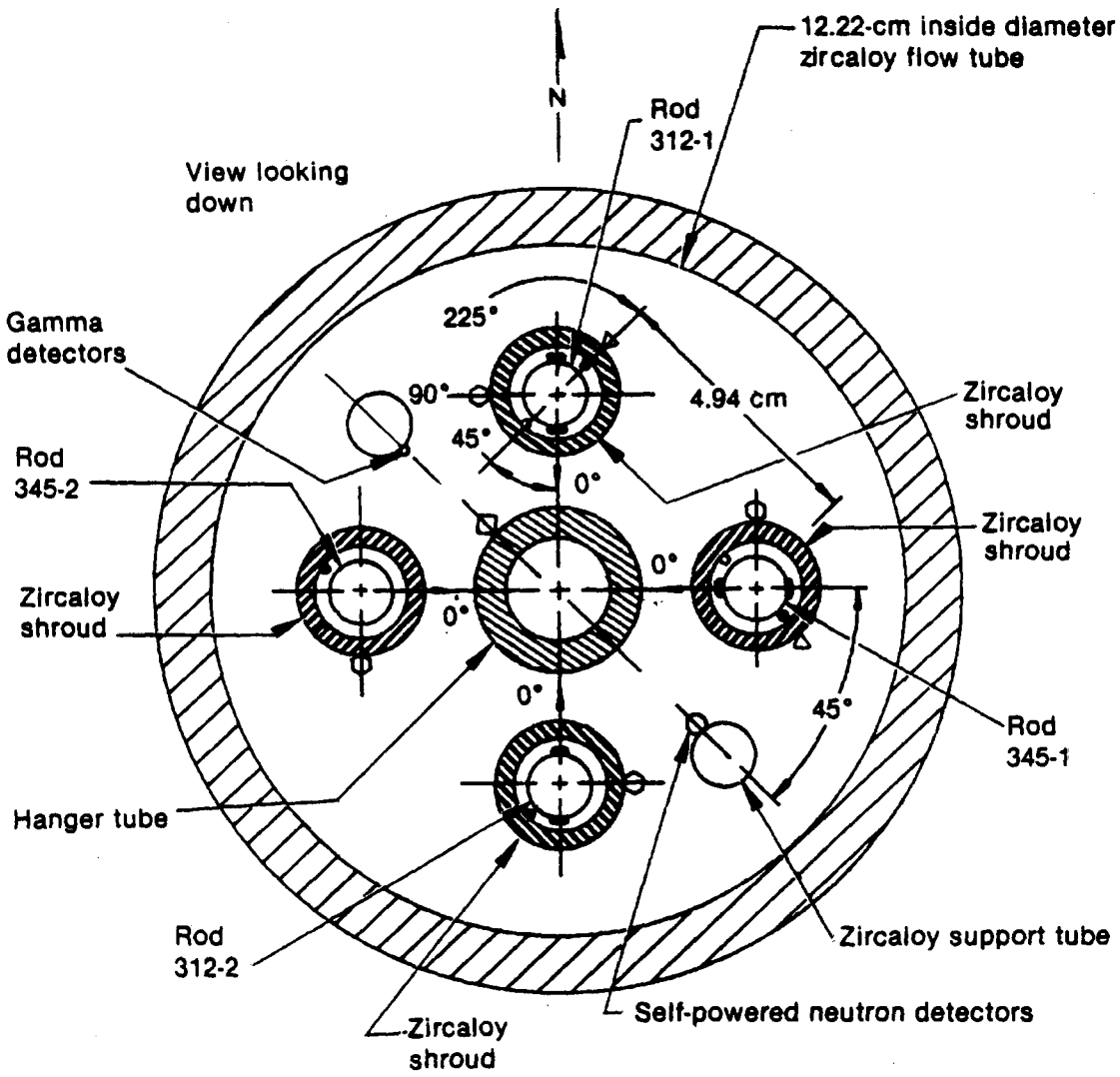

△ 3 Outer shroud thermocouples
○ 3 Midcoolant thermocouples
● Differential thermocouples
⬬ Cladding thermocouples
○ Flux wire
□ Test train flux wire

All rod shrouds have inlet and outlet thermocouples located at the 45° azimuthal location inside the shroud.

INEL-A-12 786-1

Fig. 1B Test fuel rod instrumentation schematic. Tests LLR-04 and LLR-05.

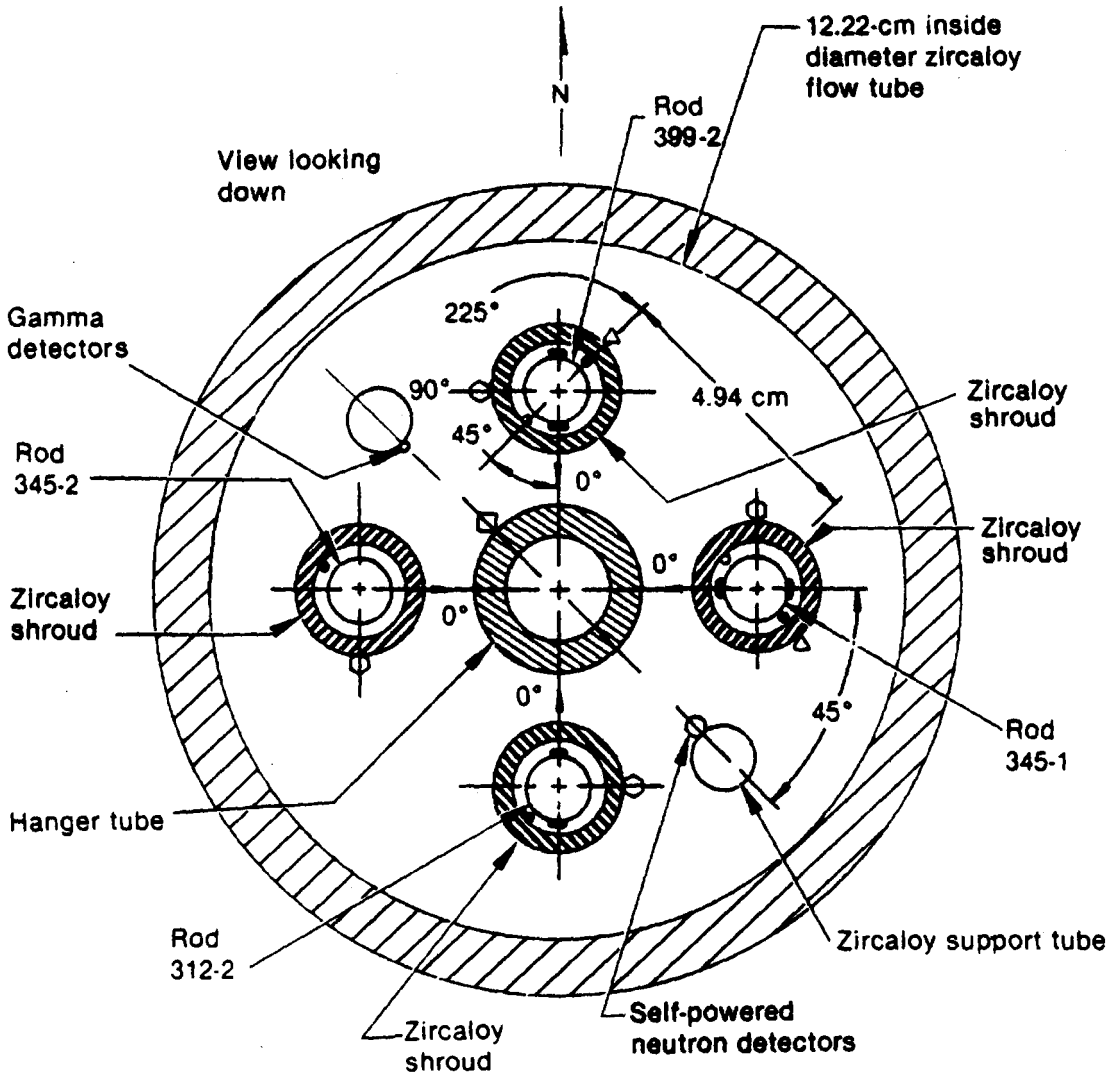

△ 3 Outer shroud thermocouples
○ 3 Midcoolant thermocouples
● Differential thermocouples
⬬ Cladding thermocouples
○ Flux wire
□ Test train flux wire

All rod shrouds have inlet and outlet thermocouples located at the 45° azimuthal location inside the shroud.

INEL-A-12 770

Fig. 1C Test fuel rod instrumentation schematic. Test LLR-4A.

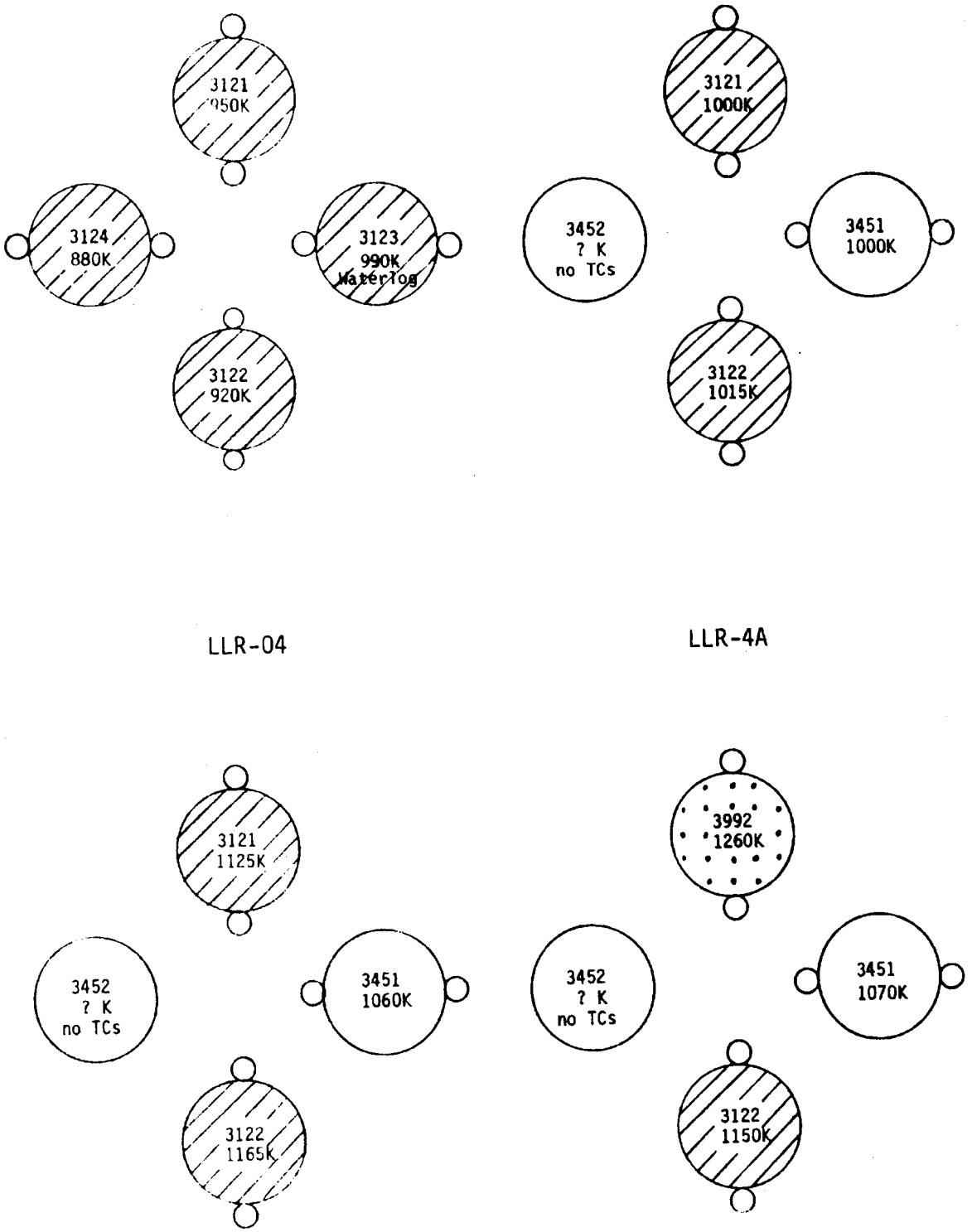

Fig. 2. Test schematic and peak measured surface temperature.

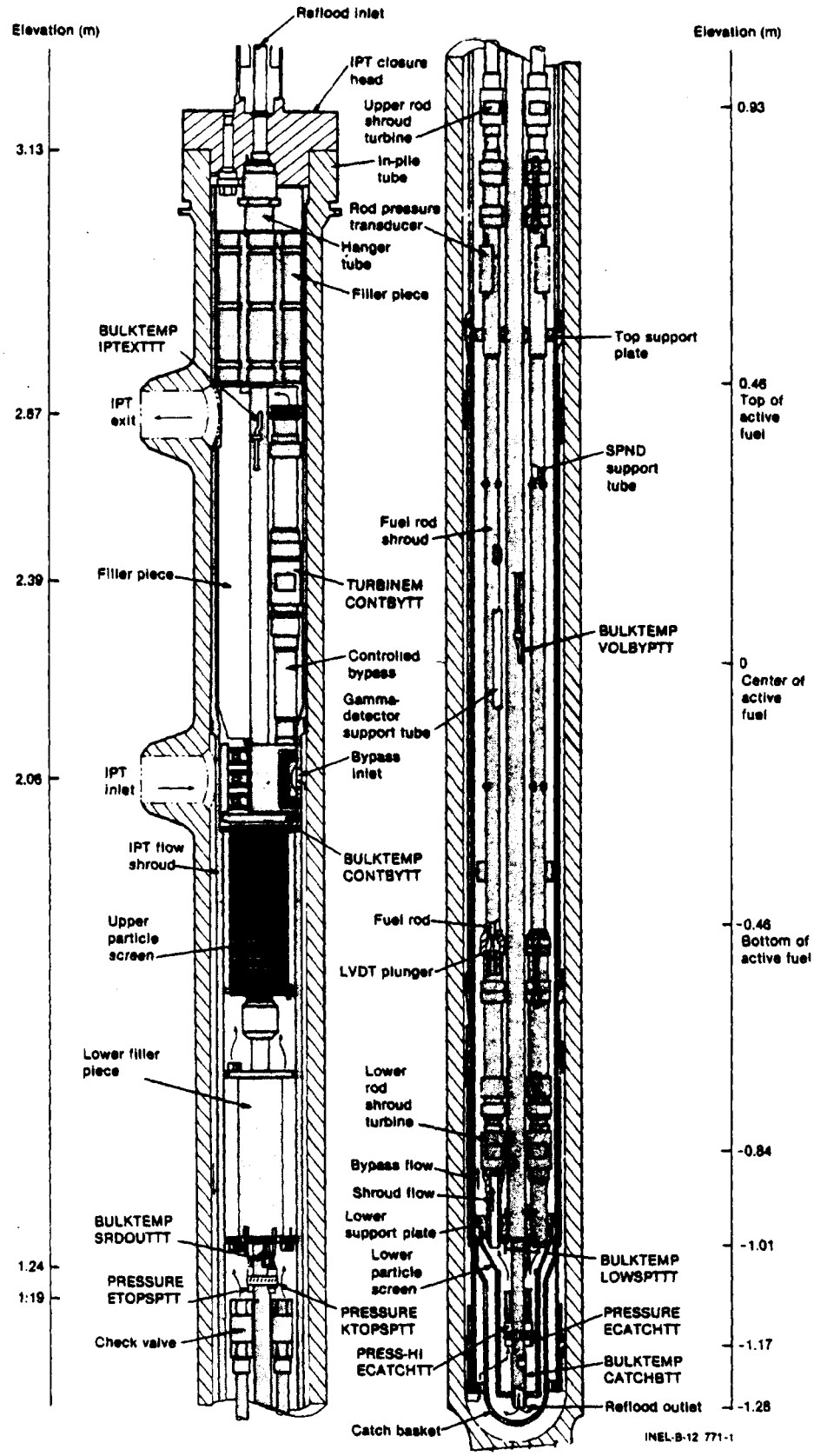

Fig. 3 LLR test train drawing.

TABLE 1

FUEL ROD DESIGNATIONS AND CLADDING SURFACE THERMOCOUPLE LOCATIONS FOR PBF/LOFT LEAD ROD TESTS

Rod	Number	Tests LLR-	Shroud	*Thermocouple Location (m) Clad T/C #1 180° Orientation	Clad T/C #2 0° Orientation	Centerline T/C
1	312-1	3,4,5	Zirc	0.533	0.533	0.533
2	312-2	3,4,5,4A	Zirc	0.533	0.457	0.457
3	312-3	3	SS	0.533	0.533	0.533
4	312-4	3	SS	0.533	0.533	0.533
5	345-1	4,5,4A	Zirc	0.533	0.533	0.533
6	345-2	4,5,4A	Zirc	-	-	0.457
7	399-1	Spare	Zirc	0.533	0.457	0.457
8	399-2	4A	Zirc	0.457	0.314	0.457

* From bottom of active fuel.
All rods were unpressurized (0.1034 MPa, 15 psia).

TABLE 2

INITIAL CONDITIONS FOR THE PBF/LLR TESTS PRIOR TO BLOWDOWN[a]

Test	Reactor Power (MW)	MLHGR (kW/m)	System Pressure (MPa)	IPT Inlet temperature	Average Core Differential temperature	Individual Shroud Flow l/s	Controlled Bypass Flow l/s	Total IPT Flow l/s
LLR-3	14.52	40.5	15.57	595.0	11.07	0.585	6.08	9.13
LLR-5	14.52	47.4	15.5	603.4	10.46	0.60	6.68	9.35
LLR-4	19.3	56.6	15.6	600.0	10.11	0.80	8.71	12.4
LLR-4A	19.3	55.6	15.5	600.0	11.5	0.78		

a. Measurement determination and location identified in References (2 and 3).

III. ANALYSIS METHODOLOGY

There are two principal techniques that will be used to analyze the PBF LLR data for possible thermocouple perturbation effects. First, for a given set of thermal-hydraulic boundary conditions, thermocouple effects can be investigated by comparing the cladding elongation response of fuel rods instrumented with and without surface clad thermocouples. Since the LLR tests 5, 4, and 4A contained rods with and without surface cladding thermocouples (note Table 1), and since all rods were instrumented with linear variable differential transformers (LVDTs) and centerline fuel thermocouples, an assessment of the thermocouple effects on fuel rod response can be made by comparing the cladding elongation and centerline temperature data. For instance, if significant differences exist between the LVDT data for rods with and without surface thermocouples, for a given test, then the possibility of a thermocouple perturbation effect would have to be seriously considered, as long as the thermocouple attachment integrity was not in question, and the thermal-hydraulic conditions existing between the comparison flow channels are the same.

The second technique that will be considered involves the comparison of LVDT data and surface thermocouple data for any one particular rod during each test. The advantage of this technique over the previous method is that the assumption of identical thermal-hydraulic conditions between separate flow channels is not necessary. However, in either case the principal disadvantage of using LVDTs to evaluate fuel rod behavior and inferring information about thermocouple effects is that the LVDTs measure the integral rod response and therefore can only project average conditions along any given rod, whereas thermocouples represent a discrete measurement and hence infer information for only one particular point on the rod. In general, the response of a given section of the fuel rod, say near a thermocouple, may not represent a typical condition existing along the

entire length of the rod, as indicated by the LVDT. For instance, thermal hydraulic conditions can have an axial dependency along the length of the fuel rod, particularly during rod rewet events, as was shown by the axial dependent thermocouple response during the LOFT L2-2 and L2-3 experiments. Consequently, it is possible that a local rewet event or precursory cooling phenomenon, not caused by a surface clad thermocouple, might occur at particular locations on the fuel rod surface where it could be detected by a thermocouple located near the phenomenon, while the LVDT instrumentation indicating the overall elongation of the rod may not indicate an abrupt change. An event of this nature might be incorrectly interrupted as a thermocouple perturbation effect when indeed the phenomenon has no relevant association with surface cladding thermocouples. Hence, one has to be careful not to infer conclusions based on only a few isolated events. Rather, the best that can be hoped for is to evaluate all the data and draw conclusions based on the evidence supported by an overwhelming collection of the data.

IV. LLR TEST RESULTS

4.1 Comparison of the LVDT and TC Responses for LLR-03

As shown in Figure 1A the fuel rods used in the LLR-03 test were designated as 3121, 3122, 3123, and 3124. For the LLR-03 test, rods 3121 and 3122 were encased in zircaloy-4 flow shrouds, and rods 3123 and 3124 were encased in stainless steel flow shrouds. The different shroud materials caused a power tilt of 0.87/1.0 for the stainless steel (or low power rods) and the zircaloy shrouded (or high power) rods.[2] The power tilt was designed to simulate the different power characteristics of the peripheral and central rods in the LOFT core. During the LLR-03 test, however, rod 3123 developed a leak, became waterlogged, and later failed during the blowdown. Consequently, an accurate interpretation of the test data for rod 3123 is difficult. After completion of the LLR-03 experiment, the stainless steel shrouded rods were replaced with zircaloy shrouded rods. Therefore, for tests LLR-05, -04, and -4A, all test rods experienced similar power conditions.

Figures 4 through 11 compare the response of the cladding thermocouples and LVDT data for each of the LLR-03 fuel rods 3121, 3122, 3123, and 3124 for time intervals of -1 to 10 and 0 to 50 seconds. Figures 8B, 9B, 10B, and 11B display the system pressure and hydraulic data (i.e., turbine measurements of the volumetric flow rates) for each test rod in LLR-03. This data can be directly compared with the LVDT and cladding thermocouple data in Figures 8A through 11A, respectively. Figure 12 shows an overlay of the responses of the four LVDTs and Figures 13 and 14 show overlays of the thermocouple data. The events of particular importance that will be discussed with regard to thermocouple perturbation effects are the time to DNB (departure from nucleate boiling) and rod quench indicated by these figures. An interpretation of the data will be presented when feasible.

The data displayed in Figures 4, 5, 6, and 7 illustrate the rod DNB during the early portion of the blowdown. Here, the saturation temperature curve (not shown in these figures) and the coolant temperature data, taken at the outlet of the flow channel are nearly identical. Consequently, an estimate of the cladding temperature departure time from saturation conditions, indicating DNB, can be made relative to the displayed coolant temperature data. Also, an estimate of DNB can be made from the LVDT data. These estimates are collected in Table 3.

All of the data in Table 3, except for one point, suggest that the LVDT detects an earlier time for DNB than that determined by the surface clad thermocouples. In symbols, this could be written as

$$t_{LVDT}^{DNB} \leq t_{TC}^{DNB} . \qquad (1)$$

Two possible reasons for this correlation are discussed below.

Since DNB conditions are attained at different times for different axial locations along the rod, one reasonable hypothesis for explaining the early DNB response of the LVDT rests on the assumption that the LVDT instrumentation can detect the first localized film boiling event occurring at some location along the length of the rod. Meanwhile, the surface thermocouples, representing a point measurement, can only indicate the time when the neighboring clad surface experiences DNB. Consequently, the time to DNB as determined by the LVDT should be less than or equal to that determined by the TCs. The only time when the two quantities should be equal would be when the initial DNB condition occurs near enough to a thermocouple junction to be detected simultaneous with the LVDT response. The single inconsistency in the early LVDT/DNB theory occurred on the high power rod 3121. As is evident from Figure 4, the LVDT on this rod indicated a later DNB time than the surface clad thermocouple located at 0^{o} azimuthal orientation

TABLE 3

LLR-03

ESTIMATED TIME OF INITIAL DNB

	Rod Number			
Instrument	3121	3122	3123*	3124
LVDT	2.8	2.0	2.0	1.8
TC 180° 0.533 m	2.8	4.5	2.5	2.4
TC 0° 0.533 m	2.4		2.5	2.4
TC 0° 0.457 m		2.6		

The above numbers indicate the approximate time (in seconds) during blowdown that the rod temperature significantly deviates from the saturation temperature, indicating DNB, as determined from the given instrumentation. Interpretation of the data, especially the LVDT data, with regard to the initiation of DNB is somewhat subject and might be open to alternative evaluations.

Numbers reported in the above table have been suggested by PBF personnel[5].

* Rod 3123 failed at 12.3 seconds into the blowdown transient. The rod failure resulted from a water-log condition that existed prior to blowdown.

and 0.533 m from the bottom of the rod. It has been suggested[4] that this discrepancy may be due to a timing offset error in the LVDT data because it is not likely that the high power rod 3121 experienced DNB, as determined by the LVDT, later than the low power rods 3123 and 3124.

Although the above hypothesis explains the early LVDT DNB data and does not involve thermocouple perturbation effects, there is another hypothesis that is also possible, explains the data, and is directly linked to surface thermocouple cooling phenomena, i.e., "fin effects." To begin, it is possible to look at Figures 4 through 7 and say that the "delayed" response in the thermocouple DNB data relative to the LVDT data, and sometimes the wide discrepancies between oppositely positioned thermocouples, suggests that selective cooling effects are taking place near the thermocouples and thereby "delaying" DNB at these places while other more remote sections of the rod are experiencing film boiling, as shown by the LVDT data. This can occur because thermocouple sheaths extend only down to about the core midplane and consequently the lower half of the rod may be experiencing DNB while the upper section with "fin" TCs may be cooling the cladding surface and thereby delaying DNB. Whether or not this is true cannot be determined from the presently available data for a variety of reasons: (a) the thermal response of the rod at other axial positions is not known, (b) the hydraulic conditions between flow channels may be non-uniform, (c) a comparison response for rods without external surface clad thermocouples is not possible for this test, and (d) the response of rods with full length TC/rod sheaths is not known.

The presently available data are simply not sufficient to decide between the above two theories or even alternate interpretations of the LVDT and thermocouple data. The strongest statement that can presently be made about the first 10 seconds of the LLR-03 data is that the LVDT generally leads the response of the thermocouples in

determining the time to DNB, and that this may result from either thermocouple "fin" effects or axially dependent DNB conditions not dependent on cladding thermocouples.

There is one final observation that should be made. Notice that in Figure 5 there is a significant delay in the response of the thermocouple located at 0.533 m and 180^{o} compared with the TC at 0^{o}. As will be seen in some later tests this same thermocouple also behaves in a rather atypical fashion. One conceivable explanation for this thermocouple response anomaly involves the possibility of a thermocouple attachment problem. If for any reason the sensitive junction of the TC is perturbed from its intended position, then the thermocouple may not accurately measure the cladding temperature. Furthermore, the TC attachment geometry can vary slightly from test to test, due to rod power changes, cycling effects, and other factors. In the above case, it is possible that the TC junction is slightly farther away from the cladding surface than the other TCs. Consequently, the TC might be cooler than the clad and therefore enters into DNB at a later time than the cladding surface, as indicated by the other thermocouples. This explanation appears to explain other anomalies in later tests; however, not all of the test data are consistent. Other theories including leaking check valves and rod bowing effects are also possible. Additional observations will be pointed out as the behavior of this rod is studied in the later tests.

Figures 8A, 9A, 10A, and 11A present overlay plots of the intermediate time behavior of the cladding thermocouples, cladding elongation, the outlet coolant temperature, and the midplane shroud temperature for each of the four test rods 3121, 3122, 3123, and 3124, respectively. These figures show that all rods quenched between about 36 and 40 seconds into the blowdown transient. This particular rewet was initiated by opening a hot leg blowdown valve at 22 seconds and then closing the large cold leg blowdown valve at 35 seconds,

subsequently changing the test system hydraulic resistances and thereby allowing a low quality two-phase mixture to enter the test region and rewet the rods.

By comparing the LVDT rod quench and clad elongation turnaround, with the cladding thermocouple quench and temperature turnaround data, an evaluation of possible thermocouple "fin" effects can be made during reflood. Table 4 lists estimates of the time to rod quench and turnaround times for the cladding surface thermocouples and LVDT instrumentation, as determined from Figures 8A through 11A.

Before interpreting the data in Table 4 it should be pointed out that at approximately 12.3 seconds into the transient, fuel rod 3123 ballooned and ruptured. This failure resulted from a water-logged condition that existed in the rod prior to blowdown. Consequently, it may be difficult to assess the behavior of this rod, especially during rod quench, with regard to surface clad thermocouple effects when the rod geometry and structural properties may be markedly different than non-failed rods. Nevertheless, rod rewet times have been estimated for rod 3123 and are listed in Table 4. A review of the data for rod 3123 will be presented after the behavior of the three non-failed rods has first been studied.

From Table 4 it can be seen that the cladding elongation turnaround times occur approximately 0.3 seconds after the thermocouples rewet; and the rod quench, indicated by the LVDT data, occurs even later. To present some possible explanations for this response event, the behavior of each rod during rewet will be studied and compared with the responses of the other rods.

For rod 3121 (note Figure 8A), the external thermocouple experiences a very rapid quench starting at about 36.2 seconds and ending at a relatively stable value near 37.0 seconds. Little or no precursory cooling effect is evident in the thermocouple data. In contrast, the LVDT turnaround time at 36.5 seconds suggests a

TABLE 4

LLR-03

ESTIMATED ELONGATION TURNAROUND TIME AND ROD QUENCH TIME

	Rod Number			
Instrument	3121	3122	3123*	3124
LVDT	36.5/40.0	36.5/	36.5/	36.5/
TC 180° 0.533 m	36.2	36.2	36.0/37.5	36.2
TC 0° 0.533 m	36.2		36.0/37.5	36.2
TC 0° 0.457 m		36.2		

The first number indicates the approximate turnaround time (in seconds) for the response of the LVDT, i.e., the time of maximum rod elongation prior to rod cooldown. The second number represents the approximate rod quench time as indicated by the LVDT. A blank entry in the LVDT data indicates that a unique rod quench time could not be assessed. The temperature turnaround time and the rod quench time, as determined from the TC data, are nearly the same for non-failed rods, and are therefore reported as a single number.

* Rod 3123 failed at 12.3 seconds into the blowdown transient. The rod failure resulted from a water-log condition that existed prior to blowdown.

classical precursory cooling period of approximately 3.5 seconds, followed by a rapid rod quench at 40 seconds. This behaviorial anomaly between the responses of the two instruments suggests that the thermocouple may have indeed selectively enhanced rod cooling effects, as supported by the precursory cooling tendancy in the LVDT data, to such a point when the rod itself could rewet at 40 seconds. However, the LVDT response of this rod is different than the responses of the other rods, even though all rods experienced similar hydraulic conditions. For example, consider the response of rod 3122 in Figure 9A. Again we see the sudden thermocouple quench starting at 36.2 seconds and the LVDT turnaround time at about 36.5 seconds with a precursory cooling period evident in the LVDT data until about 40.5 seconds where the cladding elongation data has stabilized. No clearly definable quench time is evident in the LVDT data for rod 3122, as compared with rod 3121. Likewise, rod 3124 shows a corresponding turnaround time in the LVDT data near 36.5 seconds, and then decreases to a stable value at 41 seconds. Between 36.5 and 41 seconds cooling effects and perhaps local rewet events take place; however, nowhere is there evidence that the entire rod experienced such a rapid and entire rewet as seen in the data for rod 3121.

Another interesting observation can be made about the TC behavior of rods 3121, 3122, and 3124. Shortly after the thermocouples rewet, the TCs noticed a sudden and rapid increase in temperature, essentially another DNB. This is not as noticeable in Figure 8A with rod 3121 as it is evident in Figures 9A and 11A with rods 3122 and 3124 respectively. This thermocouple "flutter" behavior may be indicative of a thermocouple selective cooling effect. That is, the thermocouples being slightly cooler than the adjoining clad surface are subsequently more likely to rewet as the coolant floods the test assembly than the cladding surface. Then, as heat is transported from the clad to the thermocouple the liquid boils off the thermocouple and it experiences another DNB. This could be followed by another thermocouple rewet and possibly another DNB. This "flutter" might continue until the stored energy and/or clad temperature of the rod

permitted rewetting. During this time period the LVDT notices only a gradual decrease in the rod length, relative to the shroud, and no typical overall rewetting response, except for rod 3121 near 40 seconds. These data suggest that the TCs may be experiencing preferential rewetting conditions.

Without having discussed the response of rod 3123, the data at present suggests that no sudden overall rewet occurred at any given time for rods 3122 and 3124; but rather a time varying rewet over the axial length of the rod or possibly several very localized rewets or even rewets of extremely short duration so that the energy stored in the rods was gradually dissipated. Whether or not the external thermocouples influenced rod cooling and the rewetting behavior of the rod cannot be established with reasonable certainty. Perhaps the strongest statement that can be made so far is that the response of the thermocouples are not representing the overall response of the cladding temperature. This does not mean that the thermocouples are giving inaccurate data about the cladding temperature near the TCs, but rather the entire clad cannot be experiencing a rapid quench at 36.2 seconds, because the LVDT should have detected such an event. In other words, the local cladding surface near the TCs may be rewetting and then going into DNB as heat is transported into the region from other axial sections. Either hypothesis is possible, i.e., (a) TC rewet followed by TC DNB, or (b) clad rewet near the TC followed by a subsequent clad DNB near the TC. About the only thing that can be said with any certainty is that one cannot adequately determine fuel rod behavior with TCs located at only one axial position along the rod. Nor can one adequately compare the response of an integral type instrument, i.e., LVDT, with a single pair of thermocouples located at one axial position.

Now consider the behavior of rod 3123, shown in Figure 10A. As was mentioned before, rod 3123 failed at 12.3 seconds into the transient and interpretation of the data for this rod is somewhat questionable. Nevertheless, there are a few interesting observations

that should be pointed out. First, as in the previous cases, the LVDT response begins to turn around at about 36.5 seconds and moves downward rather quickly until at about 38.5 seconds an unexplained increase occurs. Since the data after 38.5 seconds is not fully understood, discussion of the data will be limited to the time interval between 36 and 38.5 seconds.

At about 36.0 seconds the thermocouples for rod 3123 show a temperature turnaround followed by a precursory cooling period to 36.5 seconds where they experience a rapid quench that ends at a stable temperature base at 38.5 seconds. The response of the thermocouples on this rod appear to be more representative of a non-uniform rod quench than the thermocouple data for the previous rods. The geometric distortion of the rod may have had an effect on the time to quench as indicated by the surface thermocouples. Certainly the LVDT response, preceding rod quench, was affected by the rod ballooning and failure.

A synopsis of the two theories discussed above concerning possible explanations for the behavior of the LVDTs and TCs during DNB and rod rewet events are presented below.

(1) The thermocouples are accurately reflecting the local cladding temperature, rewet behavior, and DNB events. And the LVDT is accurately reflecting the overall (or average) fuel rod behavior. The difference between the two instrument responses is that the average behavior need not reflect the behavior of the rod at any given axial position on the rod, e.g., the TC sensitive junction.

(2) The thermocouples are preferentially cooling the cladding surface according to fin effects. The early quench of the thermocouples for rods 3121, 3122, and 3124 suggests that because the TCs are farther from the clad surface they are

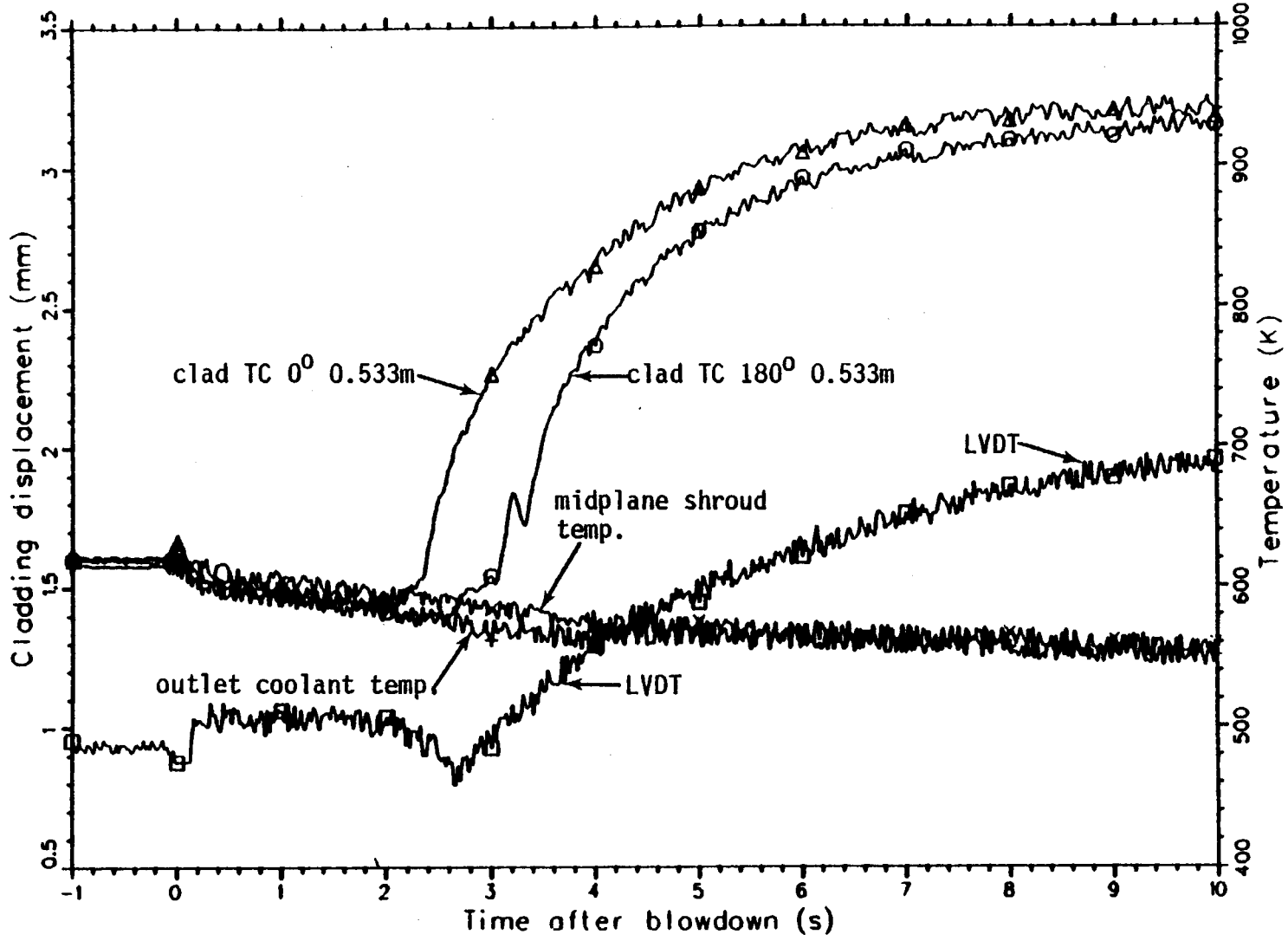

Fig. 4 Comparison of the thermal and mechanical response of fuel rod 3121. Test LLR-03.

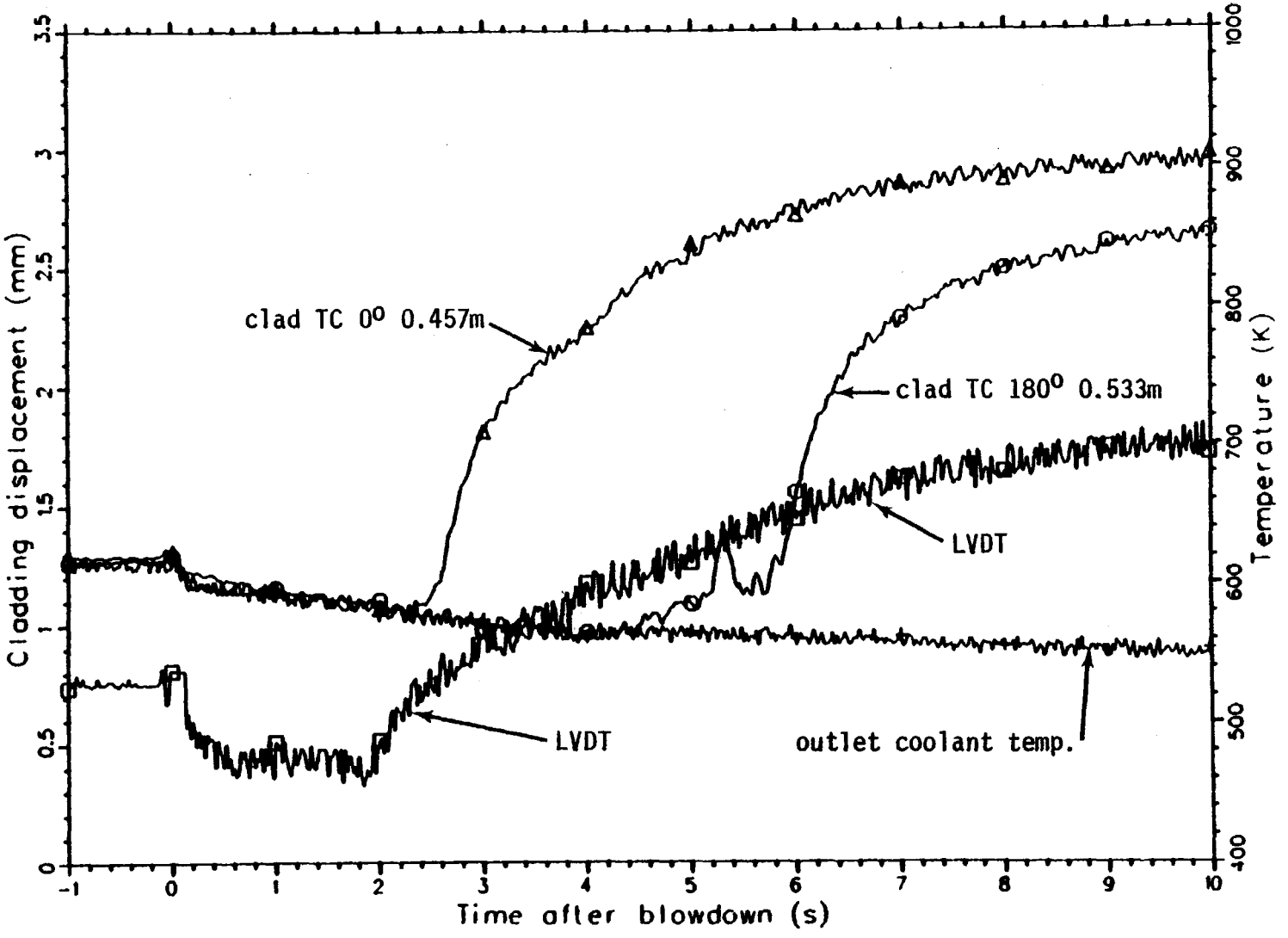

Fig. 5 Comparison of the thermal and mechanical response of fuel rod 3122. Test LLR-03.

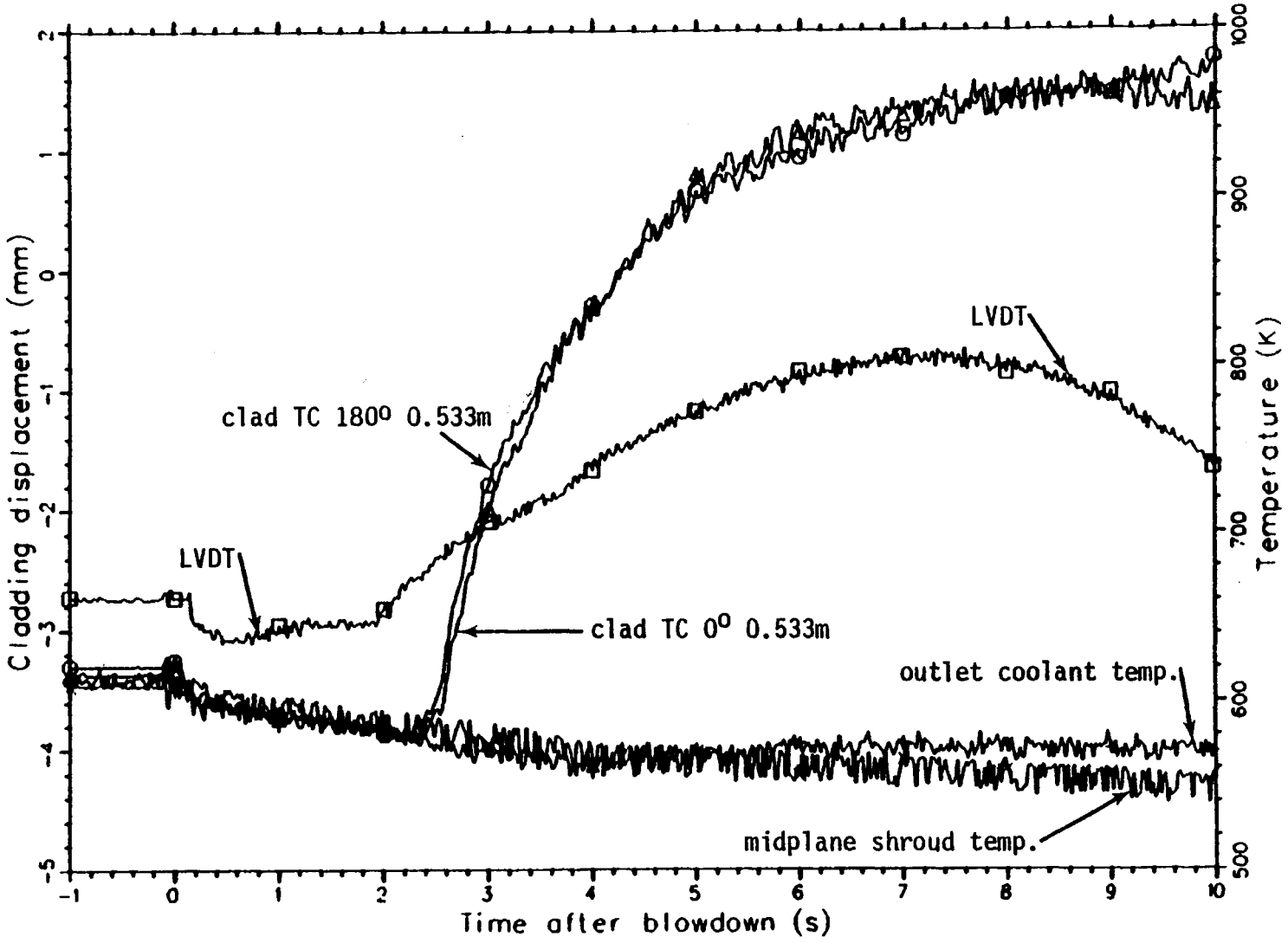

Fig. 6 Comparison of the thermal and mechanical response of fuel rod 3123. Test LLR-03.

LTR LO-00-79-108

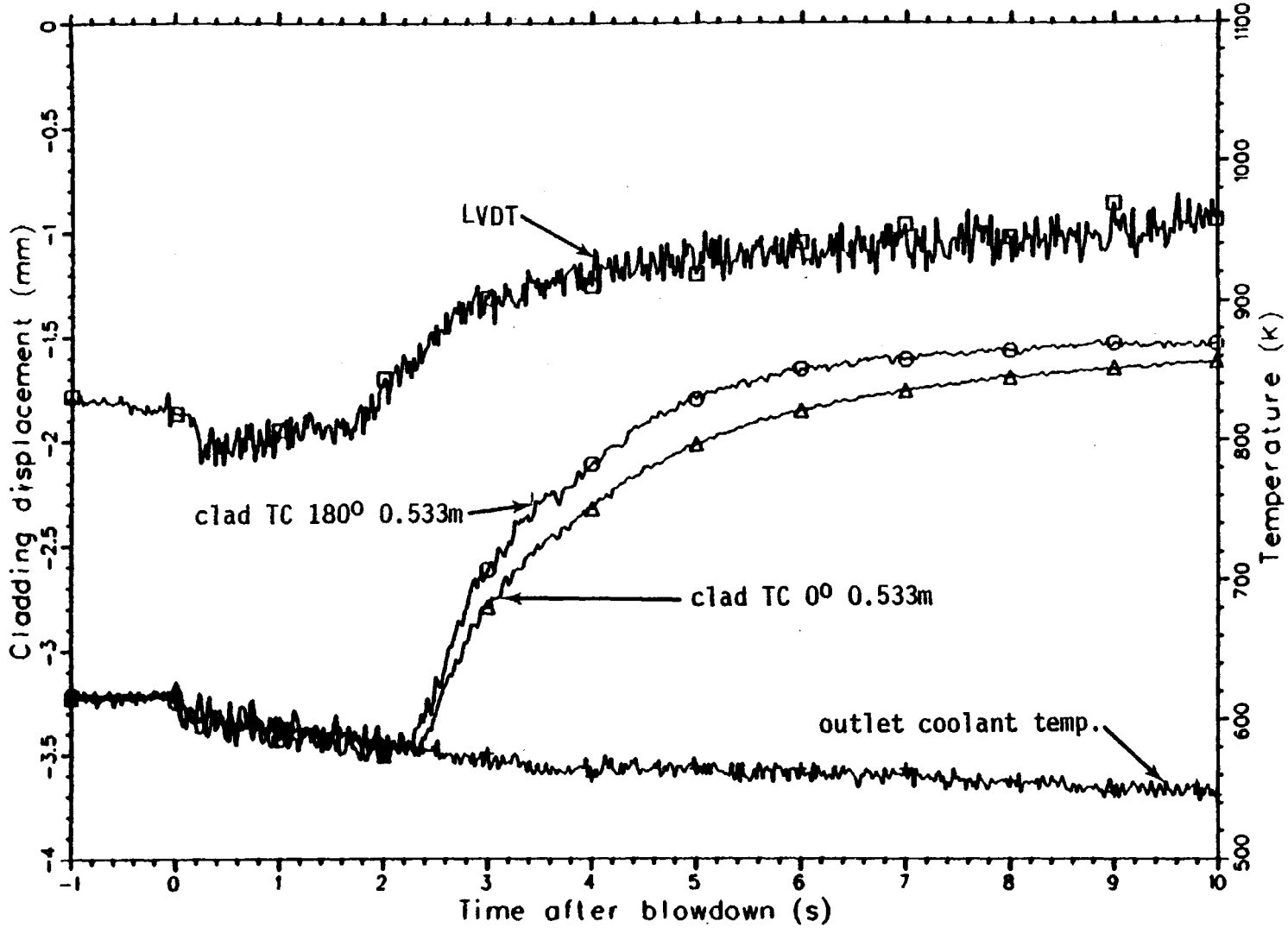

Fig. 7 Comparison of the thermal and mechanical response of fuel rod 3124. Test LLR-03.

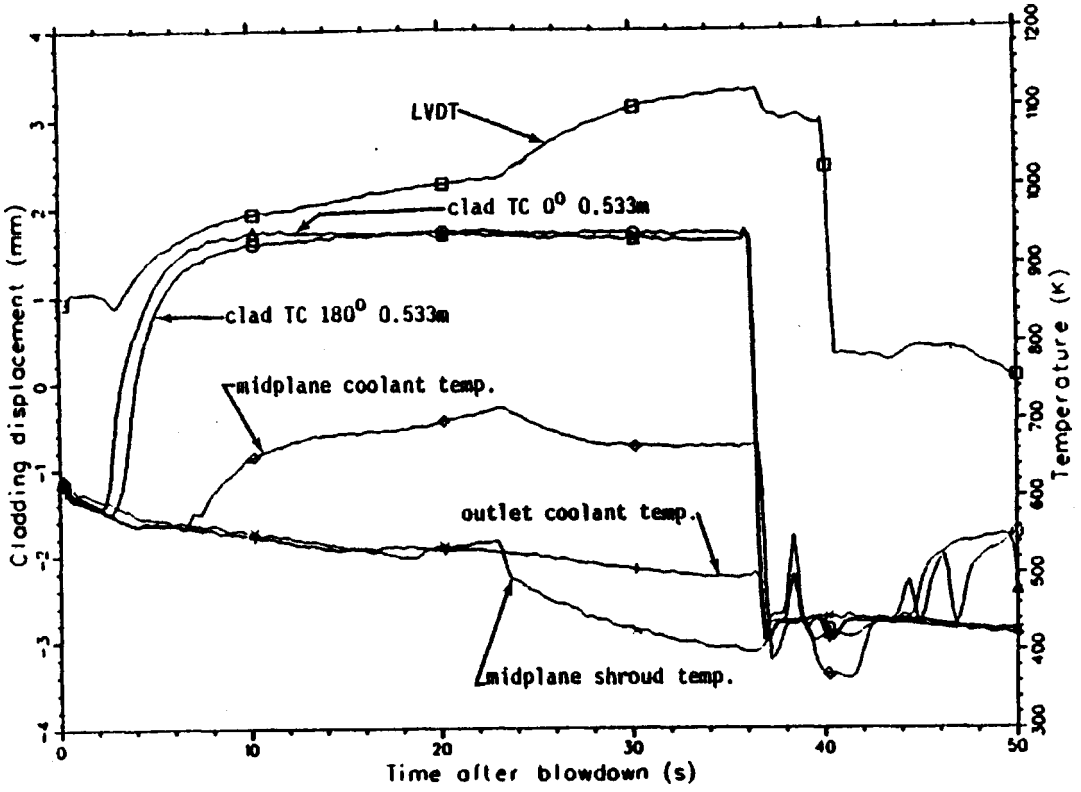

Fig. 8A Comparison of the thermal and mechanical response of fuel rod 3121. Test LLR-03.

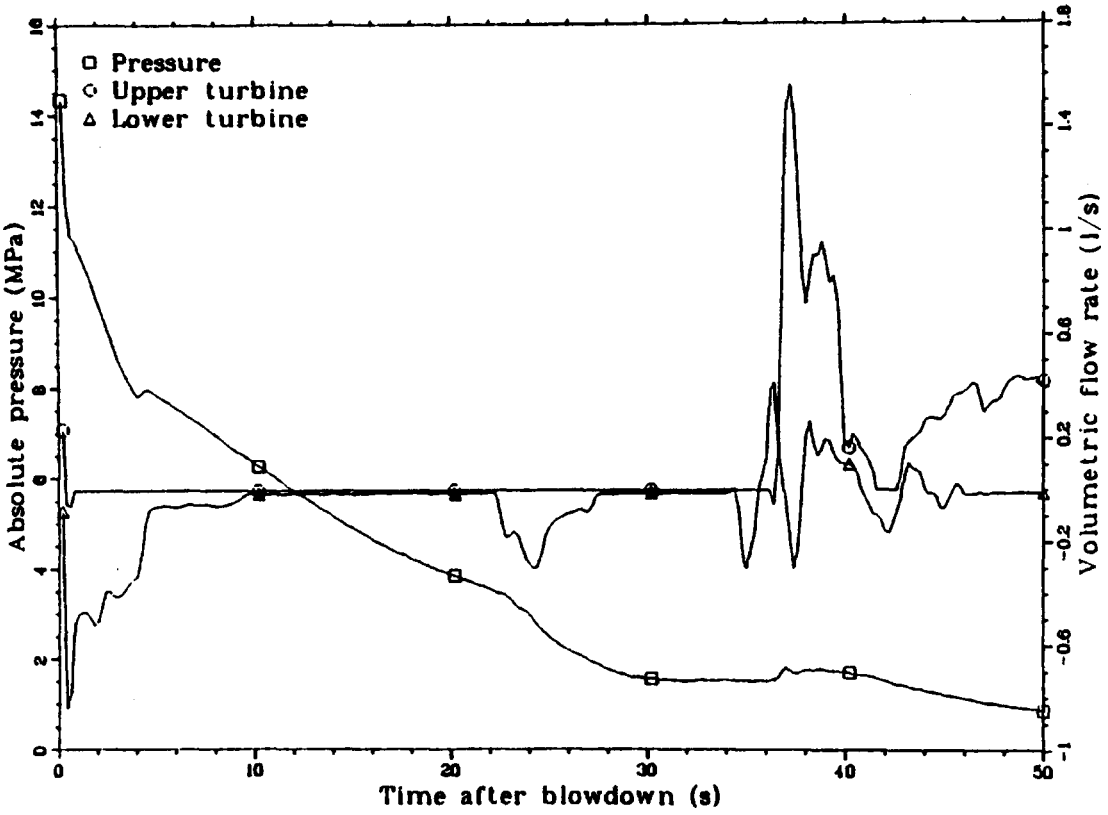

Fig. 8B An overlay showing the system pressure and the upper and lower volumetric flow rates for rod 3121. Test LLR-03.

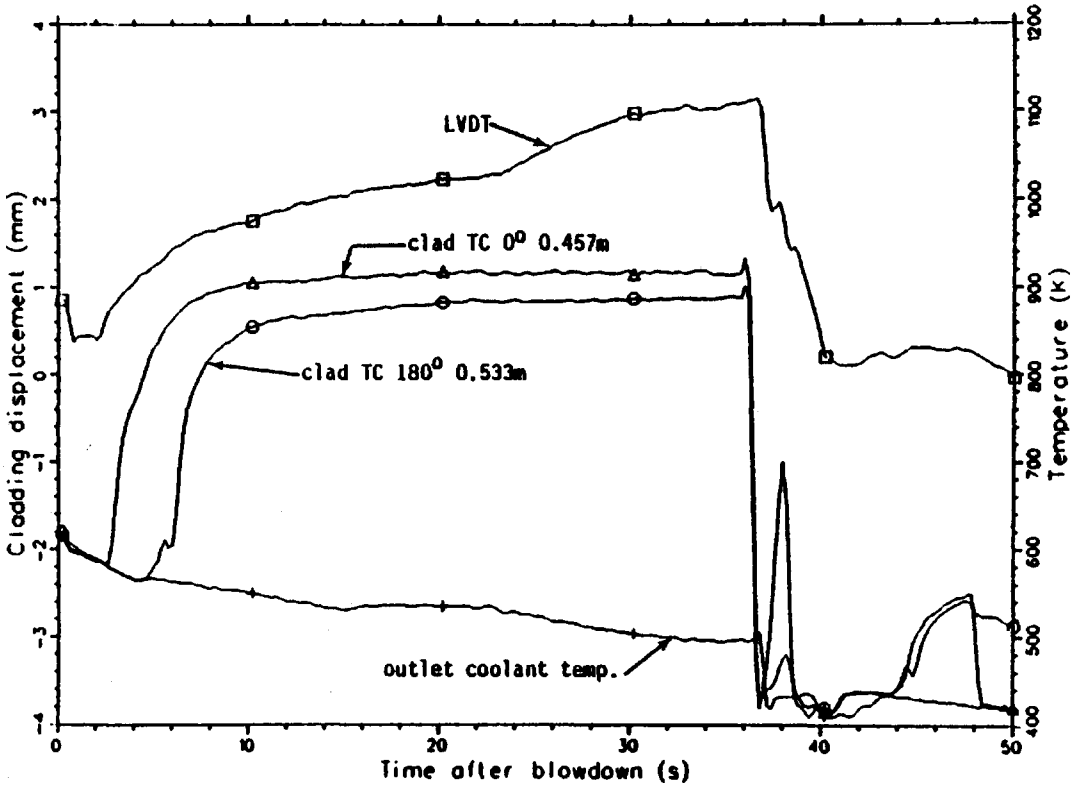

Fig. 9A Comparison of the thermal and mechanical response of fuel rod 3122. Test LLR-03.

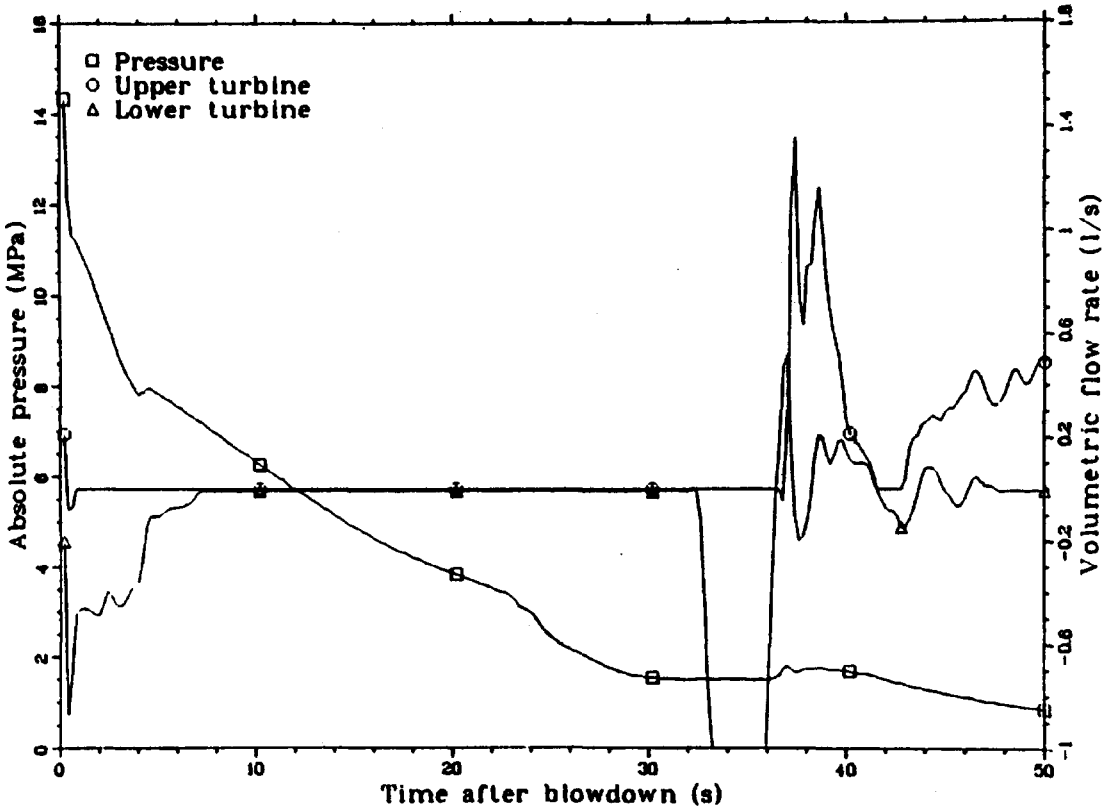

Fig. 9B An overlay showing the system pressure and the upper and lower volumetric flow rates for rod 3122. Test LLR-03.

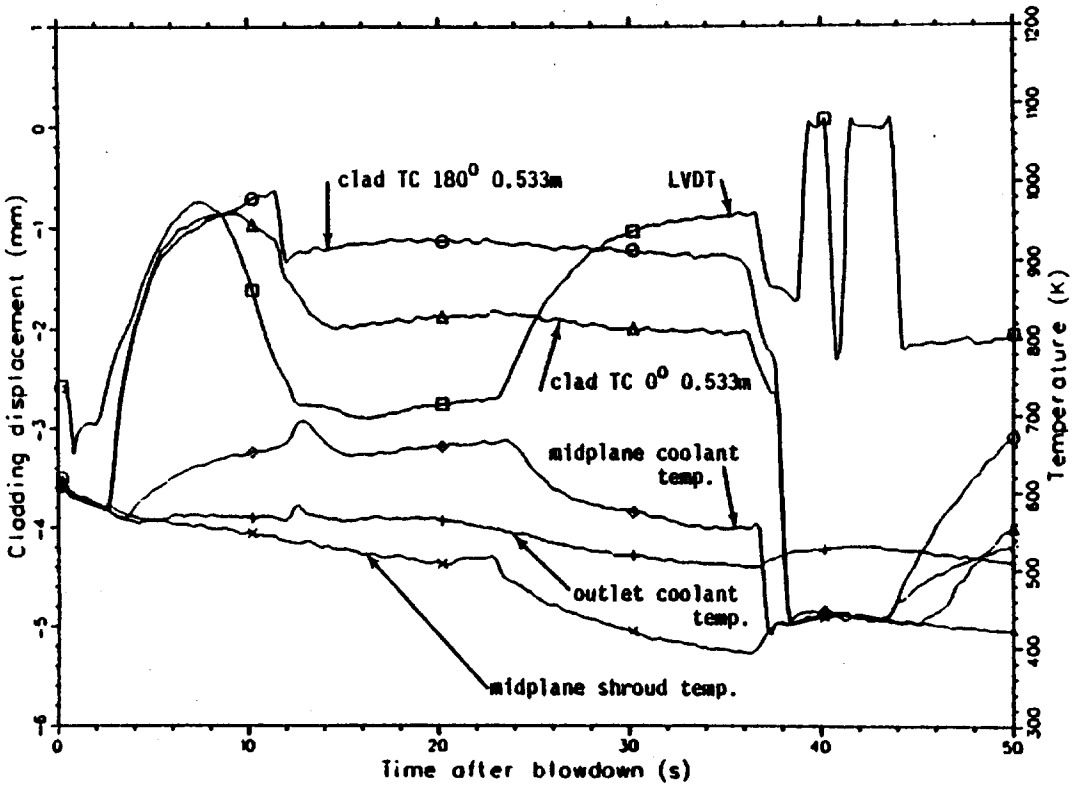

Fig. 10A Comparison of the thermal and mechanical response of fuel rod 3123. Test LLR-03.

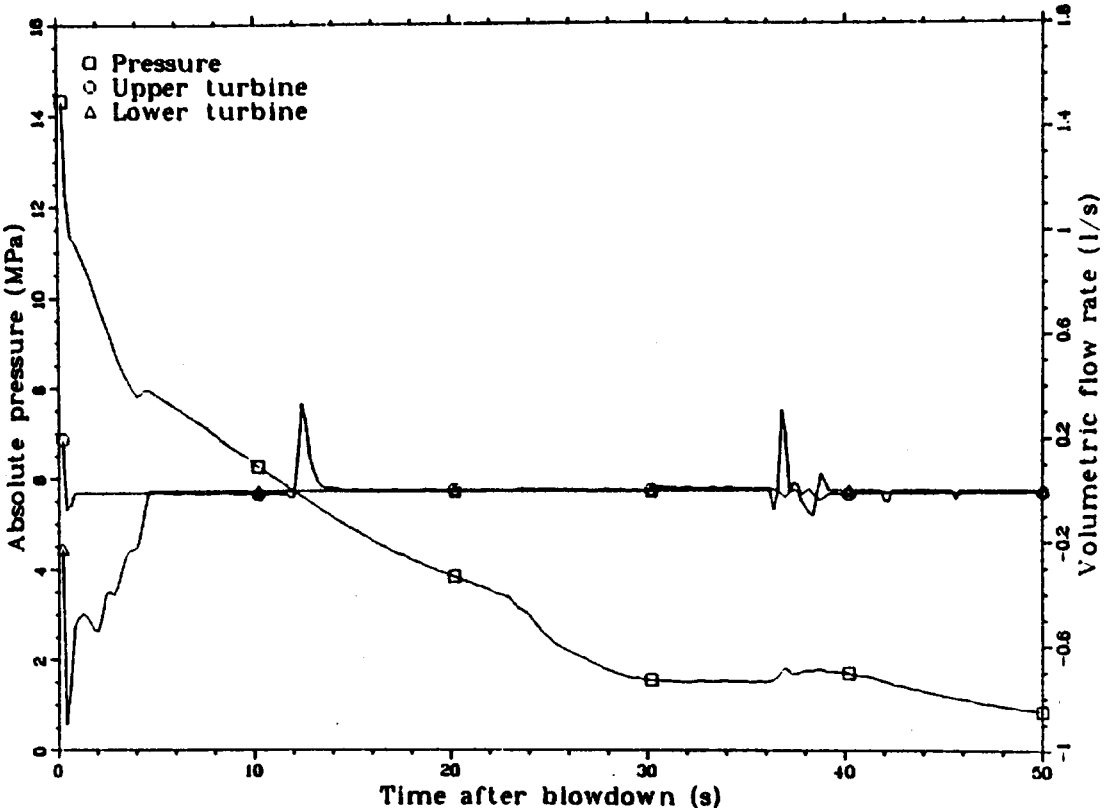

Fig. 10B An overlay showing the system pressure and the upper and lower volumetric flow rates for rod 3123. Test LLR-03.

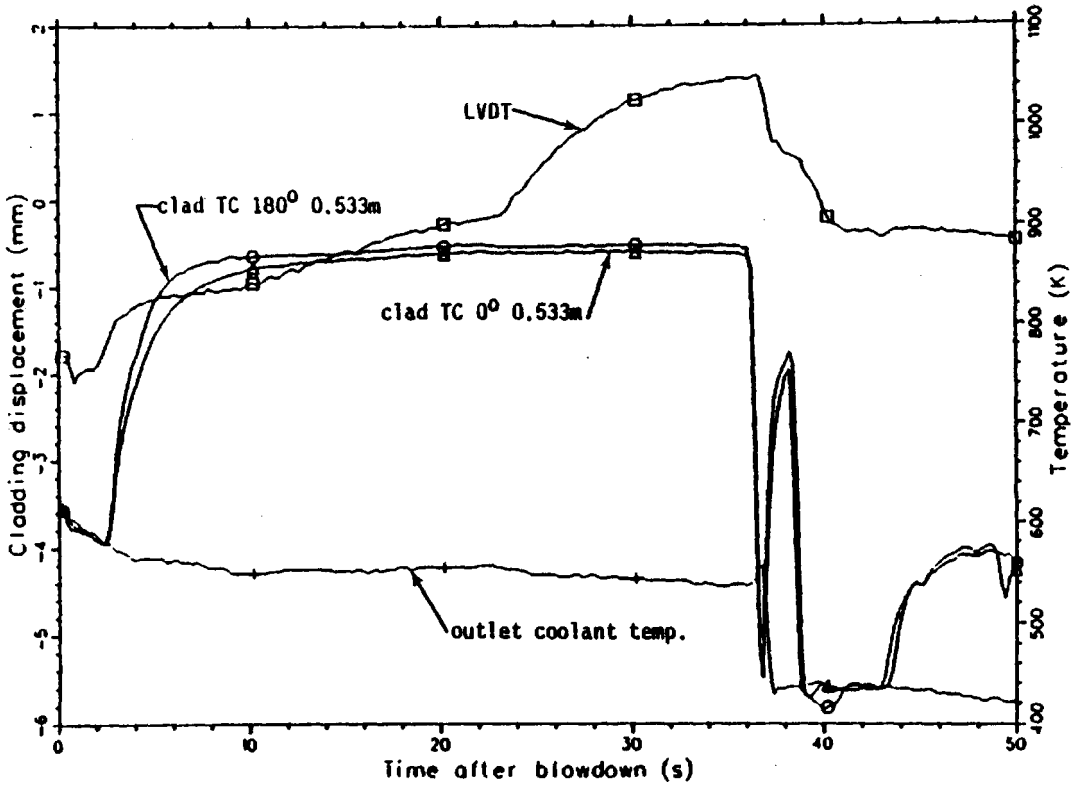

Fig. 11A Comparison of the thermal and mechanical response of fuel rod 3124. Test LLR-03.

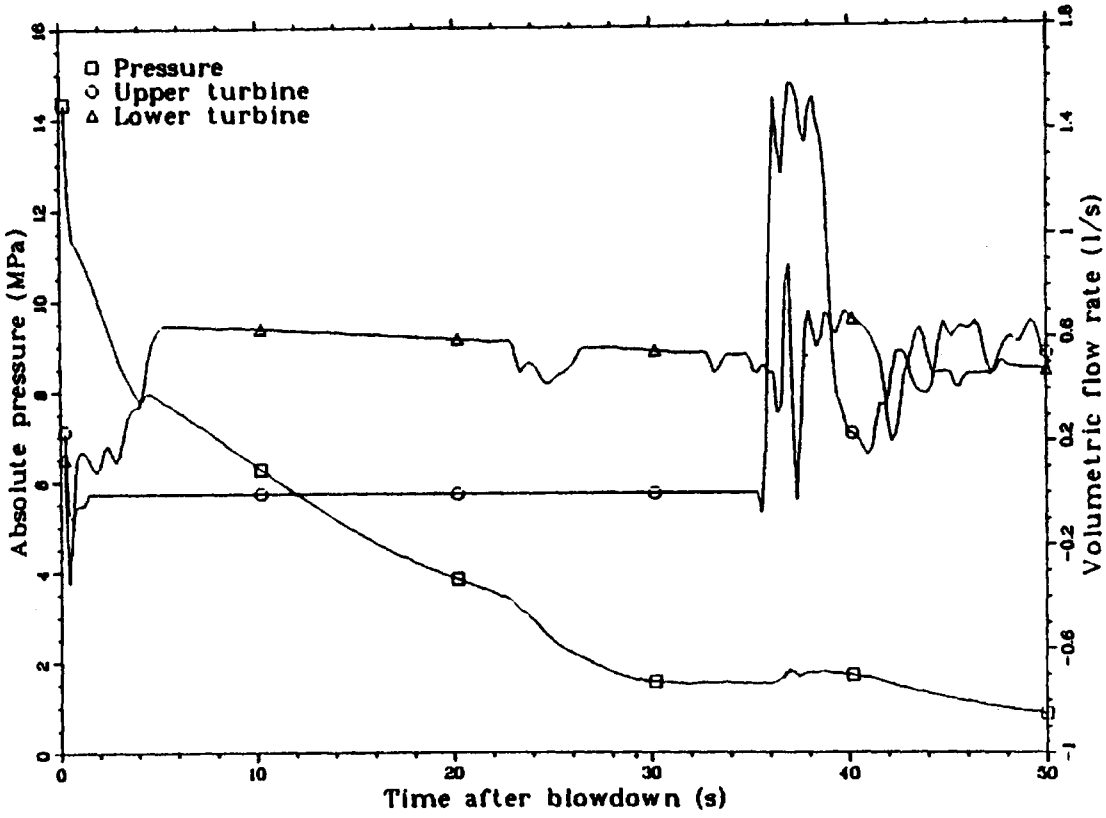

Fig. 11B An overlay showing the system pressure and the upper and lower volumetric flow rates for rod 3124. Test LLR-03.

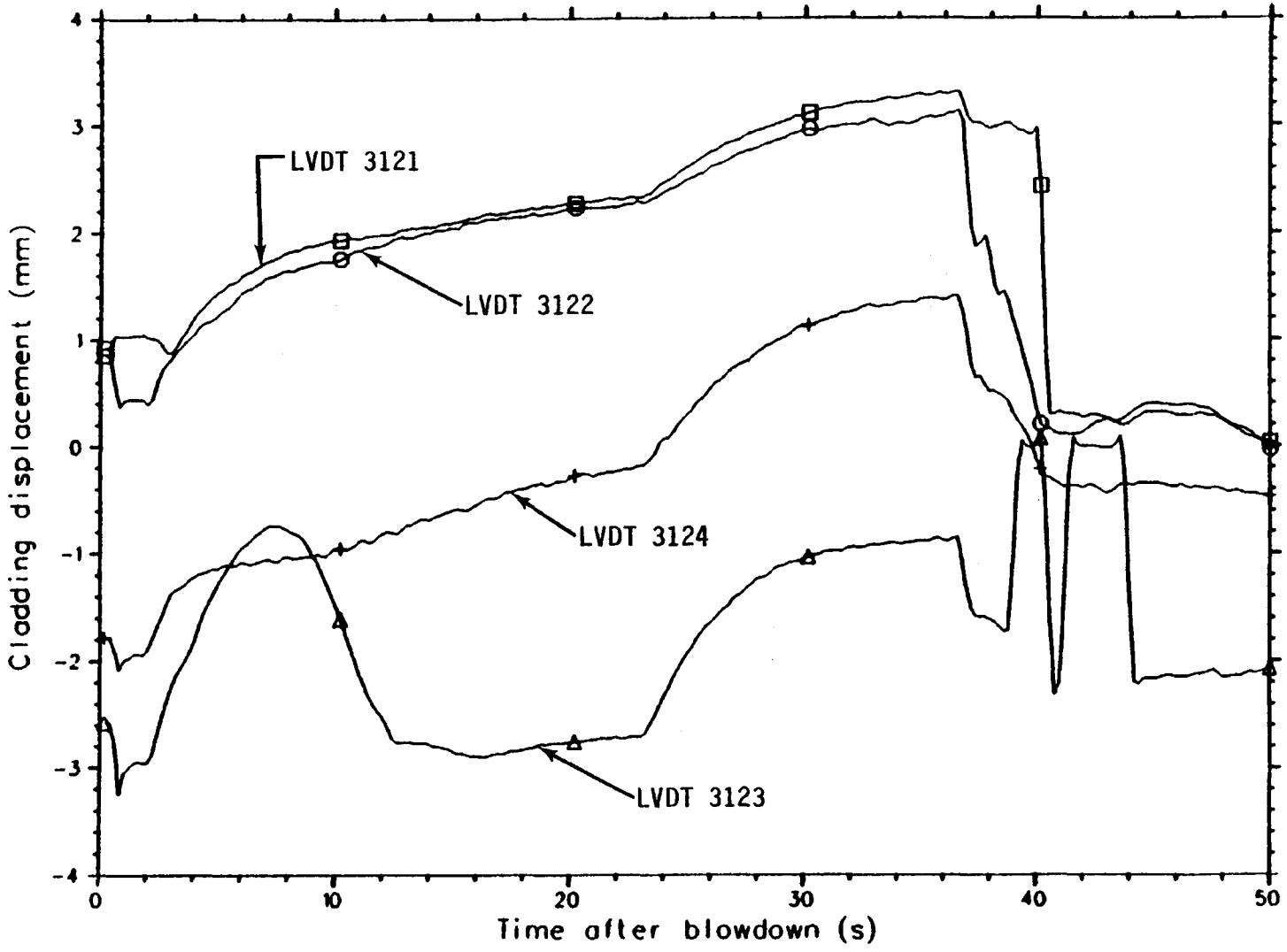

Fig. 12 An overlay showing the mechanical response of rods 3121, 3122, 3123, and 3124. Test LLR-03.

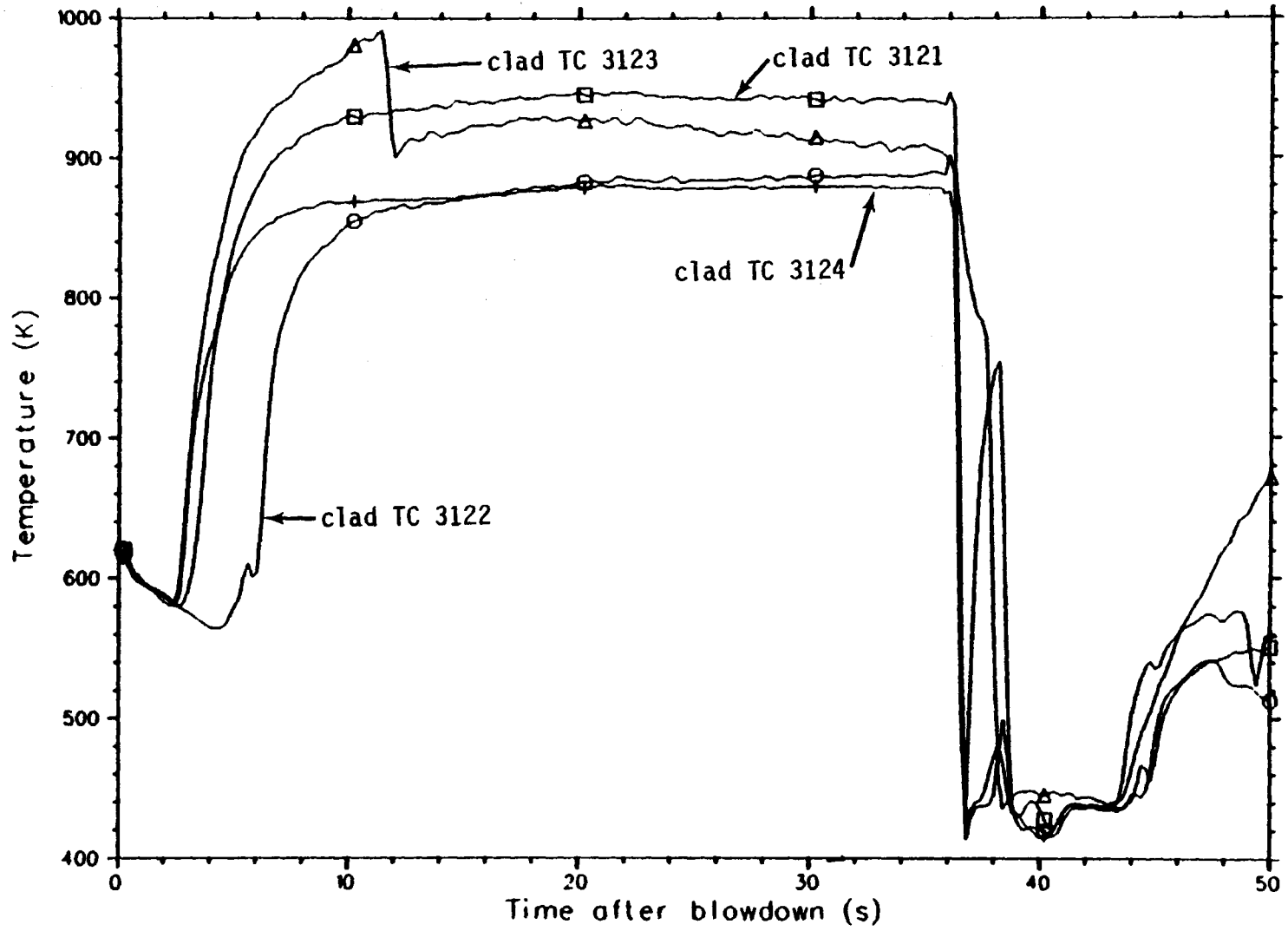

Pig. 13. An overlay showing the thermal response of rods 3121, 3122, 3123, and 3124, as determined by thermocouples located at 180° azimuthal orientation. Test LLR-03.

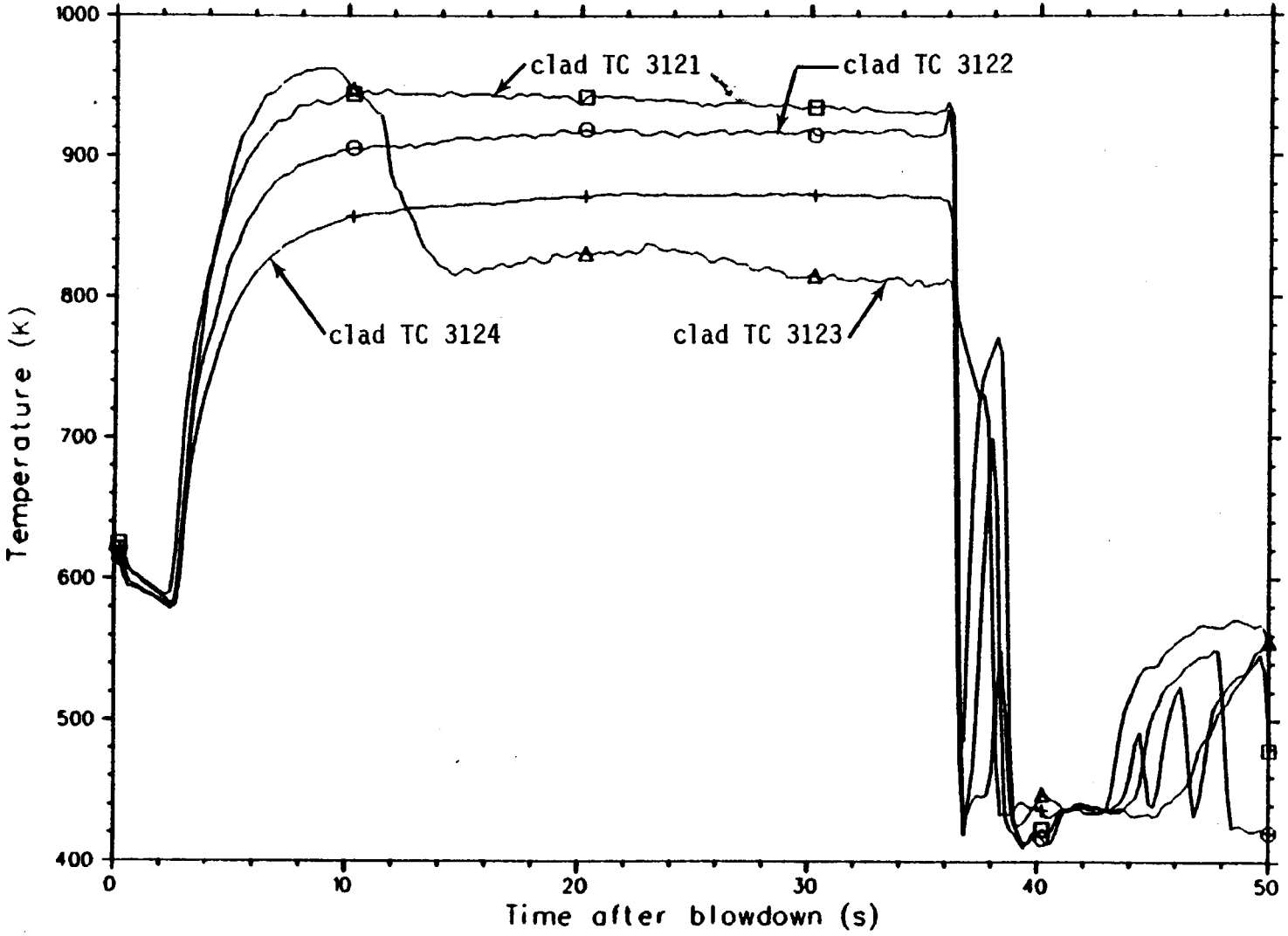

Fig. 14 An overlay showing the thermal response of rods 3121, 3122, 3123, and 3124, as determined by thermocouples located at 0^{0} azimuthal orientation. Test LLR-03.

cooler than the rod and therefore the TC rewets before the hotter surface rewets. If this occurs, then heat could be transported from the clad to the TC and the TC would dissipate the heat as a fin. This could lower the temperature of the clad to the Leidenfrost temperature where it too could quench. Consequently, the thermocouples would be preferentially influencing the behavior of the rod according to a TC perturbation effect.

4.2 Comparison of the LVDT and TC Responses for LLR-05

The second test in the LOFT Lead Rod test series was LLR-05. The principal test train design modifications undertaken between LLR-03 and LLR-05 involved the replacement of the two low power stainless steel shrouded rods: 3123, which failed during LLR-03, and 3124, with high power zircaloy shrouded rods 3451 and 3452, respectively. Thus, all four rods in the LLR-05 test had nominally the same power generation. Figure 1B illustrates the general test configuration for LLR-05 and LLR-04.

With the change from stainless steel to zircaloy shrouded rods, all four rods in the LLR-05 test assembly were identical except for two items: (a) rods 3121 and 3122 had experienced one prior blowdown transient, and (b) rod 3452 had no surface clad thermocouples. Since all rods in the LLR-05 test, as well as in all other subsequent tests, were equipped with LVDTs, it is possible to compare the dynamic behavior of rods with and without surface clad thermocouples by examining the LVDT data. Further, since all rods were expected to experience similar thermal-hydraulic conditions during blowdown and reflood, an evaluation of thermocouple perturbation effects could be made by comparing the LVDT responses of rods instrumented with cladding TCs to uninstrumented rods.

Figures 15, 16, 17, and 18 overlay the response of the cladding thermocouples, coolant thermocouple data, shroud temperatures, and LVDT data for the LLR-05 fuel rods during the first 20 seconds following blowdown. Figures 19A, 20A, 21A, and 22A present the long-term history for the cladding thermocouples, cladding elongation, outlet coolant temperature, midplane coolant temperature, and shroud temperature for each of the LLR-05 fuel rods. In addition, Figures 23, 24, 25, and 26 show magnified views of the rod rewet event near 225 seconds. Corresponding to the "A" figures are Figures 19B, 20B, 21B, and 22B. The "B" figures show the system pressure and volumetric flowrate data for each of the test rods in LLR-05. Overlays of the LVDT data and thermocouple data appear in Figures 27 and 28, respectively.

As was done for the previous test, the events of particular interest that will be discussed concerning thermocouple perturbation effects are the time to DNB and rod quench data determined from Figures 15 through 28, and summarized in Tables 5 and 6. Other events will also be pointed out when deemed noteworthy.

Consider the time to DNB data presented in Table 5. The data in Table 5 are generally consistent with the observations made for the previous test LLR-03. Namely, that the LVDT instrumentation generally indicates an earlier DNB time than the surface clad TCs. The explanation for this phenomenon is the same as before. Since rod 3452 did not have surface clad TCs, the earlier time to DNB noticed for this rod suggests a possible TC "fin" effect for the other rods; however, it is difficult to say with certainity that this is true because of the magnitude of the LVDT response for rod 3452. However, if there is a TC perturbation effect resulting in a delay in DNB for "finned" rods, then this should also be evident in the later tests for rod 3452 as compared with the LVDT data for rods with surface TCs. This type of comparison will be considered in the LLR-04 and LLR-4A data analysis.

TABLE 5

LLR-05

ESTIMATED TIME OF INITIAL DNB

	Rod Number			
Instrument	3121	3122	3451	3452**
LVDT	0.5	--*	1.4	0.4
TC 180° 0.533 m	2.0	2.3	1.9	
TC 0° 0.533 m	1.8			
TC 0° 0.457 m		2.0	1.8	

The above numbers indicate the approximate time (in seconds) during blowdown that the rod temperature significantly deviates from the saturation temperature, indicating DNB, as determined from the given instrumentation. Interpretation of the data, especially the LVDT data, with regard to the initiation of DNB is somewhat subjective and might be open to alternative evaluations.

Numbers reported in the above table have been suggested by PBF personnel[5].

* PBF considers the LVDT for rod 3122 to have failed for this test[5].

** Rod 3452 had no surface clad TCs.

TABLE 6

LLR-05

ESTIMATED ELONGATION TURNAROUND TIME AND ROD QUENCH TIME

	Rod Number			
Instrument	3121	3122	3451	3452*
LVDT	175/226	175/226	175/226	175/226
TC 180° 0.533 m	175/226	175/226	175/226	
TC 0° 0.533 m	175/226		175/226	
TC 0° 0.457 m		175/226		

The first number indicates the approximate turnaround time in the response of the LVDT or TC, and the second number represents the approximate time the given instrumentation indicates rod quench.

* Rod 3452 had no surface clad TCs.

Before leaving the "20 second data" two other events should be discussed. Consider the response of rod 3122 as shown in Figure 16. The event that is clearly evident in this figure is the TC "flutter" phenomenon noticed between 2.0 and 3.0 seconds for the thermocouple located at 180^{0} and 0.533 m. At first glance this might appear to be a TC perturbation effect; however, since this thermocouple performed in a similar atypical fashion in LLR-03, while the antipodal thermocouple functioned in a more typical manner, it appears that this anomaly as well as the anomaly shown in Figure 5 might result from a thermocouple attachment problem.* The second TC "flutter" phenomenon shown in Figure 17 resulted when a check-valve above fuel rod 3451 failed to seal completely during the blowdown and subsequently allowed a significant amount of coolant to enter the flow shroud channel for about 3 seconds and caused both cladding thermocouples to rewet. This event is different than the previous TC "flutter" event in that both thermocouples quenched and the LVDT data shows a definite cooling period coincident with the TC rewet.

Consider Figures 19 through 22 and 23 through 26. All of these figures show that the cladding thermocouples quenched at about the same time the mechanical behavior of the rods dropped sharply, i.e., at about the same time the LVDT data indicated large scale cooling effects taking place along the length of the rods. This type of relationship was also evident in the LLR-03 data and will also be shown to hold for tests LLR-04 and LLR-4A. The following relations summarize these ideas:

$$t_{LVDT}^{Turnaround} \simeq t_{TC}^{Turnaround} \tag{2}$$

and

$$t_{LVDT}^{Quench} \geq t_{TC}^{Quench} \tag{3}$$

---

* Recent metallurgical tests appear to indicate that there was no attachment problem for this TC. If this is the case, then the anomalous behavior of this TC is not understood.

The reason that a suitable equality cannot always be written for the rod quench time as indicated by the LVDT instrumentation is that frequently the LVDT data do not consistently indicate a response which is typical of an entire rod rewetting at the same time. For instance, the LVDT for rod 3121, shown in Figure 8A, indicates a sudden and complete rod quench near 40 seconds while the other LVDTs show a more gradual response. The reasons for this different behavior are not completely understood; however, it is theorized that different hydraulic conditions between the flow channels may be partly responsible.

Relations (2) and (3) stipulate that there is good correlation between TC quench events and turnaround times, with LVDT quench and turnaround times, respectively. This tends to support the hypothesis of no significant TC perturbation effects during rod rewet. Additional evidence supports this conclusion. For example, Figure 27 shows an overlay of the LVDT data for rods 3121, 3122, 3451, and 3452. As can be seen in Figure 27 the response of rod 3452, without TCs, corresponds with the response of those rods with TCs. These data indicate that surface clad thermocouples did not enhance the rewetting characteristics of the rods even though the measured temperature data indicate that the surface clad TCs did quench before large sections of the cladding surface could rewet. This two fold explanation of the data appears to present the best explanation of the present data, as well as the data to be reviewed in tests LLR-04 and -4A.

Summarizing the presently reviewed data for test LLR-03 and LLR-05, the following observations are made:

(1) The LVDT data generally indicate an earlier time to DNB than the cladding TCs.

(2) The rod quench time, as determined from the LVDT data, is greater than or equal to that determined from the cladding TC data.

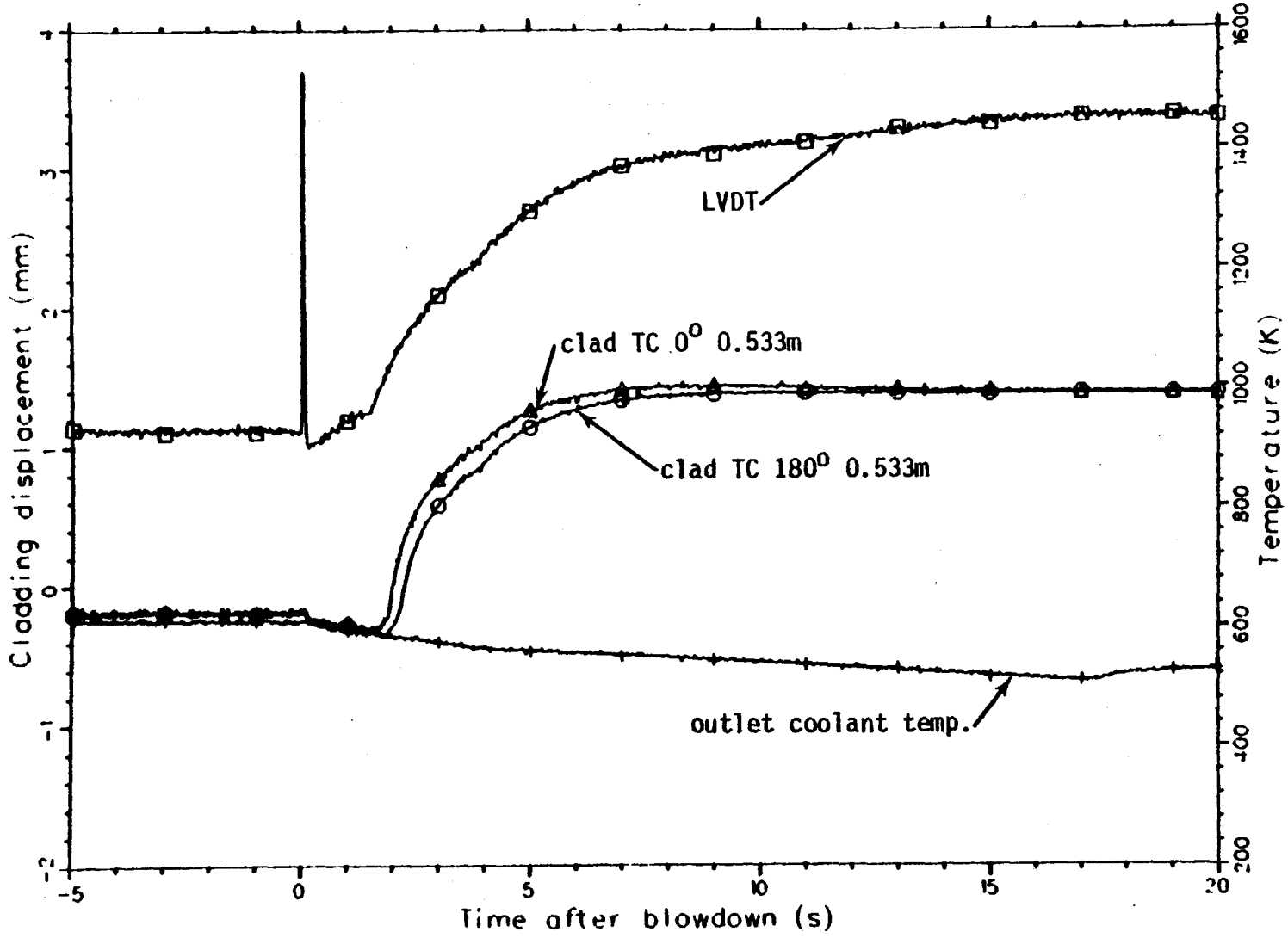

Fig. 15 Comparison of the thermal and mechanical response of fuel rod 3121. Test LLR-05.

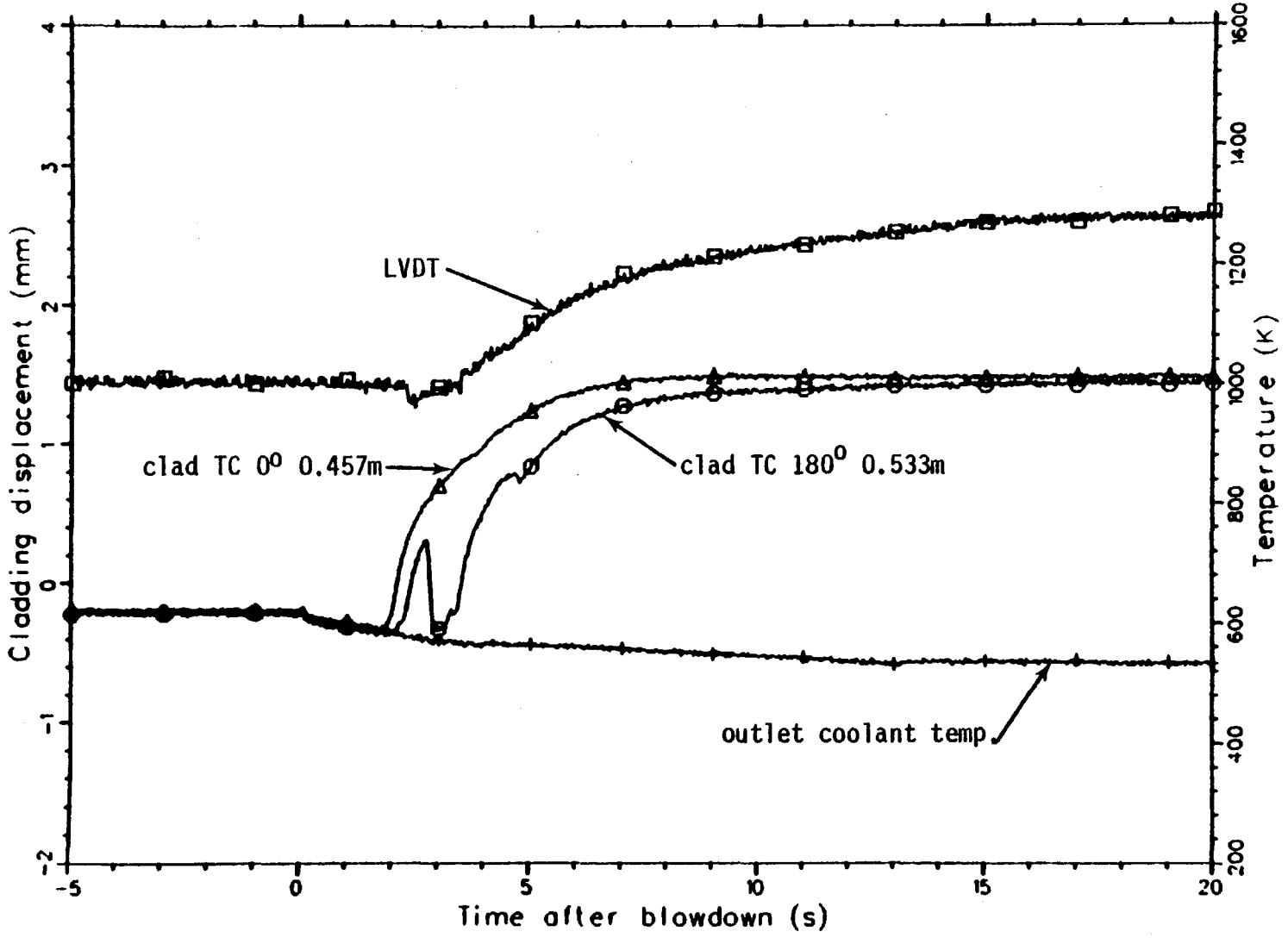

Fig. 16 Comparison of the thermal and mechanical response of fuel rod 3122. Test LLR-05.

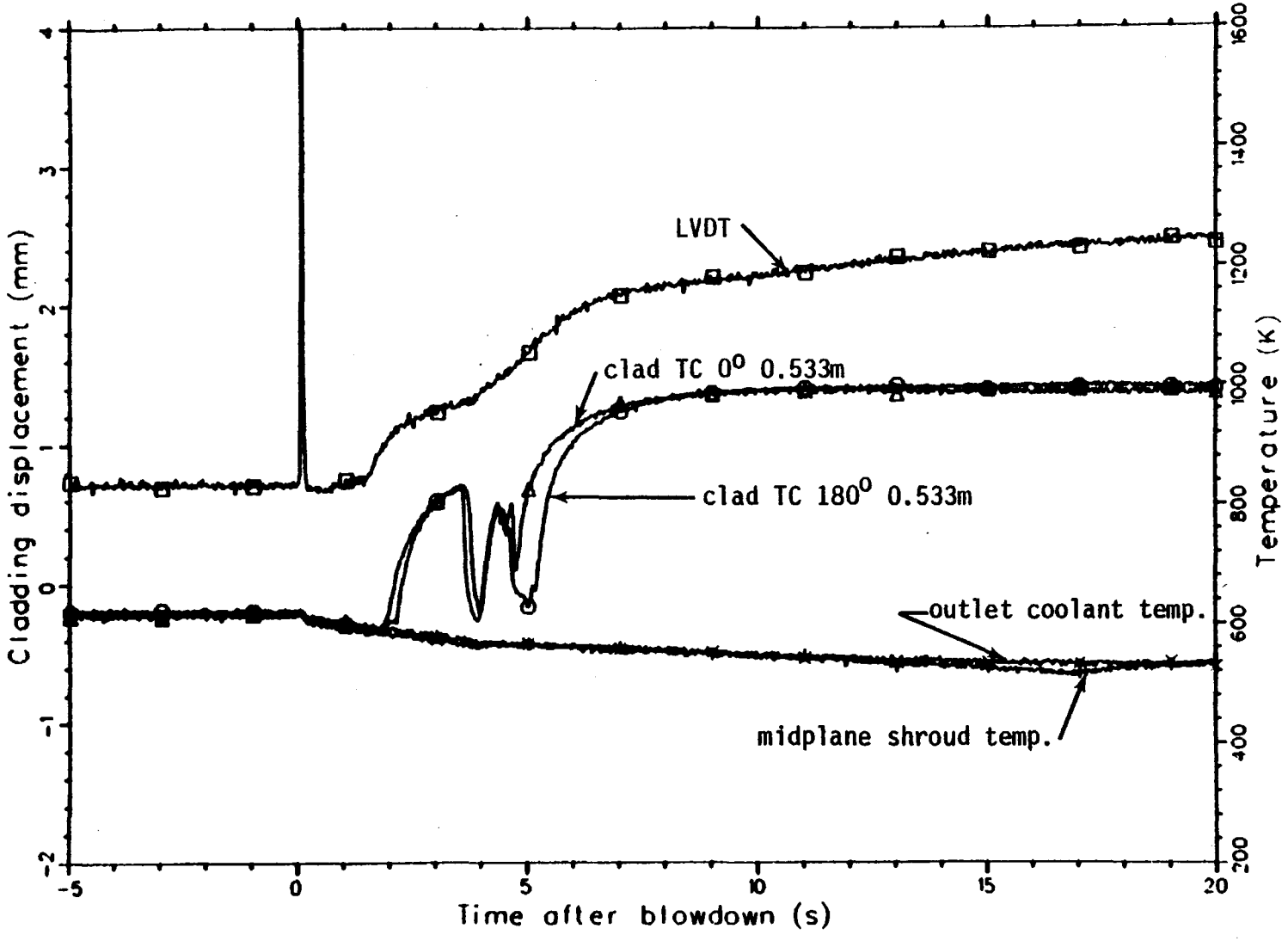

Fig. 17 Comparison of the thermal and mechanical response of fuel rod 3451. Test LLR-05.

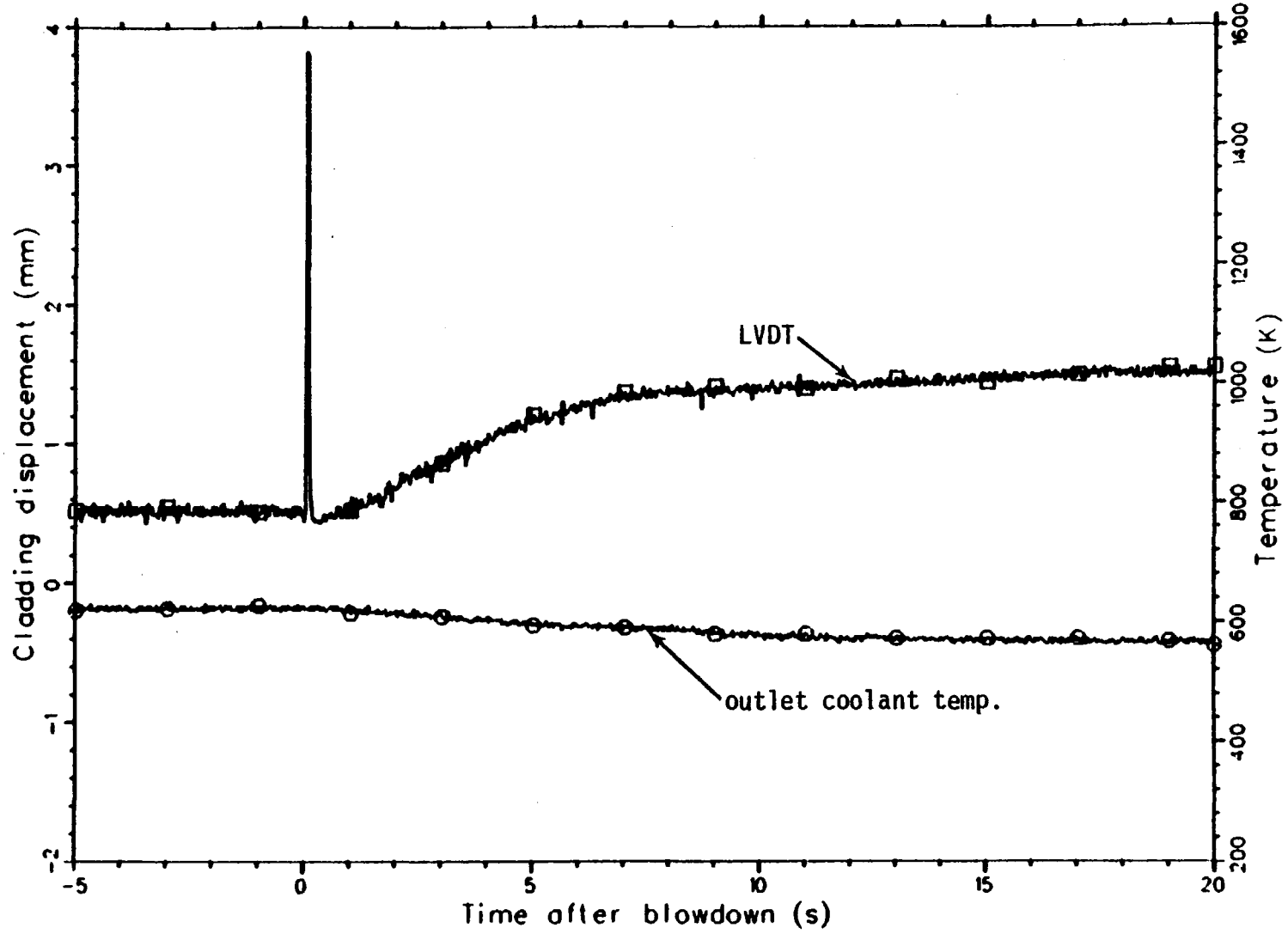

Fig. 18 The mechanical response of fuel rod 3452. Test LLR-05.

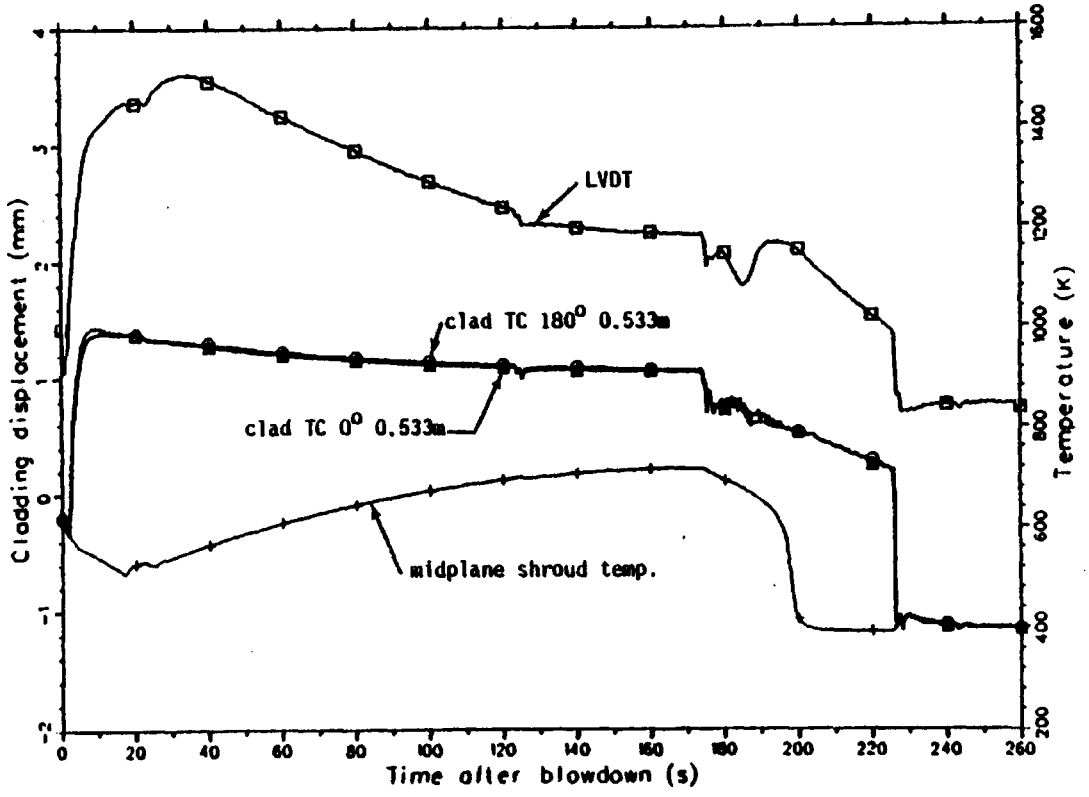

Fig. 19A Comparison of the thermal and mechanical response of fuel rod 3121. Test LLR-05.

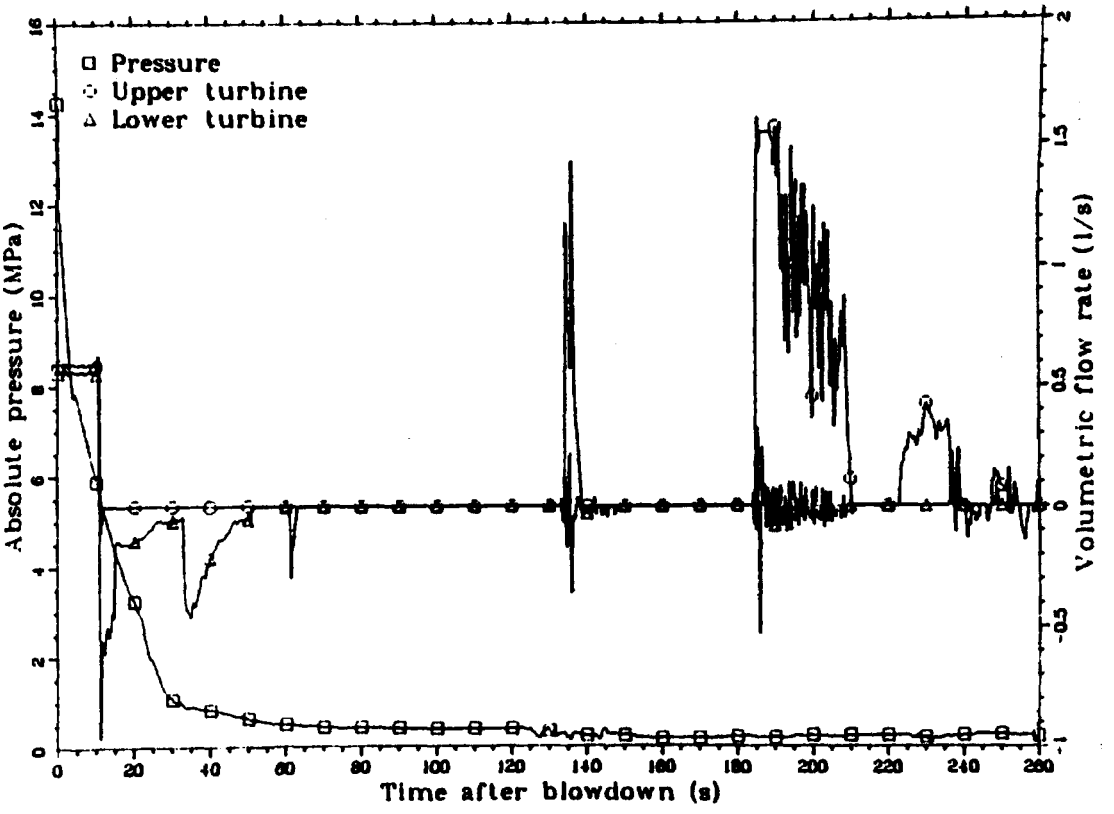

Fig. 19B An overlay showing the system pressure and the upper and lower volumetric flow rates for rod 3121. Test LLR-05.

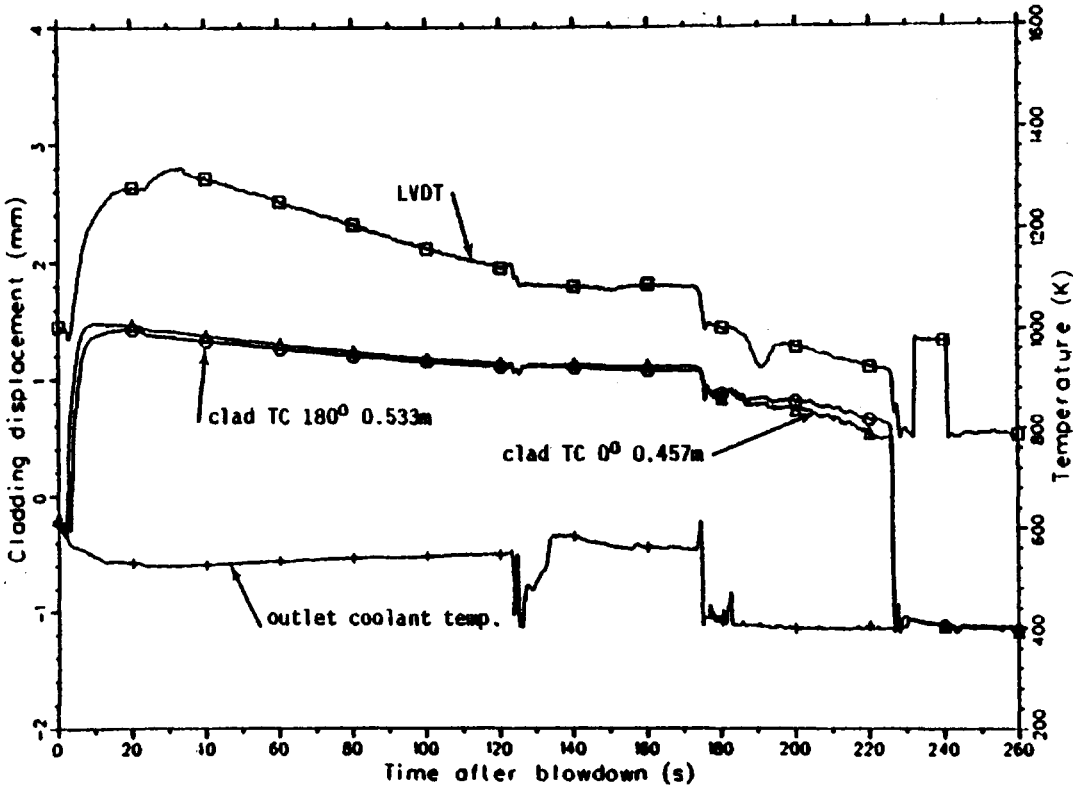

Fig. 20A Comparison of the thermal and mechanical response of fuel rod 3122. Test LLR-05.

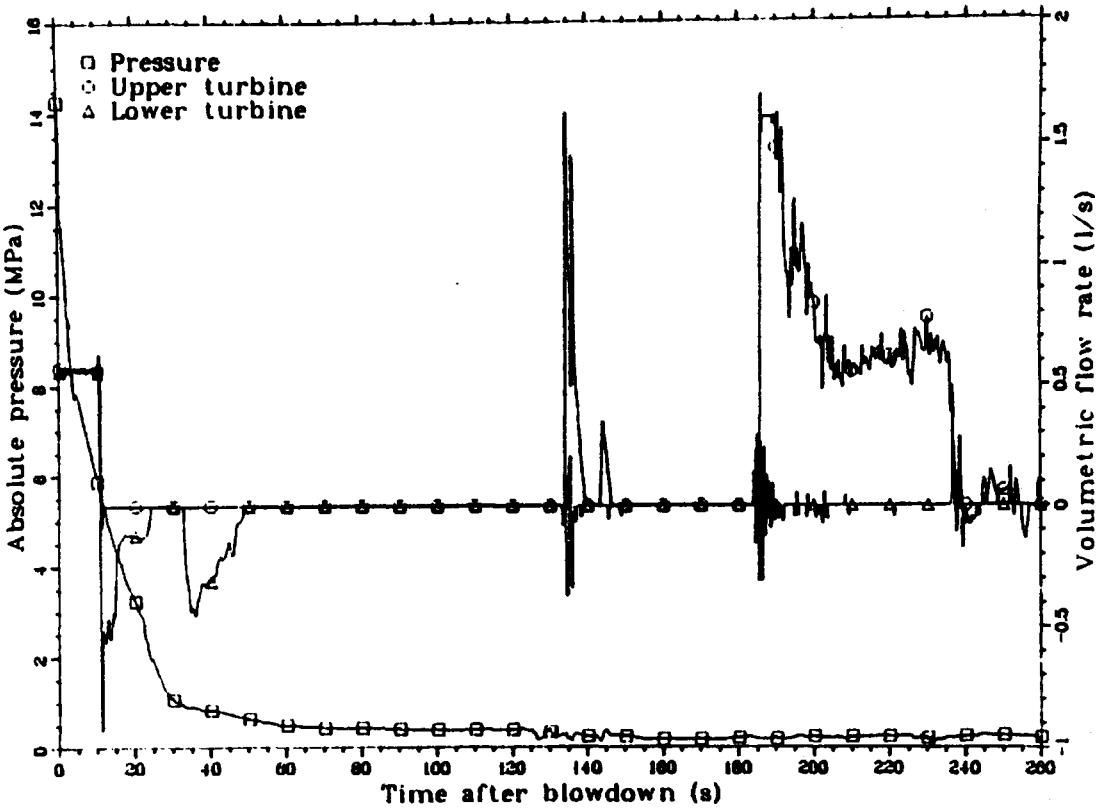

Fig. 20B An overlay showing the system pressure and the upper and lower volumetric flow rates for rod 3122. Test LLR-05.

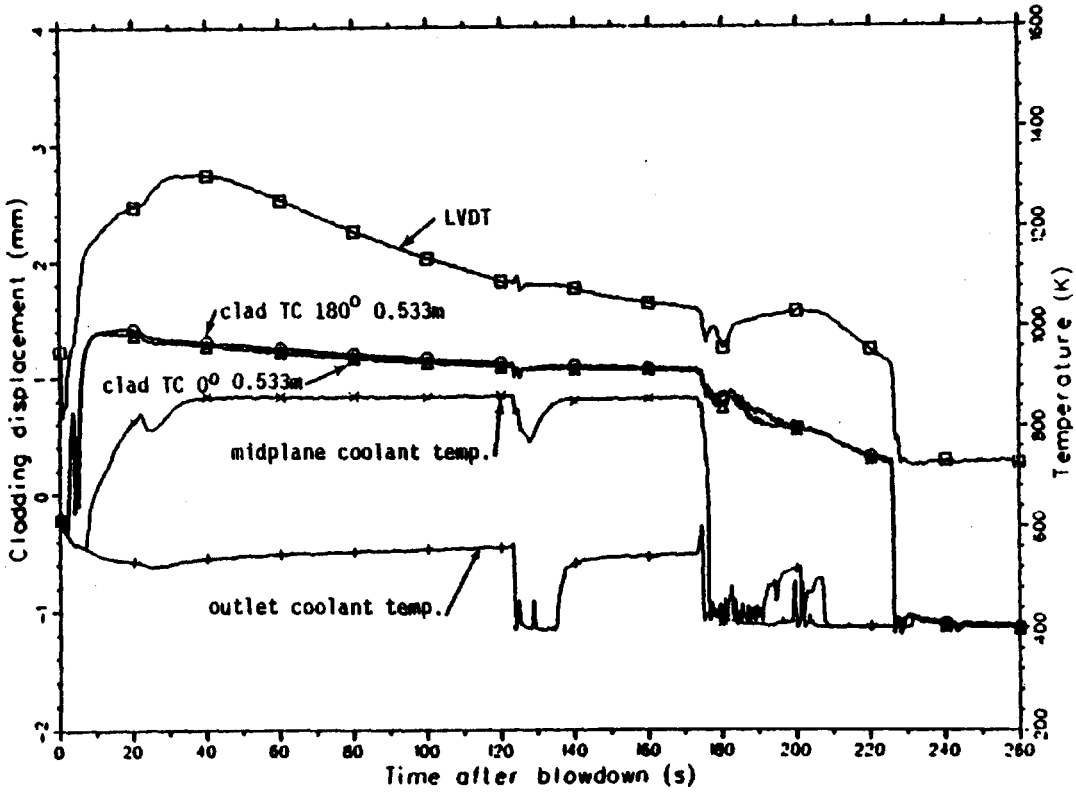

Fig. 21A Comparison of the thermal and mechanical response of fuel rod 3451. Test LLR-05.

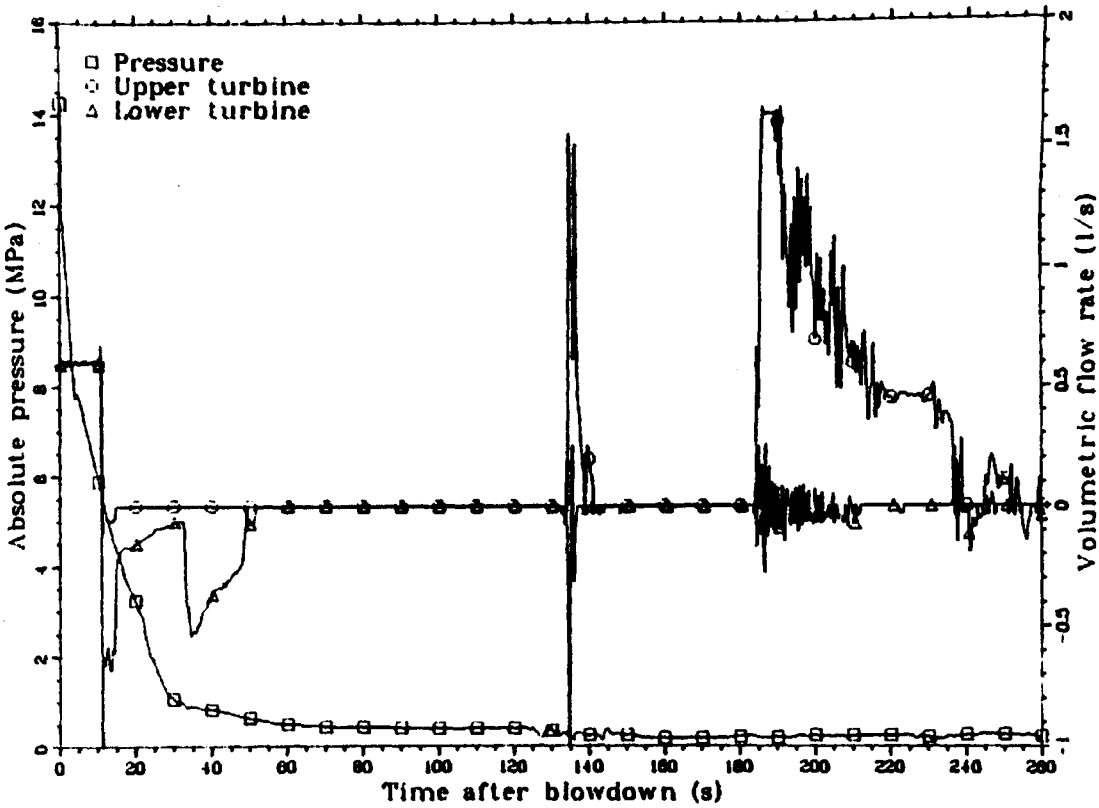

Fig. 21B An overlay showing the system pressure and the upper and lower volumetric flow rates for rod 3451. Test LLR-05.

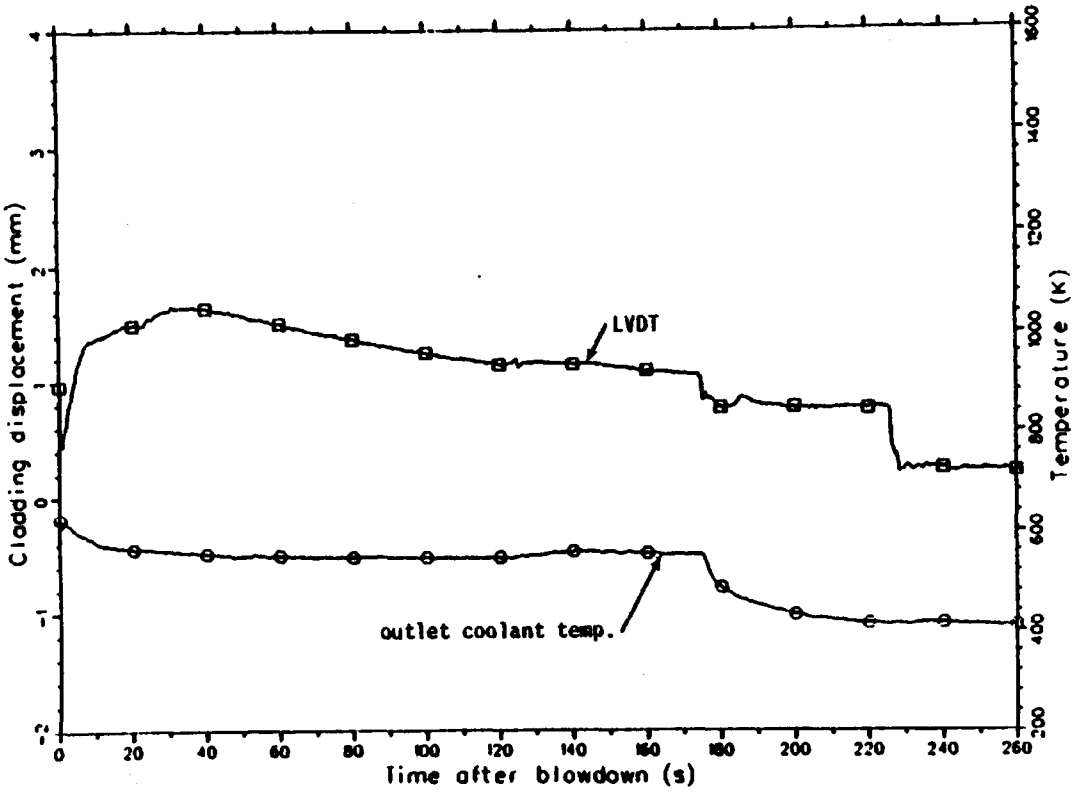

Fig. 22A The mechanical response of rod 3452. Test LLR-05.

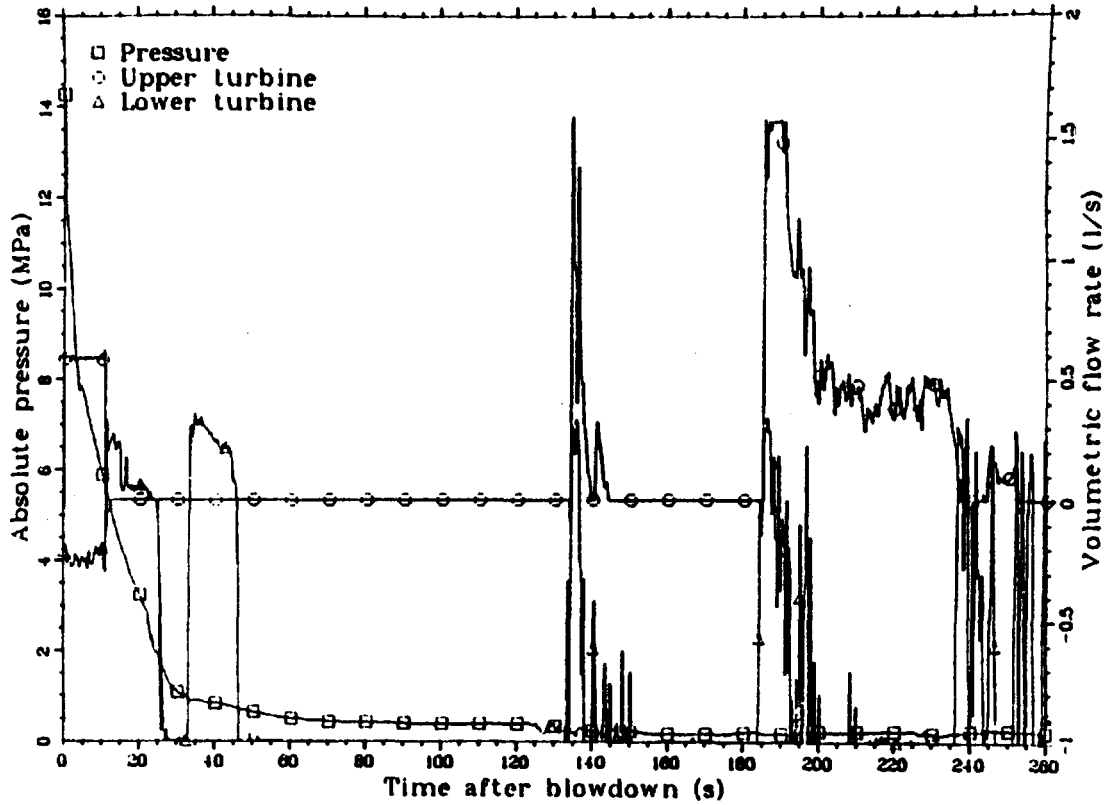

Fig. 22B. An overlay showing the system pressure and the upper and lower volumetric flow rates for rod 3452. Test LLR-05.

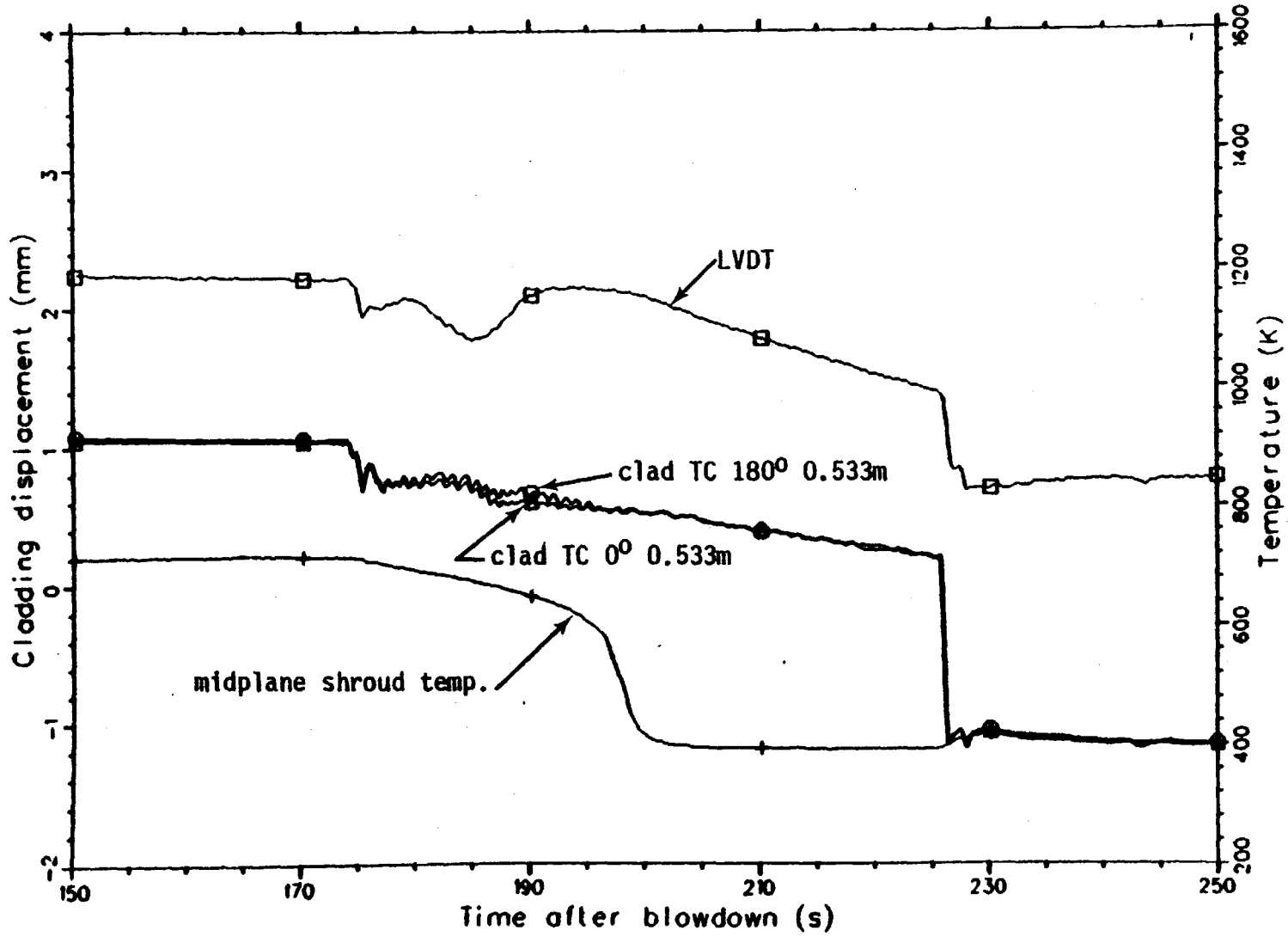

Fig. 23 Comparison of the thermal and mechanical response of fuel rod 3121. Test LLR-05.

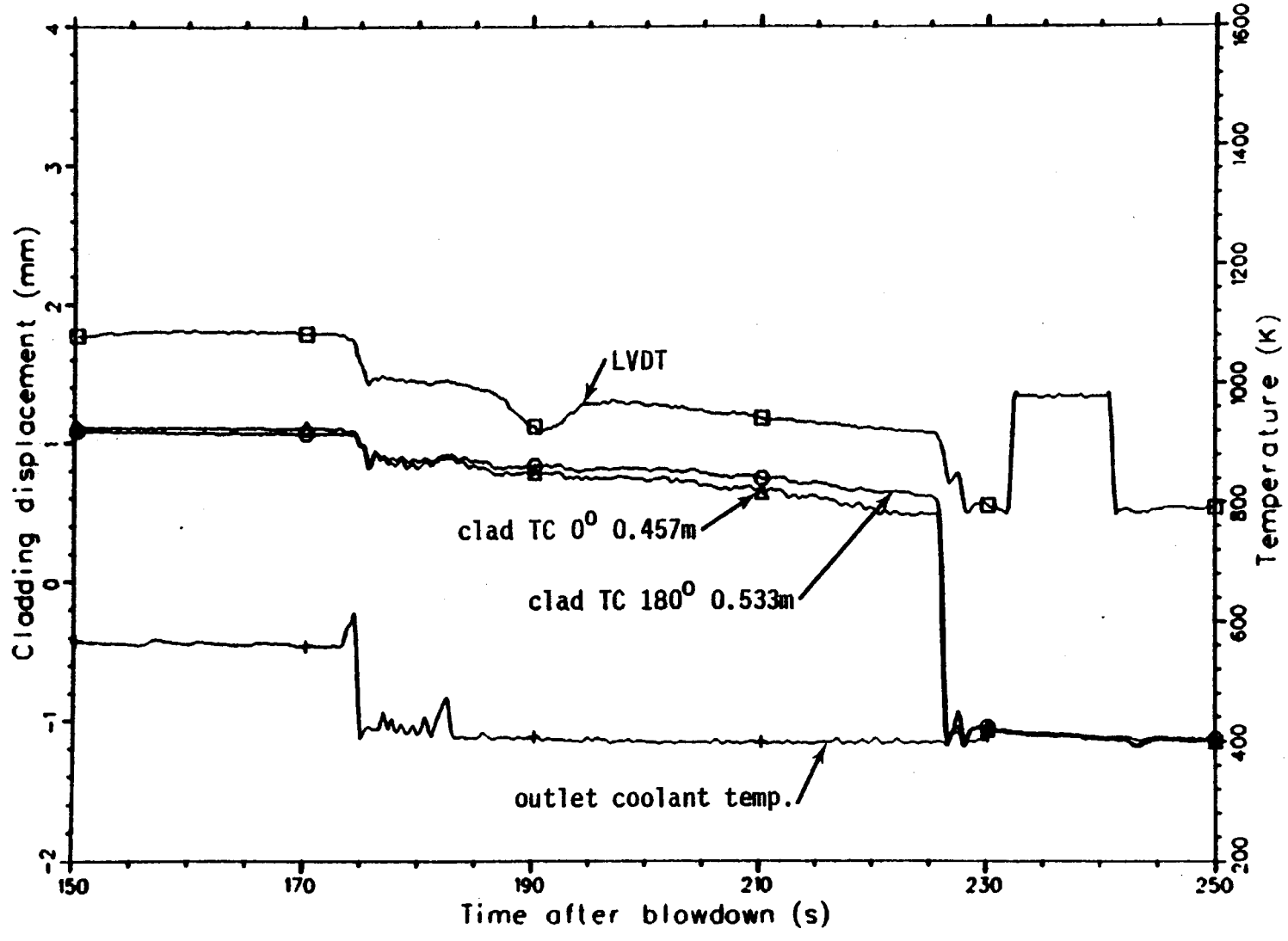

Fig. 24 Comparison of the thermal and mechanical response of fuel rod 3122. Test LLR-05.

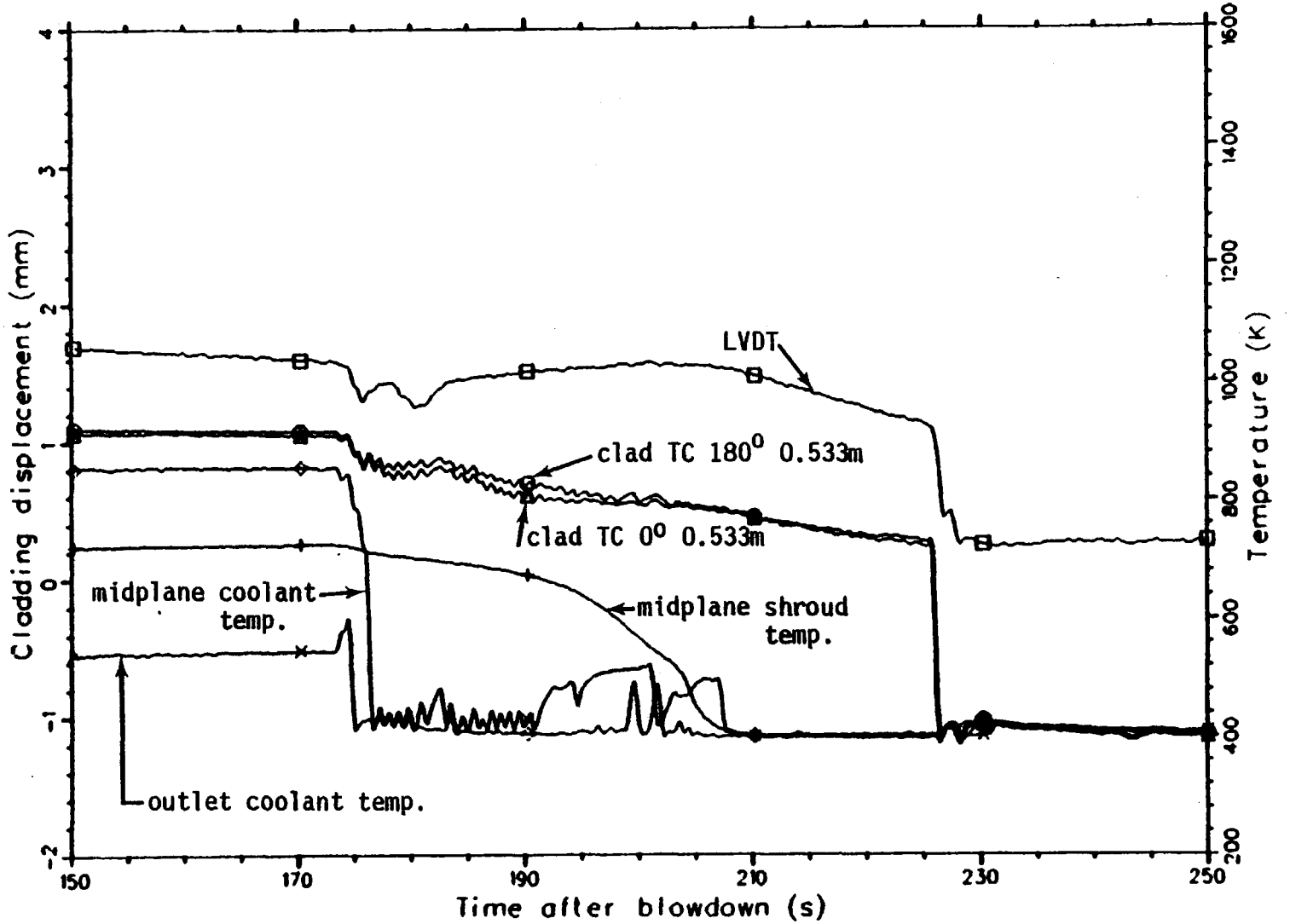

Fig. 25 Comparison of the thermal and mechanical response of fuel rod 3451. Test LLR-05.

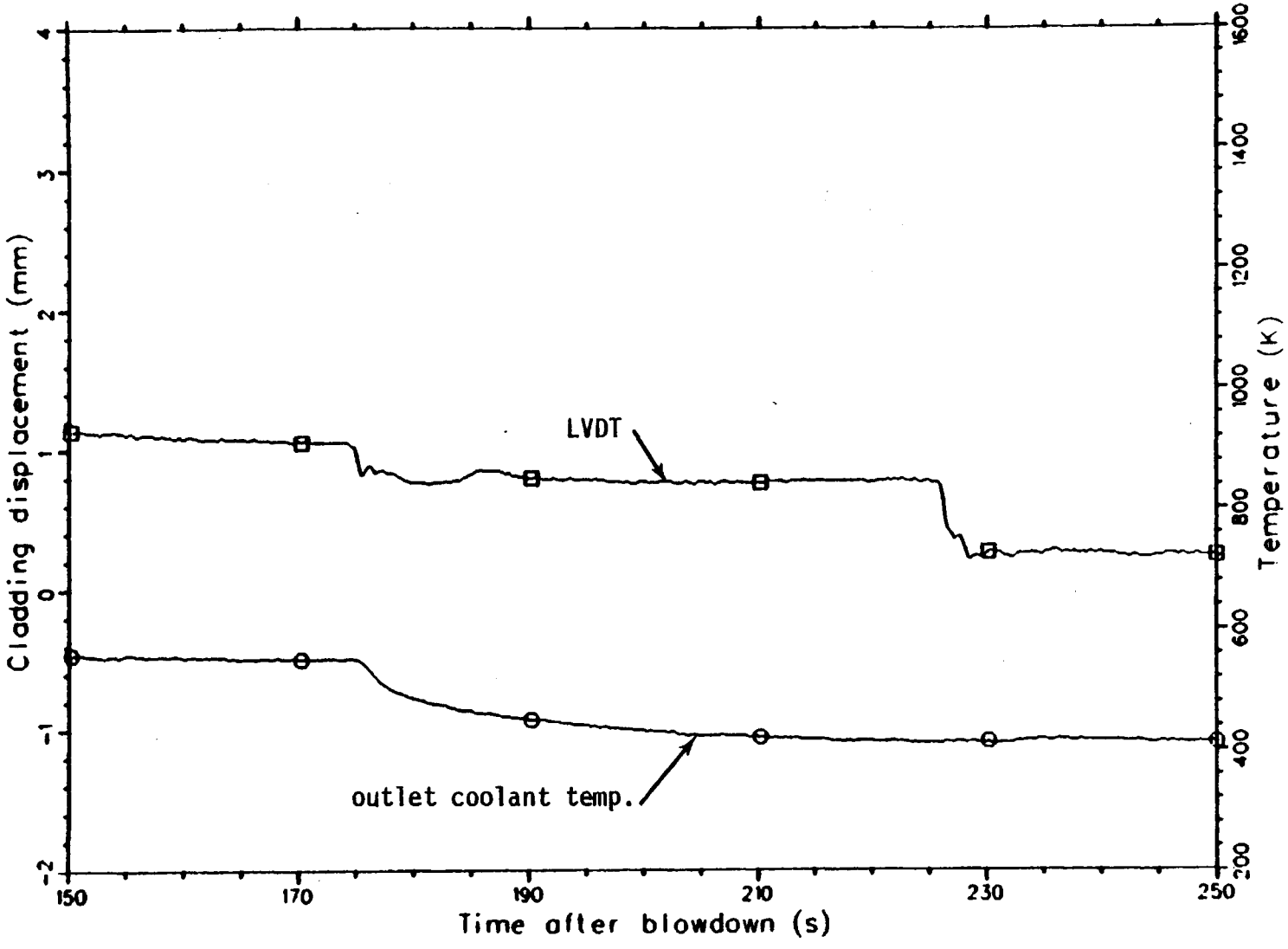

Fig. 26 The mechanical response of rod 3452. Test LLR-05.

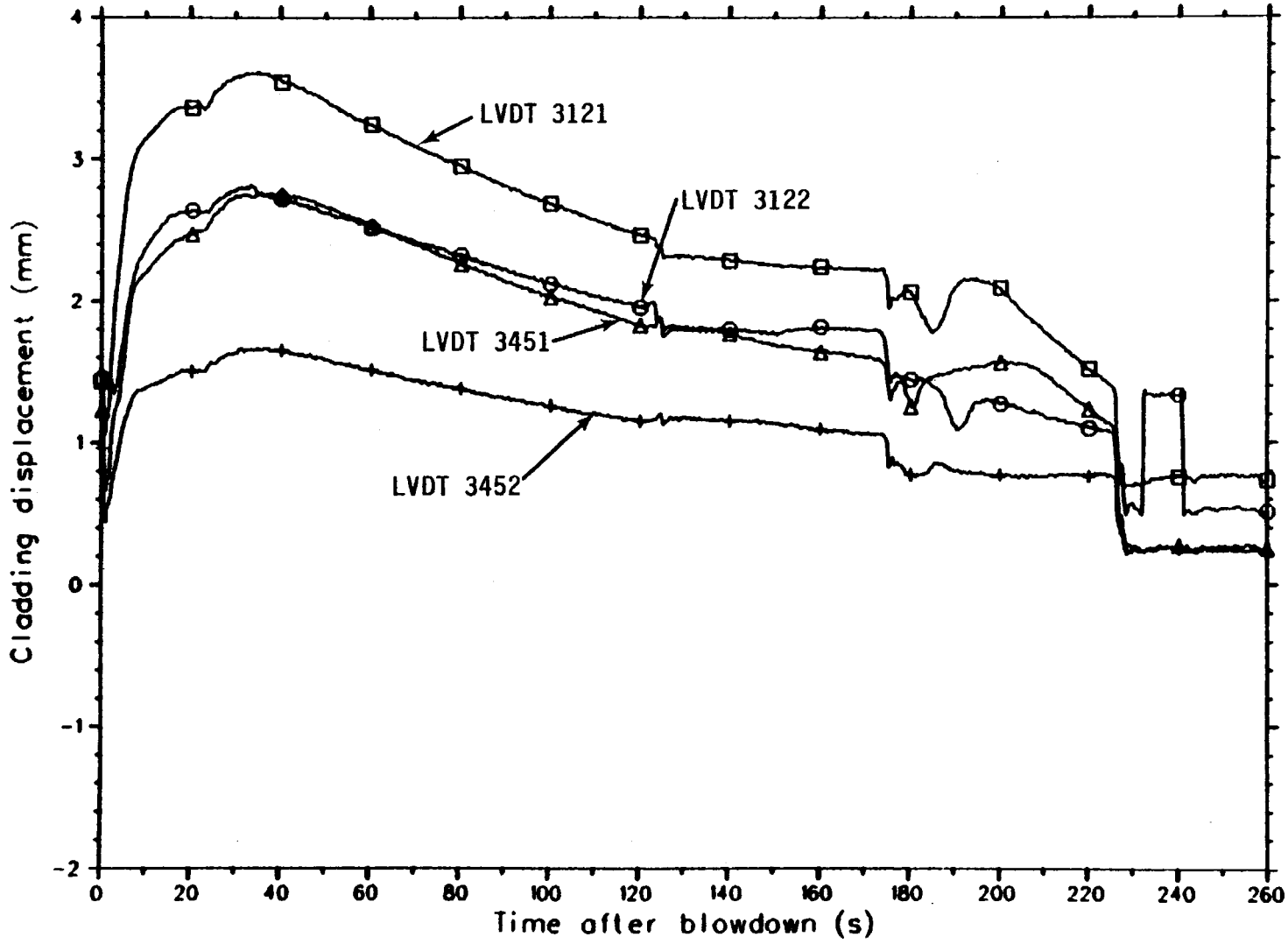

Fig. 27 An overlay showing the mechanical response of rods 3121, 3122, 3451, and 3452. Test LLR-05.

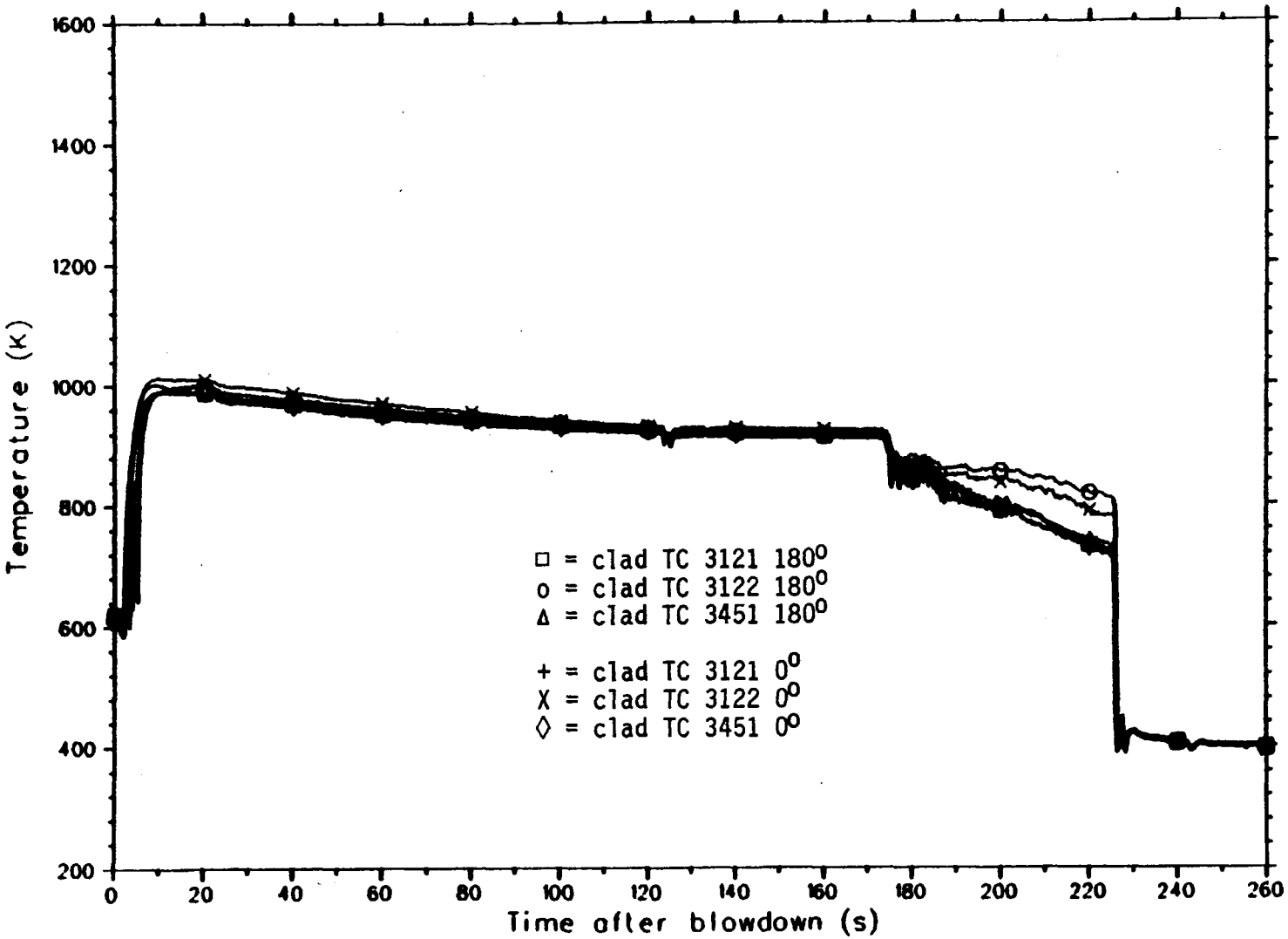

Fig. 28 An overlay showing the thermal response of rods 3121, 3122, 3451, and 3452, as determined by all thermocouples located on these rods. Test LLR-05.

(3) The LVDT turnaround times (prior to rod quench) are in close agreement with the TC turnaround times.

(4) Rods with and without surface cladding TCs have similar LVDT responses.

(5) An atypical response of the TC located at 180^{o} and 0.533 m on rod 3122 (between 2 and 5 seconds) occurred for tests LLR-05 and LLR-03.

(6) An early TC quench (between about 3 and 5 seconds) occurred for both TCs located on rod 3451. Check valve problems for this rod may have caused additional fluid to enter the flow shroud and quench the TCs. (This same type of event occurred during LLR-04 and again check valve problems seem to be responsible.)

4.3 Comparison of the LVDT and TC Responses for LLR-04

The third test in the LOFT Lead Rod test series was LLR-04. The test rod configuration for this experiment was the same as LLR-05 and is shown in Figure 1B. The test procedure for LLR-04 went as planned until at about 15 seconds into the blowdown when transient inadvertent isolation valve cycling occurred several times and caused multiple rod rewets. Since the primary test objective was to evaluate the mechanical deformation characteristics of the clad, the accidental valve cycling from 15 seconds onward resulted in cladding quenches which prevented any subsequent cladding deformation. The test data between 15 and 35 seconds is still useful, however, for providing data concerning cladding rewet conditions similar to the rapid rewet events that occurred during the LOFT tests.

Figures 29, 30, 31, and 32 overlay the response of the cladding thermocouples, coolant thermocouple data, LVDT data, and the midplane shroud temperatures for the LLR-04 fuel rods during the first 10 seconds following blowdown. The time to DNB is estimated from these figures and collected in Table 7. Figures 33A, 34A, 35A, and 36A present the overall history of the cladding thermocouples, cladding elongation, outlet coolant temperature, midplane coolant temperature, and the midplane shroud temperature for each of the LLR-04 rods from -2 to 28 seconds. Corresponding to these figures, Figures 33B, 34B, 35B, and 36B show the system pressure and volumetric flowrate data for each test rod in LLR-04. Finally, Figures 37, 38, 39, and 40 show magnified views of the cladding thermocouple and LVDT data at DNB and rod rewet events. From Figures 39 and 40 estimates of rod quench times are computed and listed in Table 8.

To begin, consider the time to DNB data presented in Table 7. The data in this table are consistent with the previous test results and satisfy equation (1). That is, the time to DNB as indicated by the LVDT instrumentation is earlier than that calculated from the cladding thermocouple data. Because of the small magnitude in the response of the LVDT for rod 3452 it is difficult to say for certain exactly when this particular rod experienced DNB. If the value reported in Table 7 is correct, then the response of rod 3452, without surface clad thermocouples, is essentially the same as that of the other rods with TCs and hence all rods first experienced DNB at about the same time, as indicated by the LVDT data. In addition, the consistency in the time to DNB data, as determined by the thermocouples, also supports the hypothesis that all rods experienced film boiling at about the same time above the core midplane.

Before leaving the "10 second data" there is one more event that deserves particular attention. Consider Figure 31, notice the TC rewet event that occurred between 2.5 and 4 seconds. This is the same rod which experienced a similar type of TC rewet in Test LLR-05. As in LLR-05 it is believed that a malfunctioning check valve above

TABLE 7

LLR-04

ESTIMATED TIME OF INITIAL DNB

	Rod Number			
Instrument	3121	3122	3451	3452**
LVDT	0.25	Failed	0.25	0.25
TC 180° 0.533 m	1.7	2.0	1.7*	
TC 0° 0.533 m	1.7		1.7*	
TC 0° 0.457 m		1.6		

The above numbers indicate the approximate time (in seconds) during blowdown that the rod temperature significantly deviates from the saturation temperature, indicating DNB, as determined from the given instrumentation. Interpretation of the data, especially the LVDT data, with regard to the initiation of DNB is somewhat subjective and might be open to alternative evaluations.

Numbers reported in the above table have been suggested by PBF personnel[5].

* A secondary DNB occurs after the TC is momentarily quenched.

** Rod 3452 had no surface clad thermocouples.

TABLE 8

LLR-04

ESTIMATED ELONGATION TURNAROUND TIME AND ROD QUENCH TIME

	Rod Number			
Instrument	3121	3122	3451	3452*
LVDT	15.2	failed	15.1	15.2
TC 180° 0.533 m	15.2	15.2	15.2	
TC 0° 0.533 m	15.2		15.2	
TC 0° 0.457 m		15.2		

Multiple rewets occurred between 15 and 23 seconds. The data presented here summarizes the first rewet event. The LVDT turnaround time also corresponds to the LVDT quench time and the TC turnaround time also corresponds to the TC quench time. Consequently, the data in this table indicate rod quench time as determined by the given instrumentation.

* Rod 3452 had no surface clad thermocouples.

rod 3451 caused fluid to leak into the test flow channel and caused the premature TC quench. Compare Figures 31 and 17; notice that for each case the LVDT responds in a similar manner. In particular, the LVDT instrumentation notices a leveling off period which directly corresponds to the TC "flutter" phenomenon. Notice also from Figure 37 that the cladding temperature of rod 3451 levels off at about 1050 K while the other rods plateau near 1150 K. In fact, the centerline thermocouple for rod 3451 also shows a lower value than those of the other rods. All of these data suggest that rod 3451 experienced a partial rod rewet early into the blowdown and that the thermocouples and the LVDT responded in a consistent manner to the increased cooling experienced by this rod.

Now consider Figures 39 and 40. From these overlay graphs it is clear that all of the cladding thermocouples responded in tantum with the LVDTs. This is also evident in the data presented in Table 8. Since rod 3452, without cladding thermocouples, showed rewet and dryout times that exactly corresponded in the same way as rods with cladding thermocouples (note Figure 40), then it must be concluded that for the thermal-hydraulic conditions existing during the rapid rod quenching events for LLR-04 (15 to 28 seconds), no significant time dependent TC perturbation effects were evident.

A careful inspection of Figures 33A through 36A shows that although the LVDT time to quench data are consistent with the TC data, the response magnitudes do not agree. That is, as illustrated in Figure 33A, the TC response from 15 to 16 seconds shows a sharp drop from a plateau temperature of slightly over $1100^{o}K$ down to a saturation temperature of approximately $550^{o}K$ (representing a 100% drop), immediately followed by another DNB. In contrast, the LVDT data show only a 40% drop from its full scale value. At present the meaning of these responses is not completely clear . For instance,

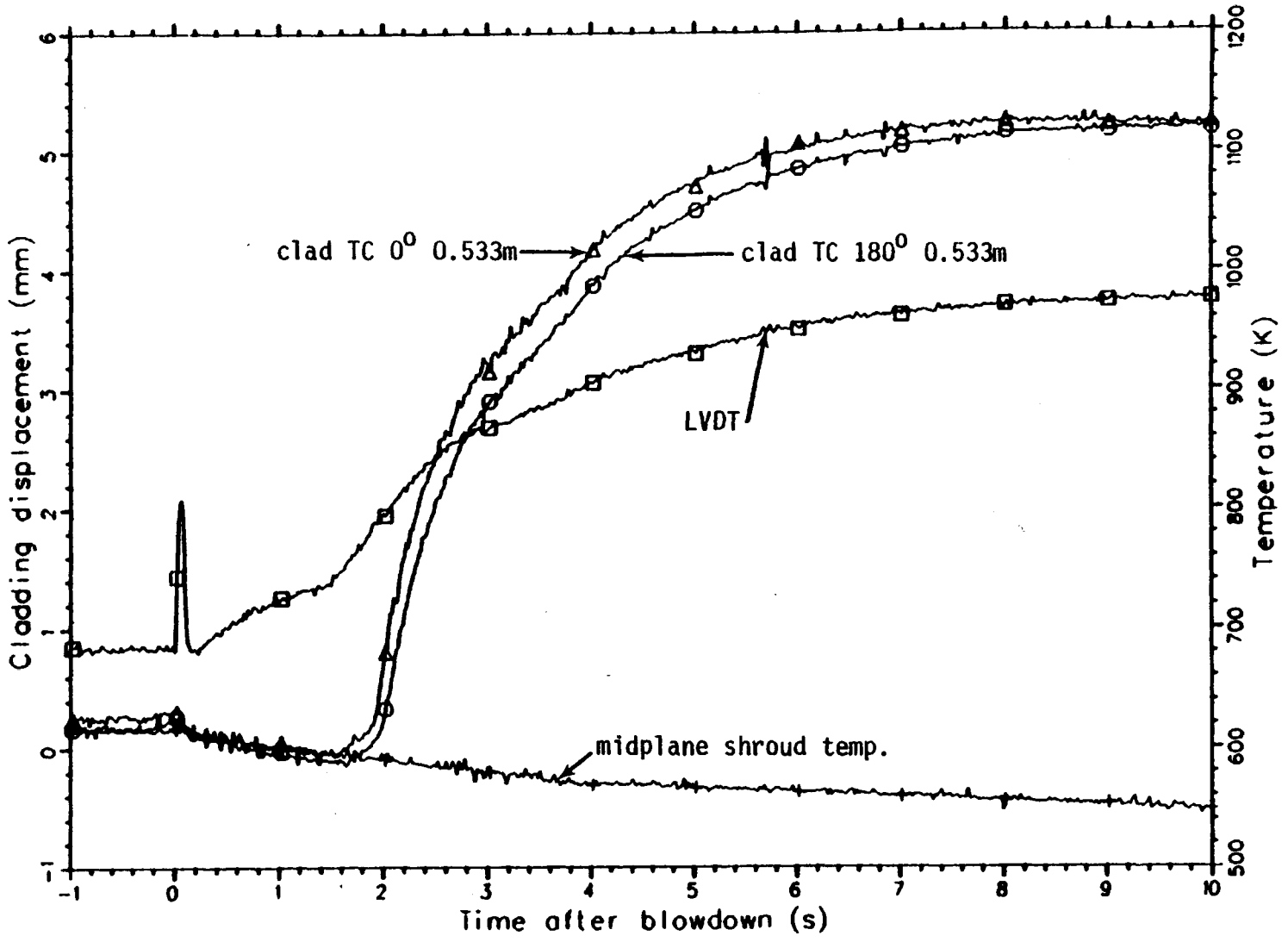

Fig. 29 Comparison of the thermal and mechanical response of fuel rod 3121. Test LLR-04.

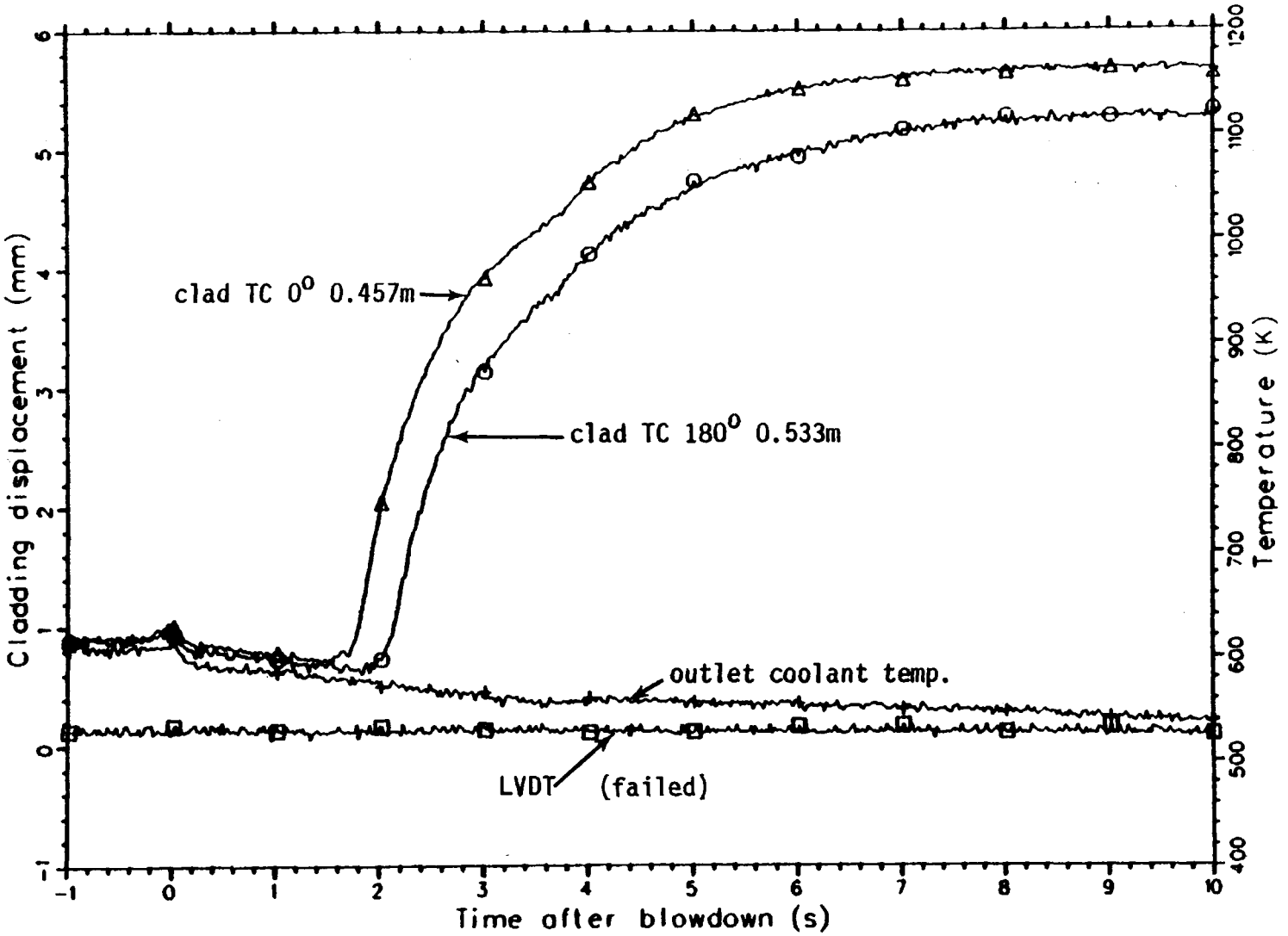

Fig. 30 Comparison of the thermal and mechanical response of fuel rod 3122. Test LLR-04.

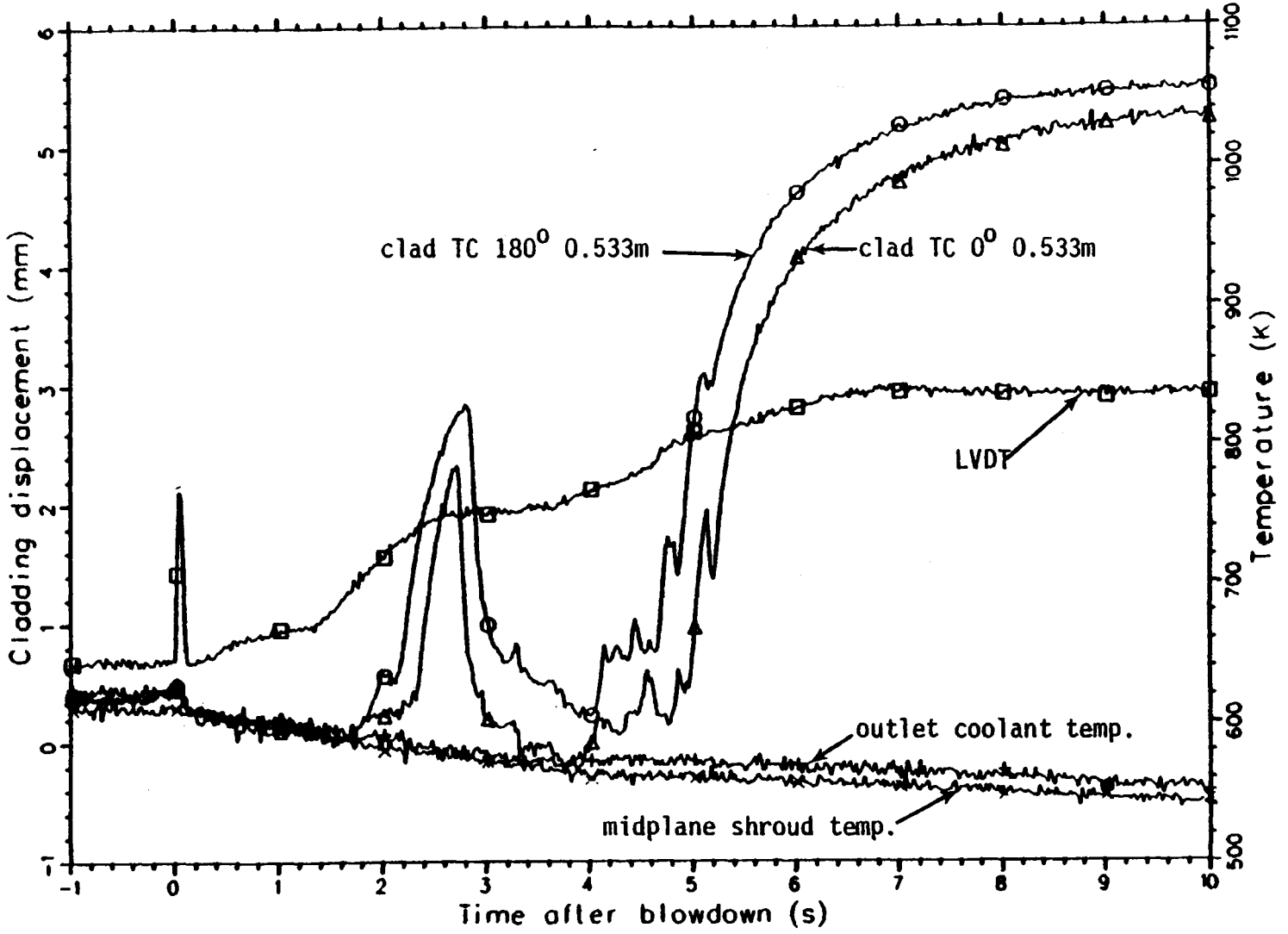

Fig. 31 Comparison of the thermal and mechanical response of fuel rod 3451. Test LLR-04.

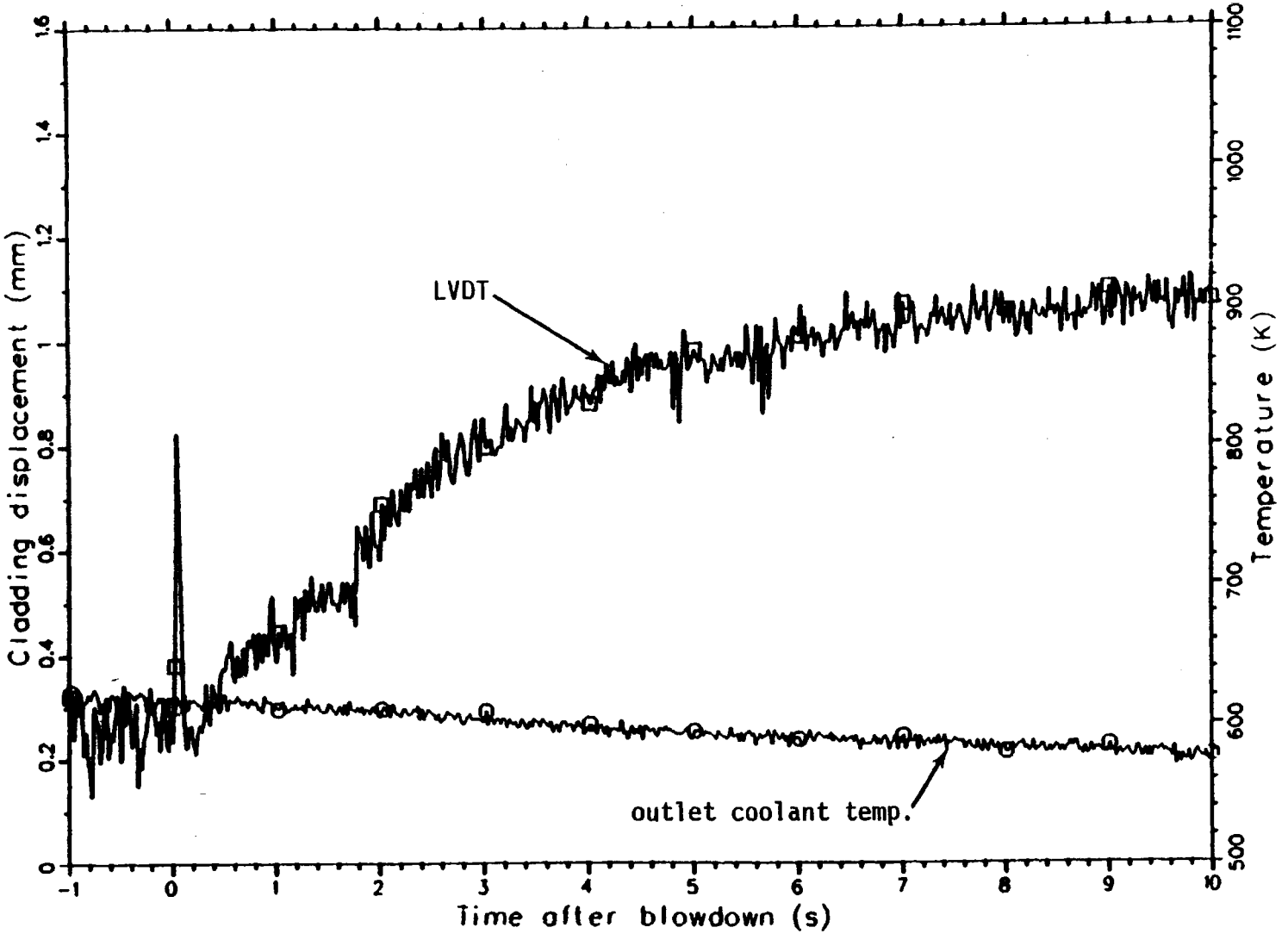

Fig. 32 The mechanical response of rod 3452. Test LLR-04.

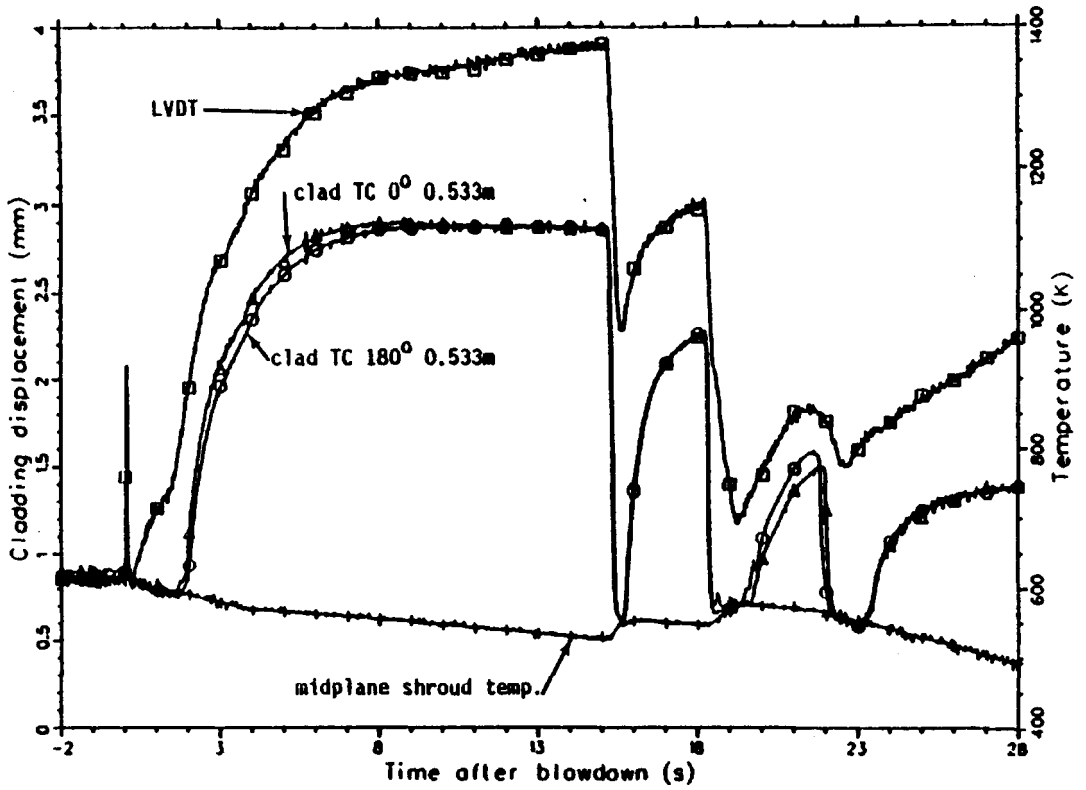

Fig. 33A Comparison of the thermal and mechanical response of fuel rod 3121. Test LLR-04.

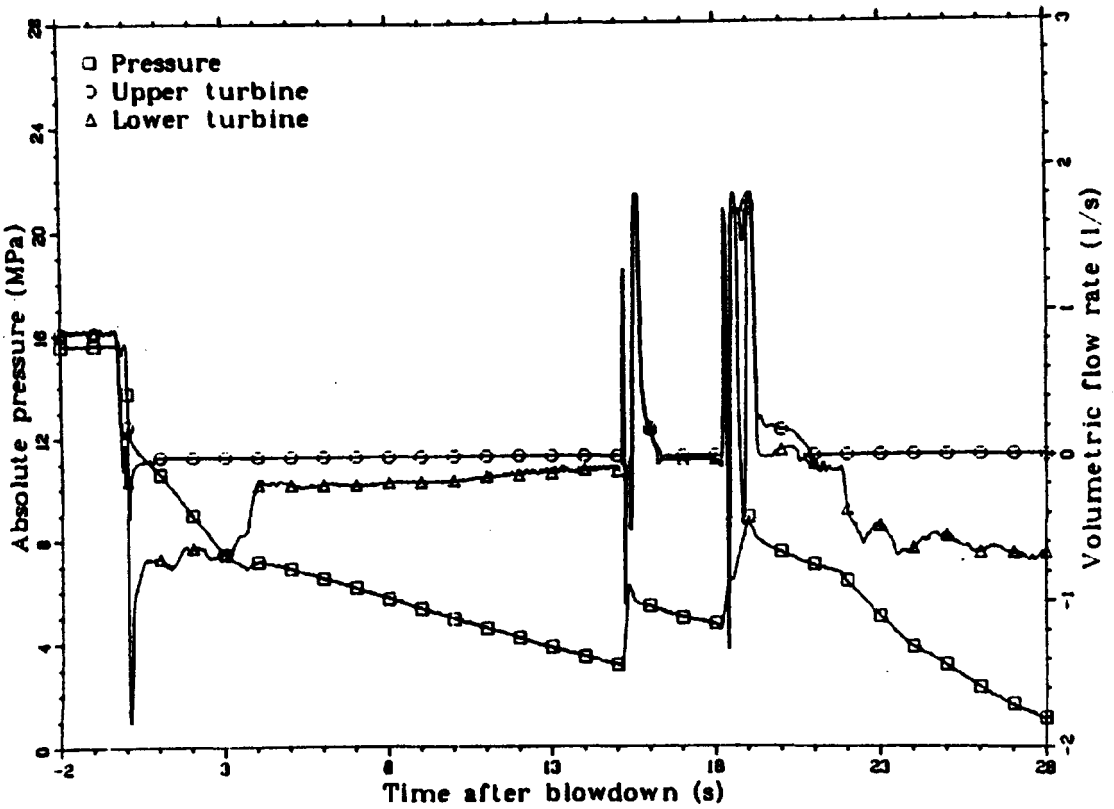

Fig. 33B An overlay showing the system pressure and the upper and lower volumetric flow rates for rod 3121. Test LLR-04.

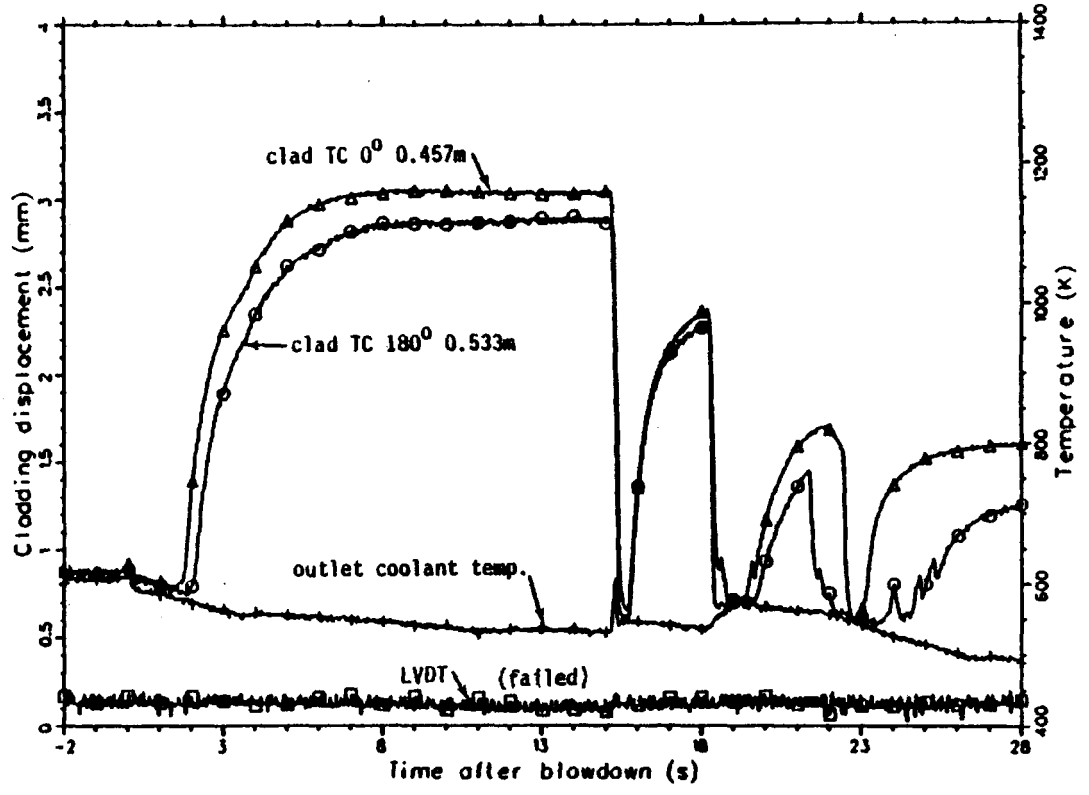

Fig. 34A Comparison of the thermal and mechanical response of fuel rod 3122. Test LLR-04.

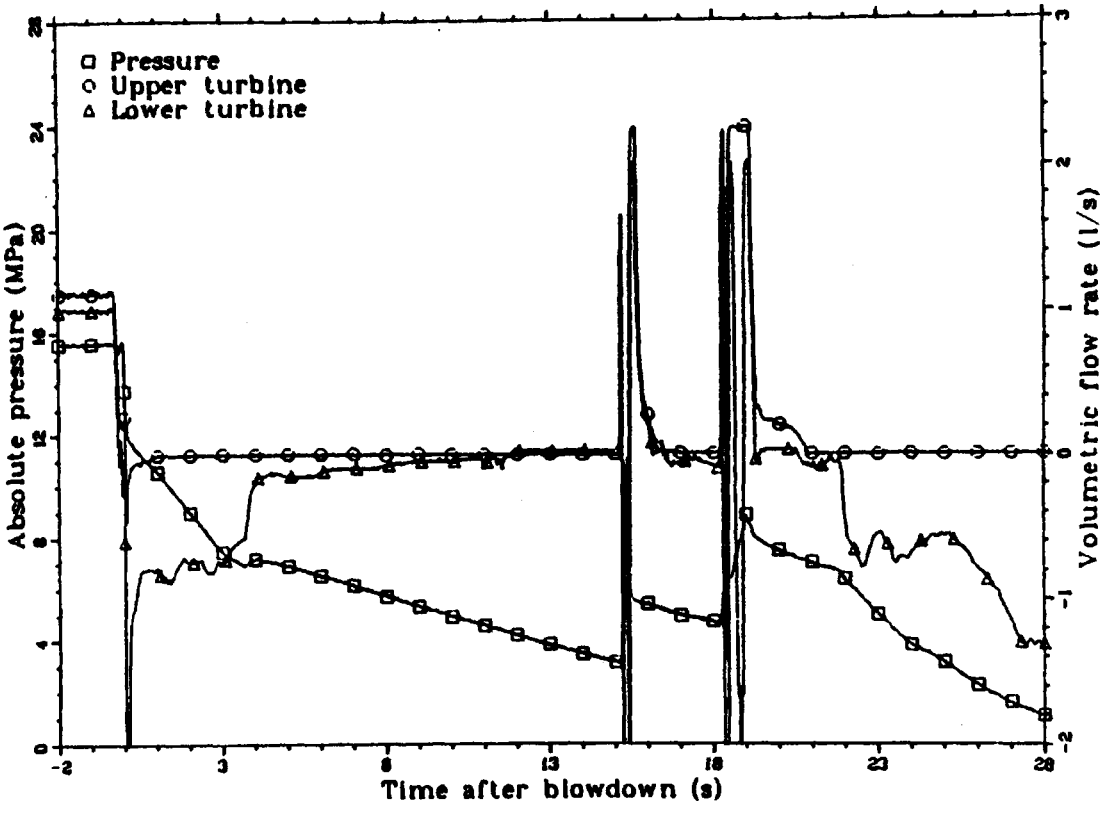

Fig. 34B An overlay showing the system pressure and the upper and lower volumetric flow rates for rod 3122. Test LLR-04.

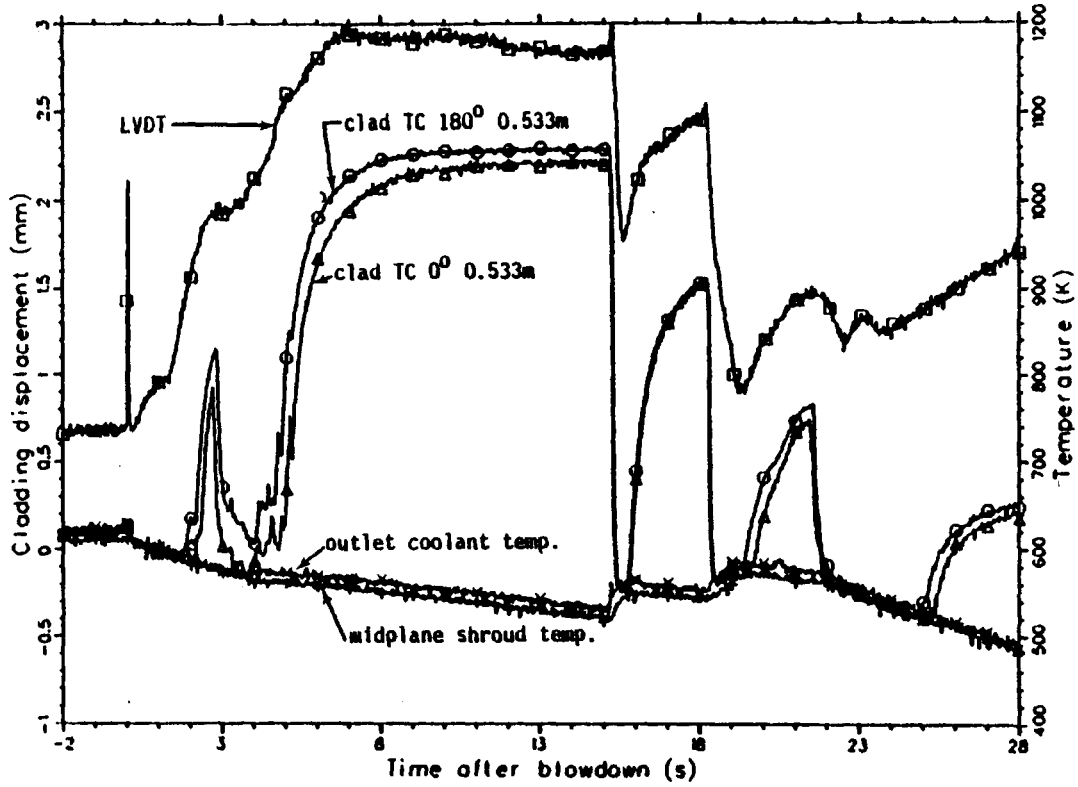

Fig. 35A Comparison of the thermal and mechanical response of fuel rod 3451. Test LLR-04.

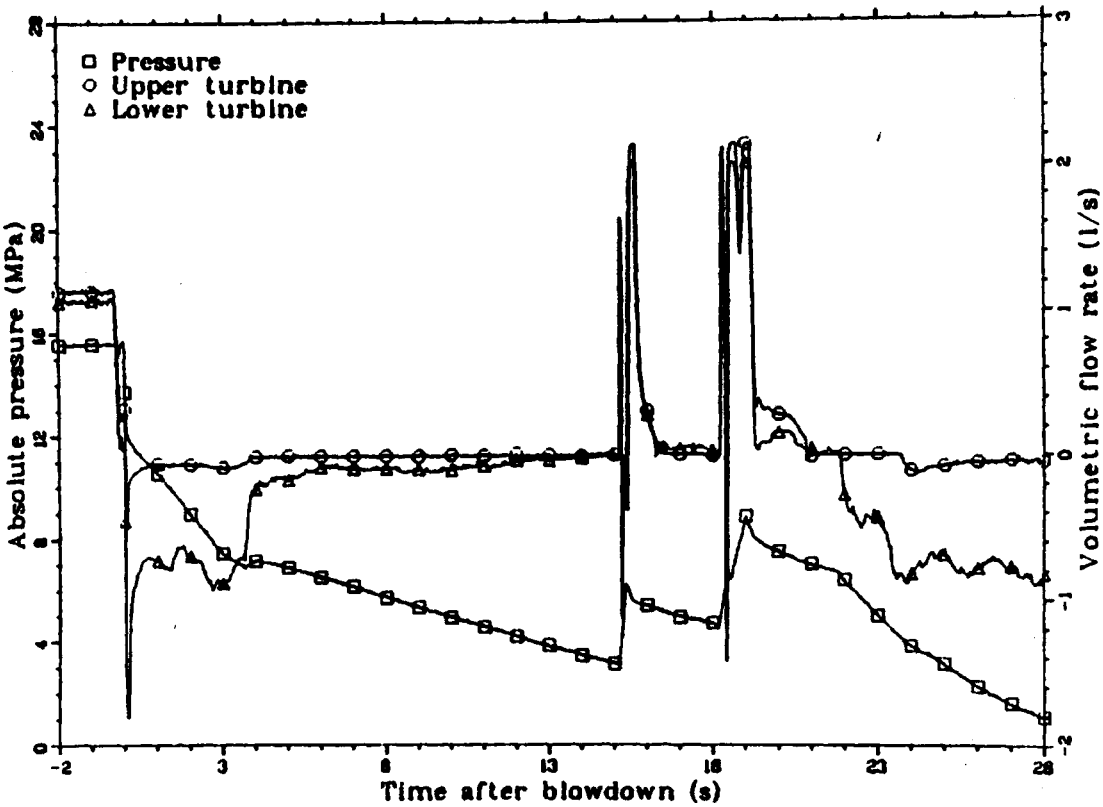

Fig. 35B An overlay showing the system pressure and the upper and lower volumetric flow rates for rod 3451. LLR-04.

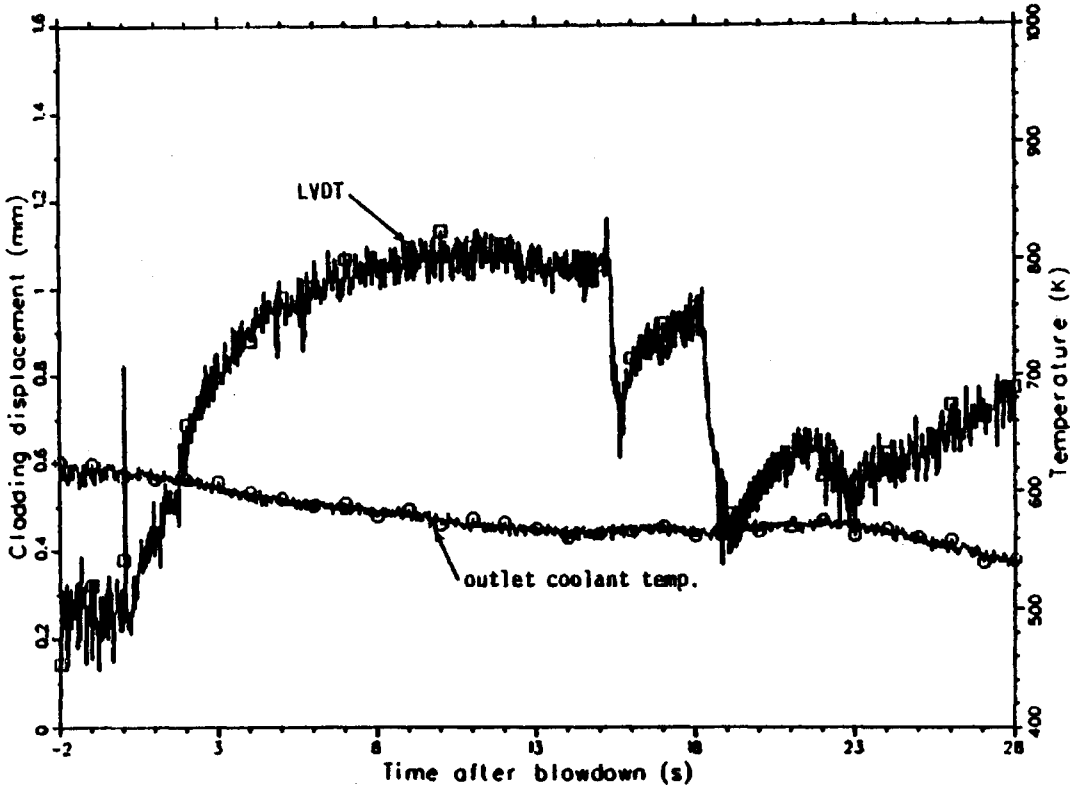

Fig. 36A The mechanical response of rod 3452. Test LLR-04.

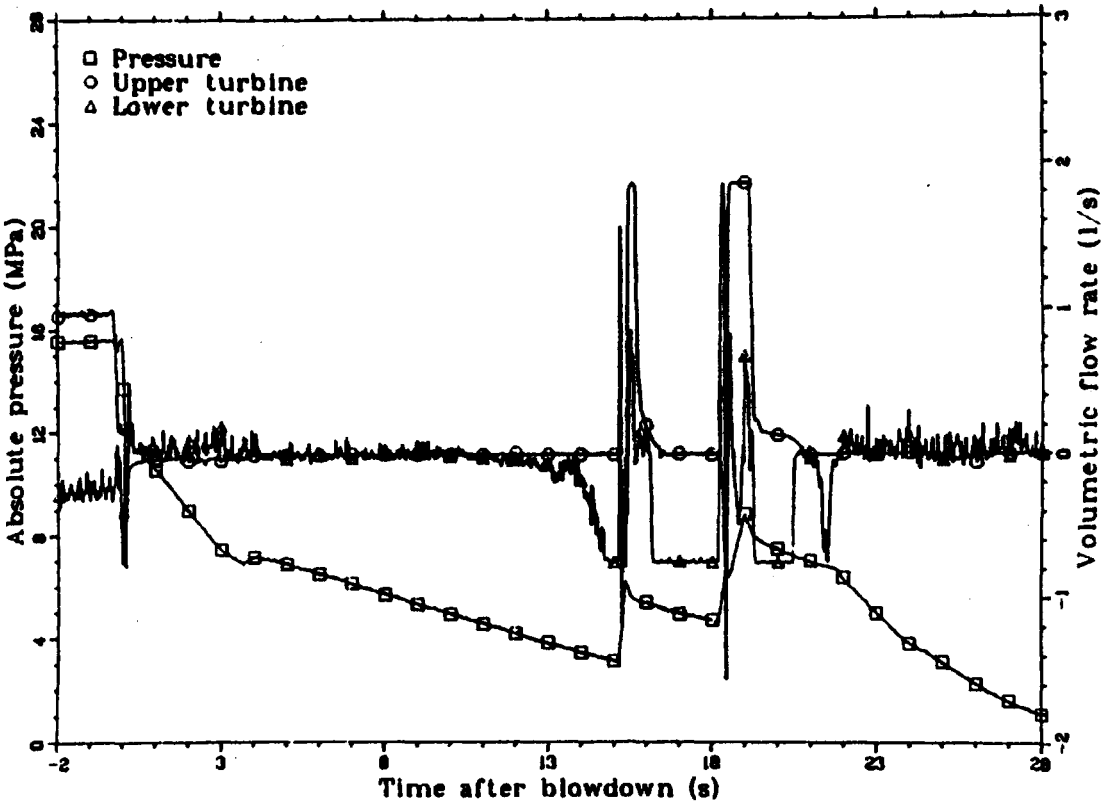

Fig. 36B An overlay showing the system pressure and the upper and lower volumetric flow rates for rod 3452. Test LLR-04.

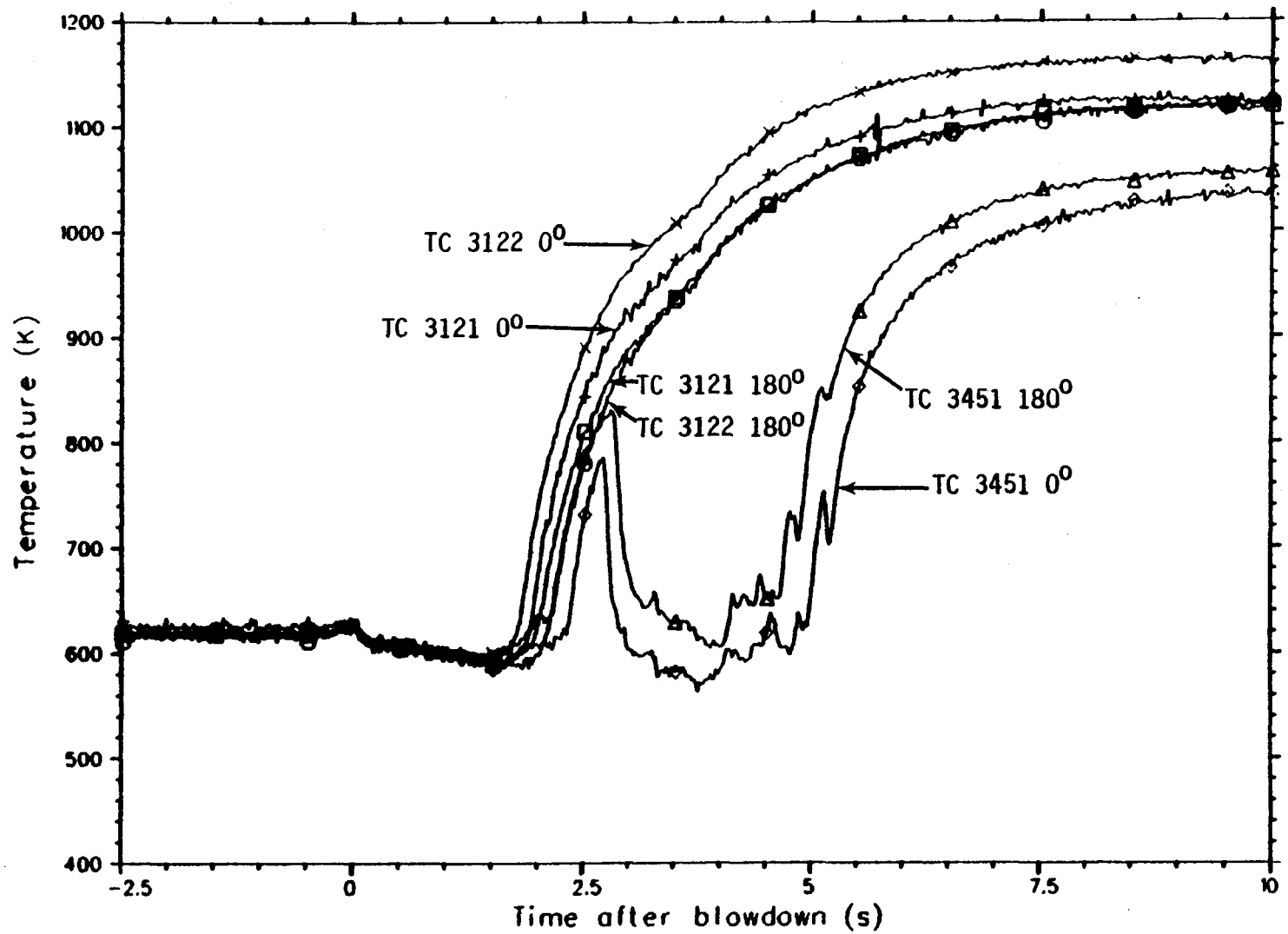

Fig. 37 An overlay showing the thermal response of rods 3121, 3122, and 3451. Test LLR-04.

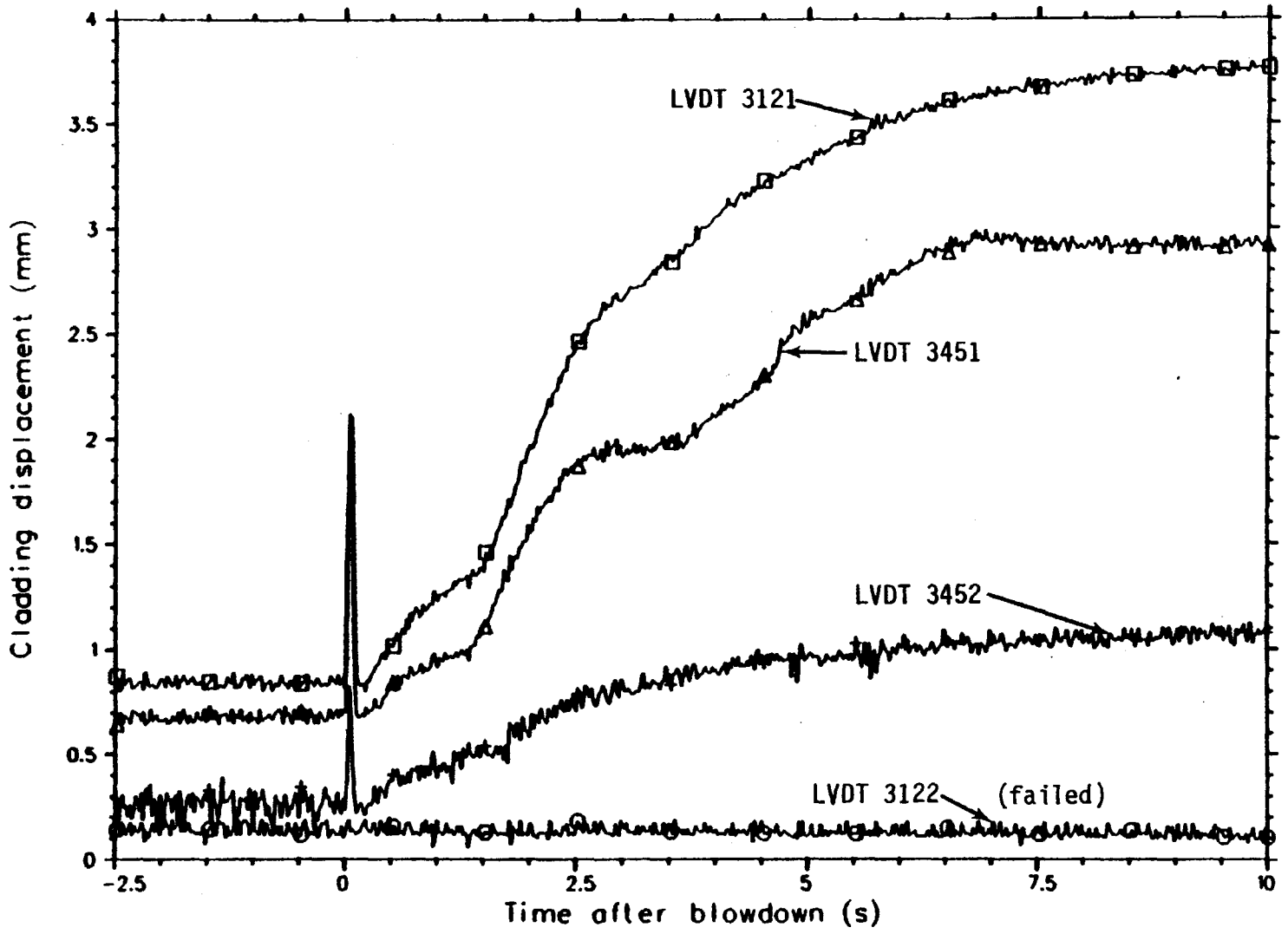

Fig. 38 An overlay showing the mechanical response of rods 3121, 3122, 3451, and 3452. Test LLR-04.

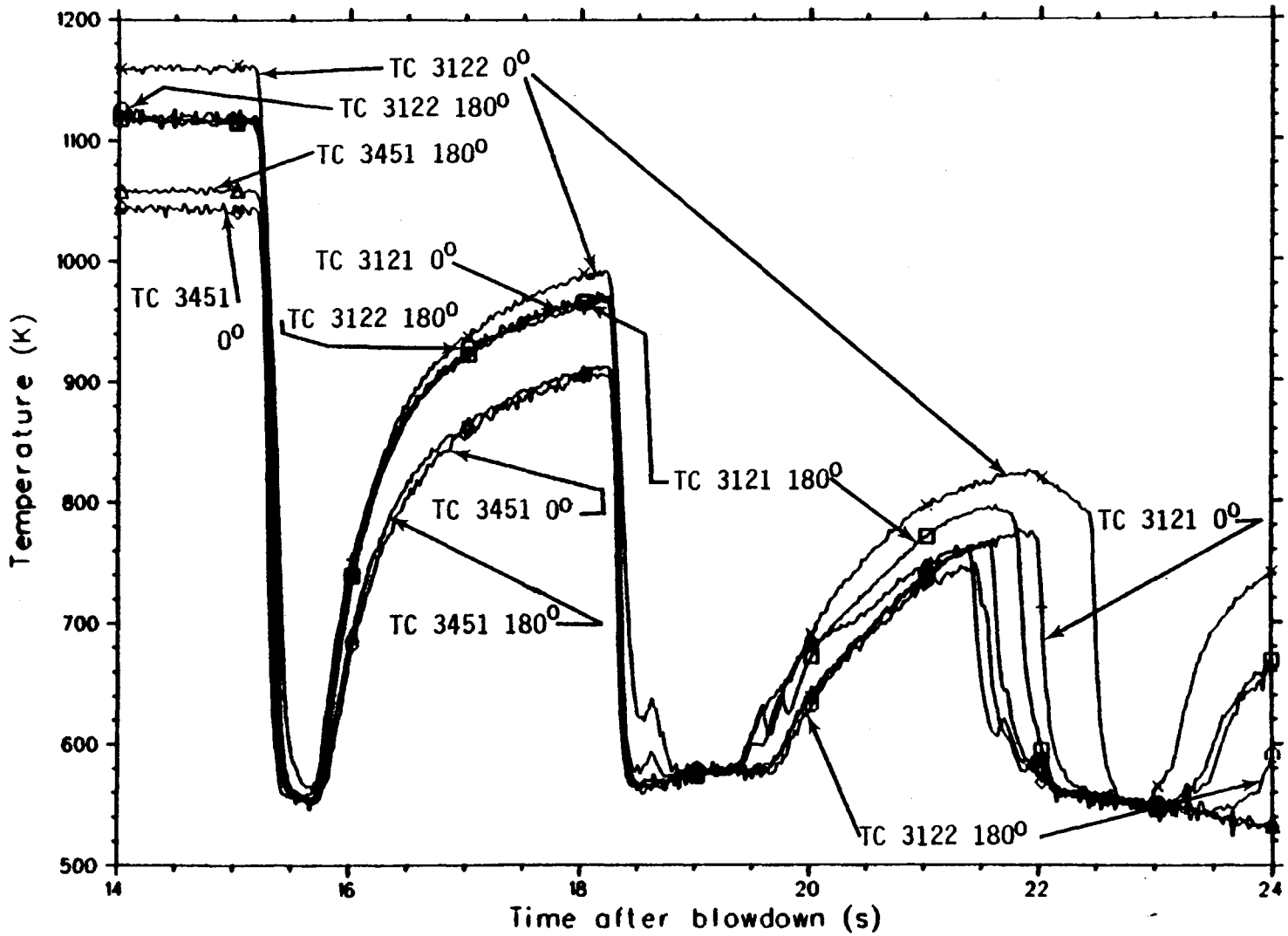

Fig. 39 An overlay showing the thermal response of rods 3121, 3122, and 3451 as determined by thermocouples located on these rods. Test LLR-04.

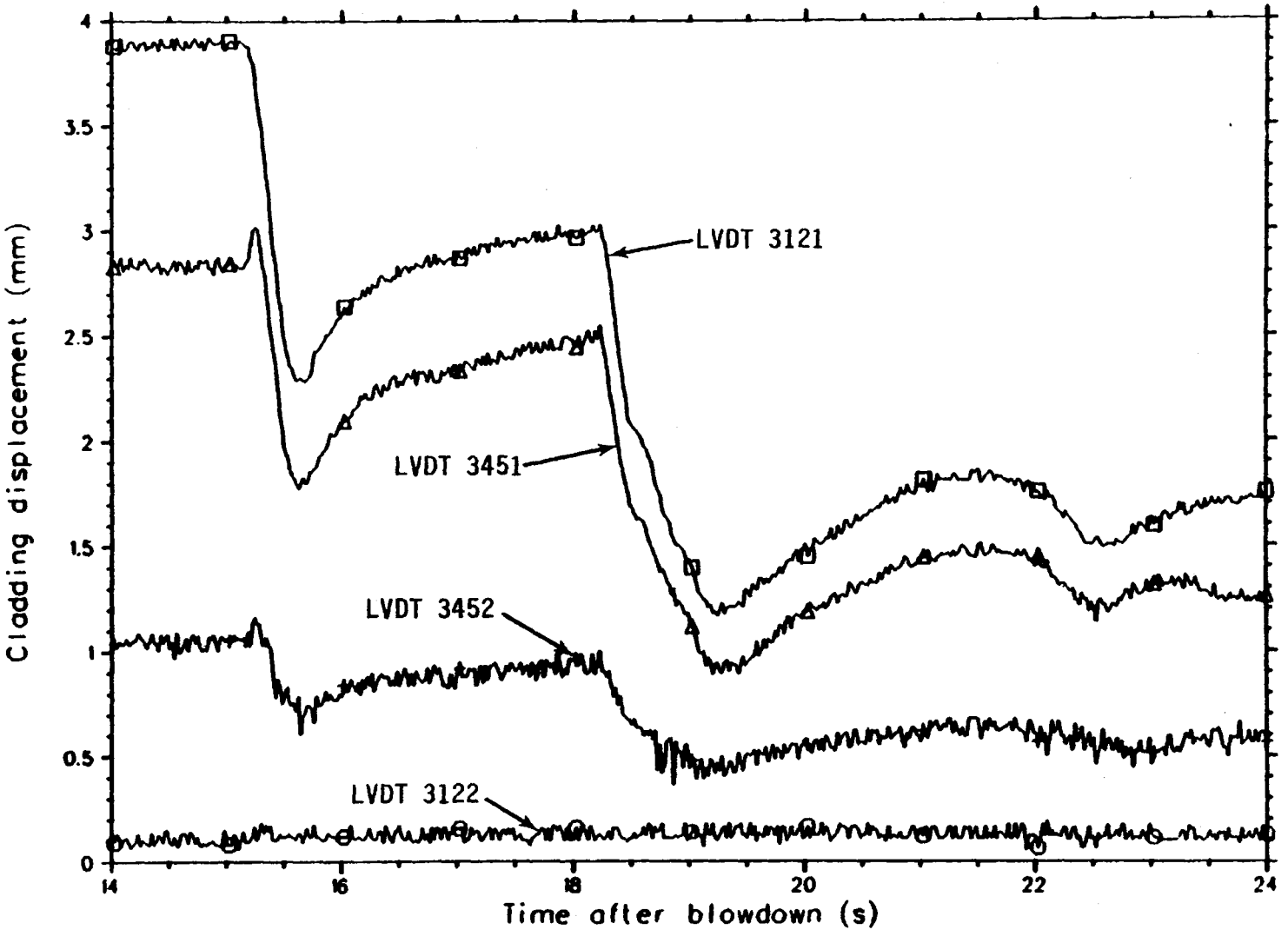

Fig. 40 An overlay showing the mechanical respones of rods 3121, 3122, 3451, and 3452 as determined by corresponding LVDTs. Test LLR-04.

does the LVDT data indicate that only "half" of the rod quenched (and if so, which half?). Did the "fin" TCs on the upper portion of the rod allow this section to preferentially quench while the lower part remained in film boiling, or was the quantity of water supplied to the test region inadequate to quench the entire rod? Part of the difficulty in trying to interpret the LVDT data with respect to these types of events is that the LVDT instrumentation can only measure rod length changes relative to shroud length changes. In addition, the LVDT output signal is sensitive to changes in the LVDT temperature. Consequently, to correctly interpret the LVDT data with regard to fuel rod elongation only, elimination of the other unwanted factors incorporated in the LVDT data is necessary. Since we have been mainly interested in time to DNB and time to quench information (believed to be mostly independent of these other factors), an indepth analysis of the LVDT data has been postponed to the appendix. Nevertheless, as is shown in Appendix A, a correction of the LVDT data, taking into account flow shroud length changes and LVDT temperature, indicates that the test rods probably did not completely quench during the initial rewet (15 to 16 s). The significance of this result is still uncertain; however, it is believed that the discrepancy between the magnitude responses of the LVDT and TC instrumentation are more likely due to limitations of the TCs to accurately measure the cladding temperature during rewet events than indicative of TC perturbation effects.

4.4 Comparison of the LVDT and TC Responses for LLR-4A

The fourth and final test in the LOFT Lead Rod test series was LLR-4A. Test LLR-4A was conducted at approximately the same test conditions as test LLR-04. The test configuration for LLR-4A is shown in Figure 1C and utilized fuel rods 3992, 3122, 3451, and 3452. Fuel rod 3992 replaced 3121 which was used in LLR-04. All rods in this test had surface cladding TCs except for rod 3452.

Figures 41, 42, 43, and 44 show the response of the cladding thermocouples, coolant thermocouples, LVDT data, and the midplane shroud temperatures for the LLR-4A fuel rods during the first 10 seconds following blowdown. From these figures DNB times are estimated and listed in Table 9. Figures 45A, 46A, 47A, and 48A present the long-term history for the cladding thermocouples, LVDT data, coolant TCs, and midplane shroud temperatures from 0 to 300 seconds. As can be seen from these figures rod quench occurs between 240 and 250 seconds. Corresponding to Figures 45A through 48A are Figures 45B, 46B, 47B, and 48B, respectively. These figures show the system pressure, and volumetric flow rates as determined by upper and lower turbine meters for each test rod. In order to better evaluate rod quench times, enlarged views of the rod rewet event appear in Figures 49 through 52. In addition, overlay plots comparing the responses of the cladding TCs and those of the LVDTs are shown in Figures 53 and 54, respectively.

To begin, consider the time to DNB data presented in Table 9. Again, as was seen before, the cladding thermocouples indicate DNB later than that determined by the LVDTs. The data in Table 9 are consistent with the previous three test results and are in agreement with relation (1).

Table 10 summarizes the estimated rod turnaround times for the thermocouples and LVDTs, as well as the estimated rod quench times indicated by these two instruments. All the data in Table 10 are consistent. That is, the LVDT turnaround times correspond with the TC turnaround times and likewise the rod quench times agree to within about 1.0 second. In addition, rod 3452 without surface clad thermocouples responds in the same way (i.e., with LVDT turnaround and quench times) as rods with surface clad thermocouples. Consequently, it is concluded that significant TC perturbation effects are not evident in the rod rewet portion of the LLR-4A data.

TABLE 9

LLR-4A

ESTIMATED TIME OF INITIAL DNB

	Rod Number			
Instrument	3922	3122	3451	3452*
LVDT	0.25	0.25	0.25	0.25
TC 180° 0.533 m		2.1	2.0	
TC 0° 0.533 m			2.0	
TC 180° 0.457 m	1.8			
TC 0° 0.457 m		1.9		
TC 0° 0.314 m	1.6			

The above numbers indicate the approximate time (in seconds) during blowdown that the rod temperature significantly deviates from the saturation temperature, indicating DNB, as determined from the given instrumentation. Interpretation of the data, especially the LVDT data, with regard to the initiation of DNB is somewhat subjective and might be open to alternative evaluations.

Numbers reported in the above table have been suggested by PBF personnel[5].

* Rod 3452 had no surface clad TCs.

TABLE 10

LLR-4A

ESTIMATED TURNAROUND AND ROD QUENCH TIMES

Instrument	Rod Number			
	3922	3122	3451	3452*
LVDT	239.4/245.0	239.4/244.6	/244.6	239.3/245.0
TC 180° 0.533 m		239.4/244.6	239.4/244.6	
TC 0° 0.533 m			239.4/244.6	
TC 180° 0.457 m	239.4/246.2			
TC 0° 0.457 m		239.4/244.6		
TC 0° 0.314 m	239.4/244.5			

The first number indicates the approximate turnaround time in the response of the LVDT or TC, and the second number represents the approximate beginning of rod quench as indicated by the LVDT or TC instrumentation respectively.

* Rod 3452 had no surface clad TCs.

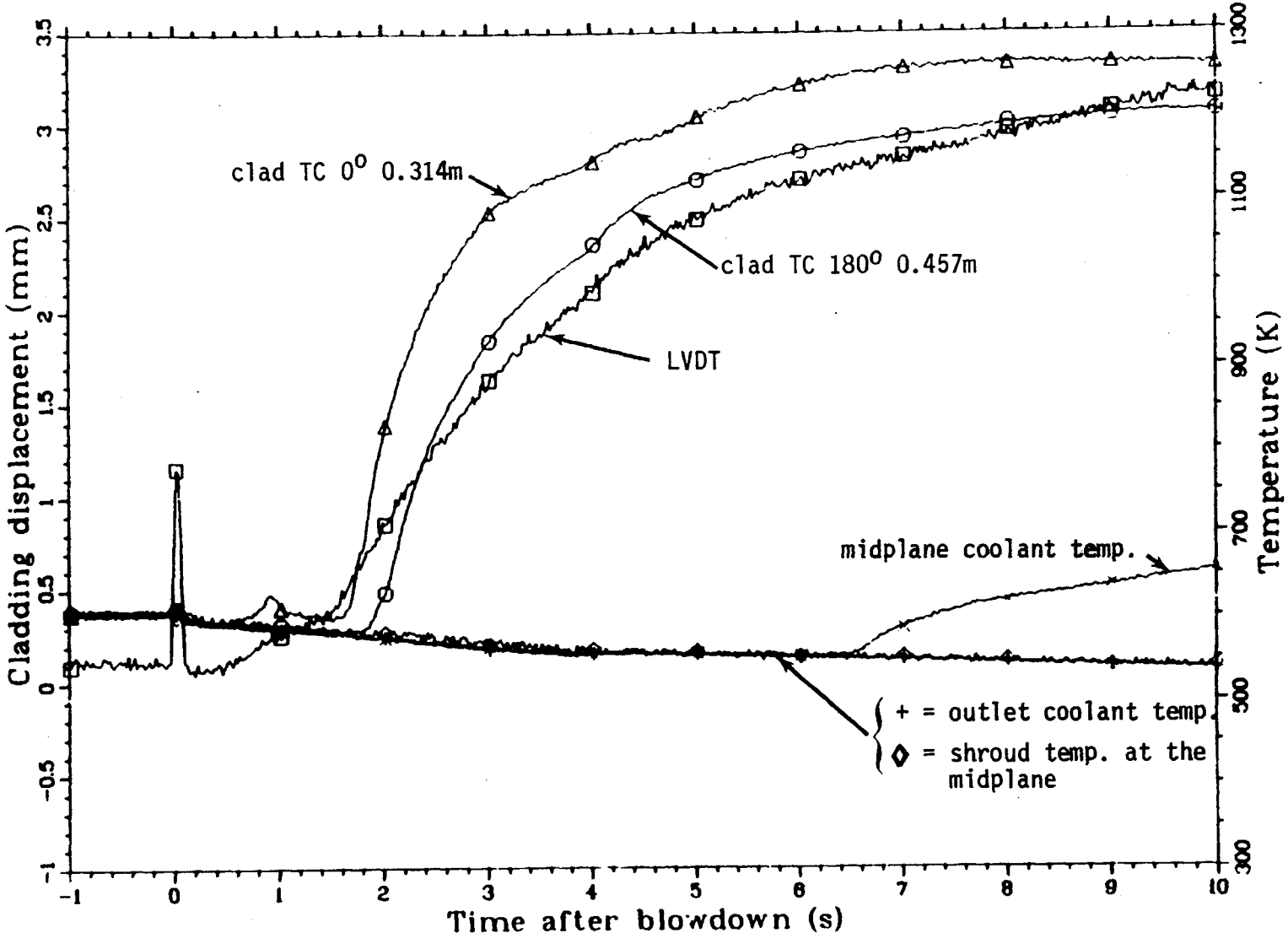

Fig. 41 Comparison of the thermal and mechanical response of fuel rod 3992. Test LLR-4A.

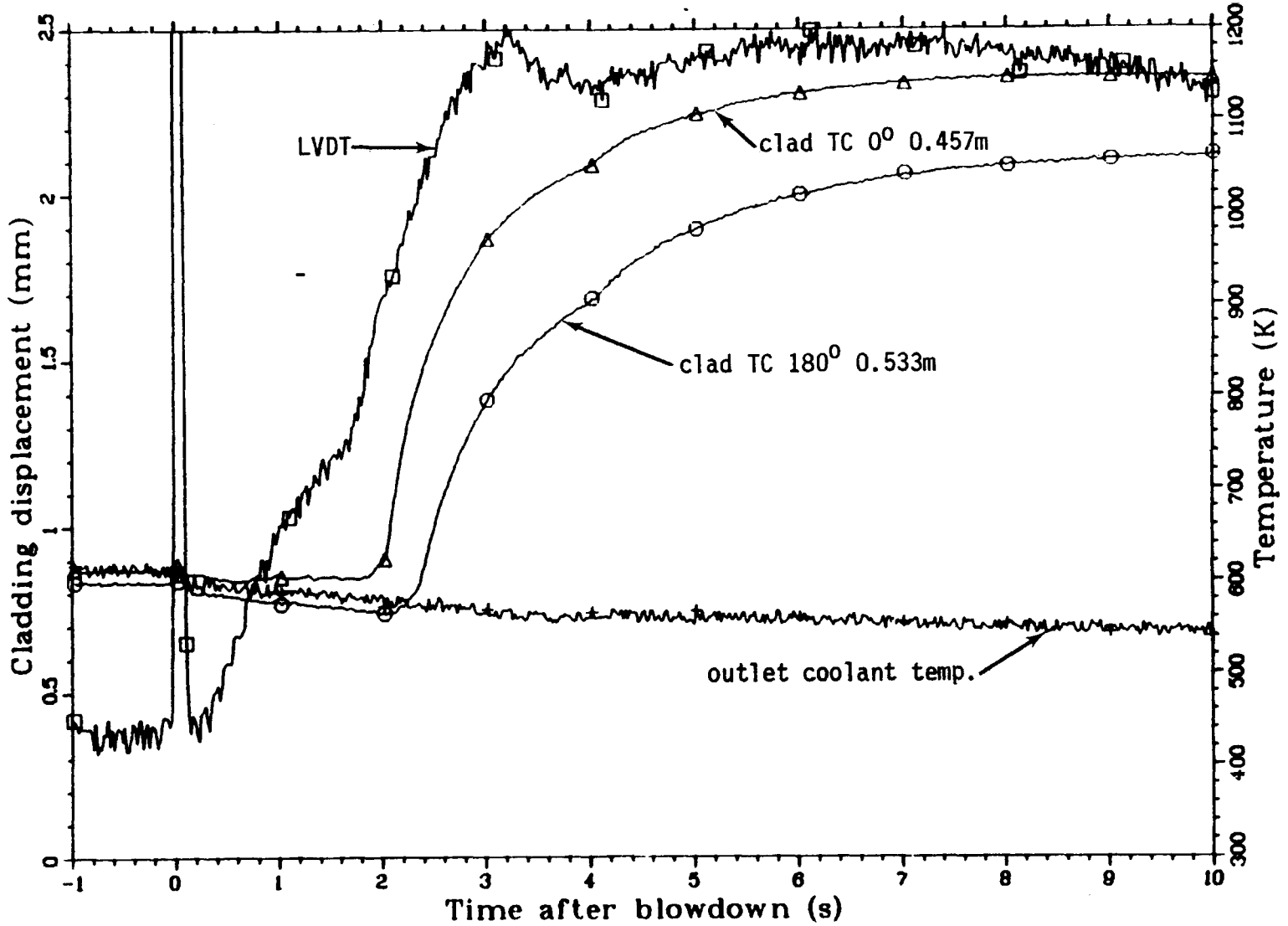

Fig. 42 Comparison of the thermal and mechanical response of fuel rod 3122. Test LLR-4A.

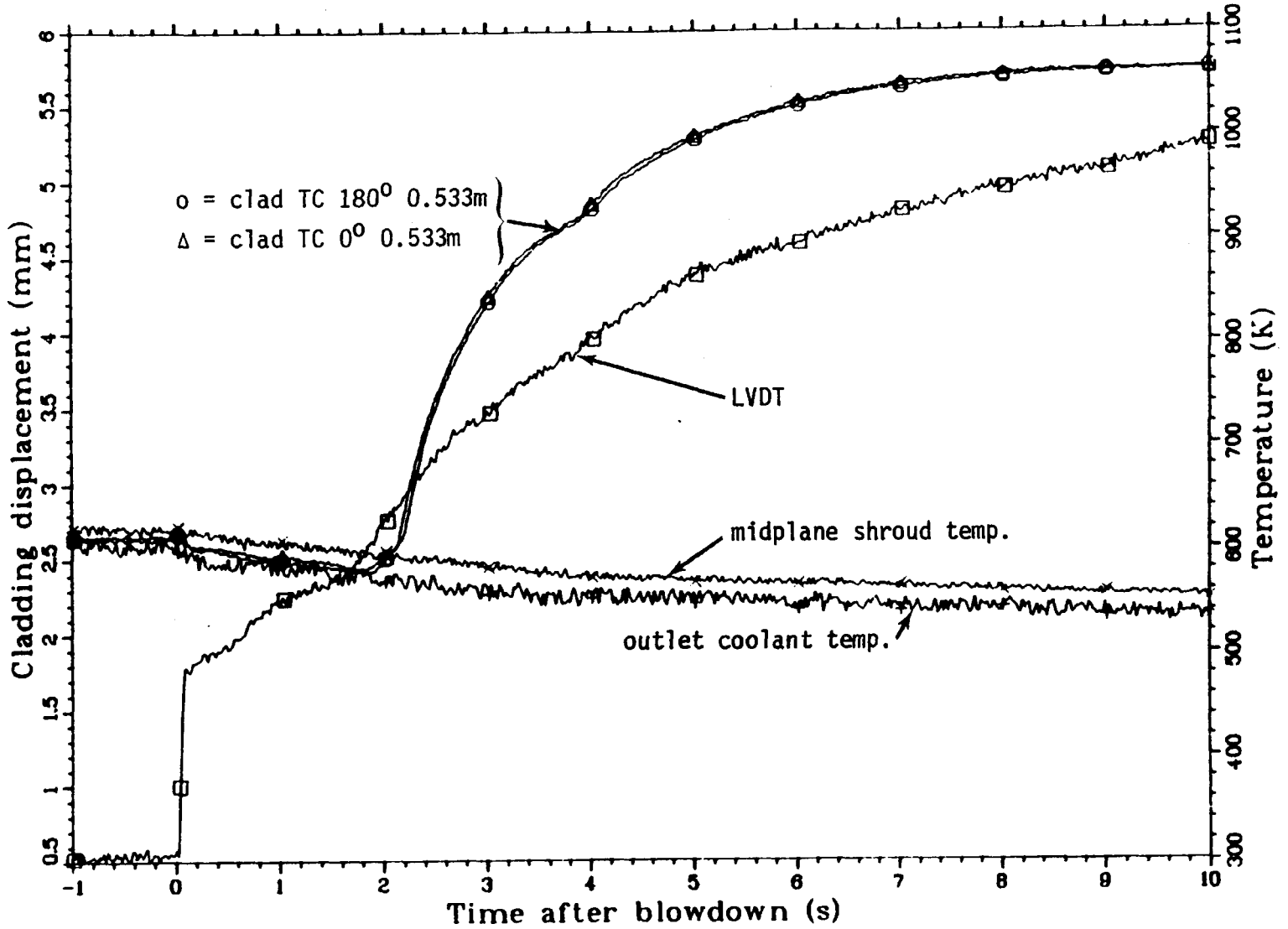

Fig. 43 Comparison of the thermal and mechanical response of fuel rod 3451. Test LLR-4A.

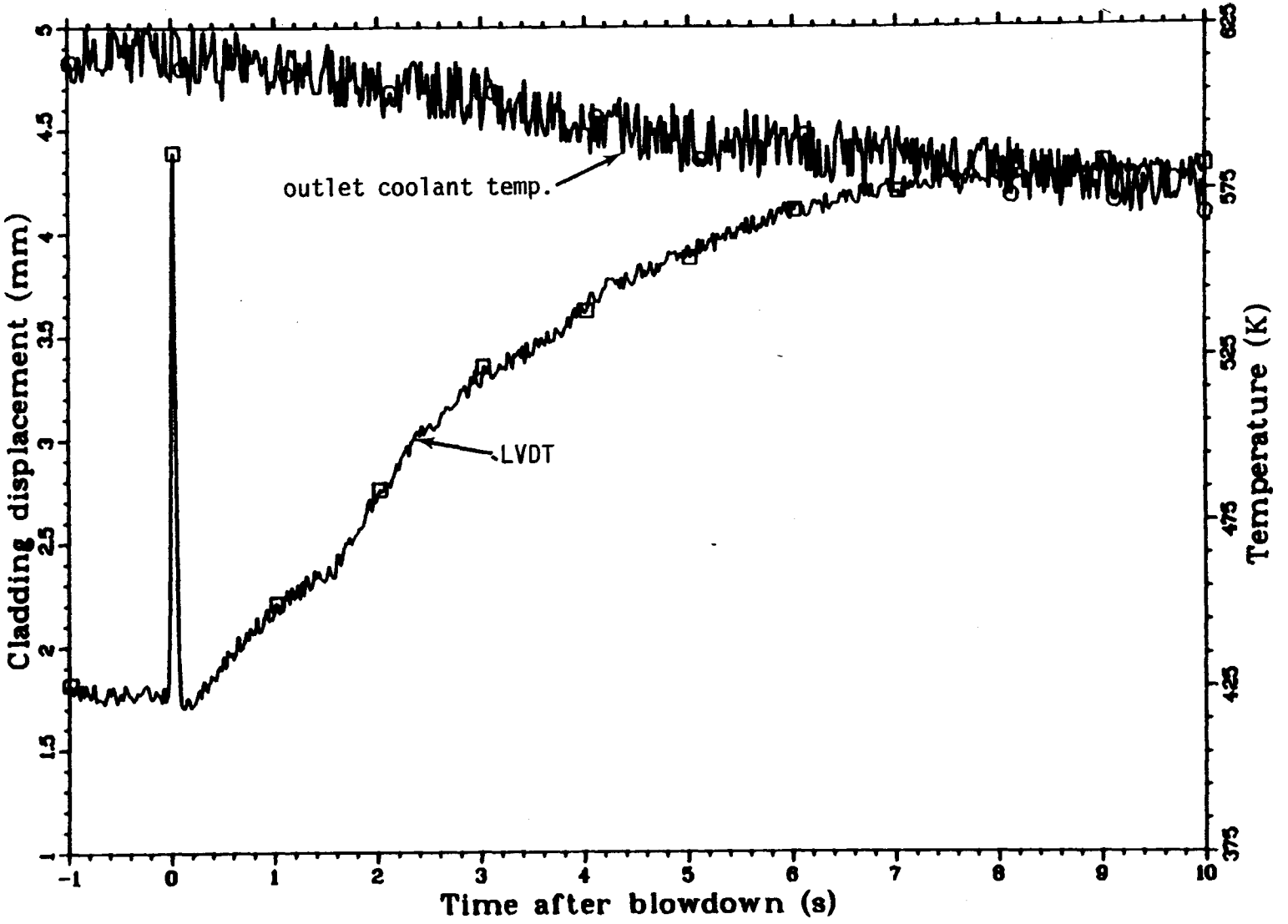

Fig. 44 The mechanical response of fuel rod 3452. Test LLR-4A.

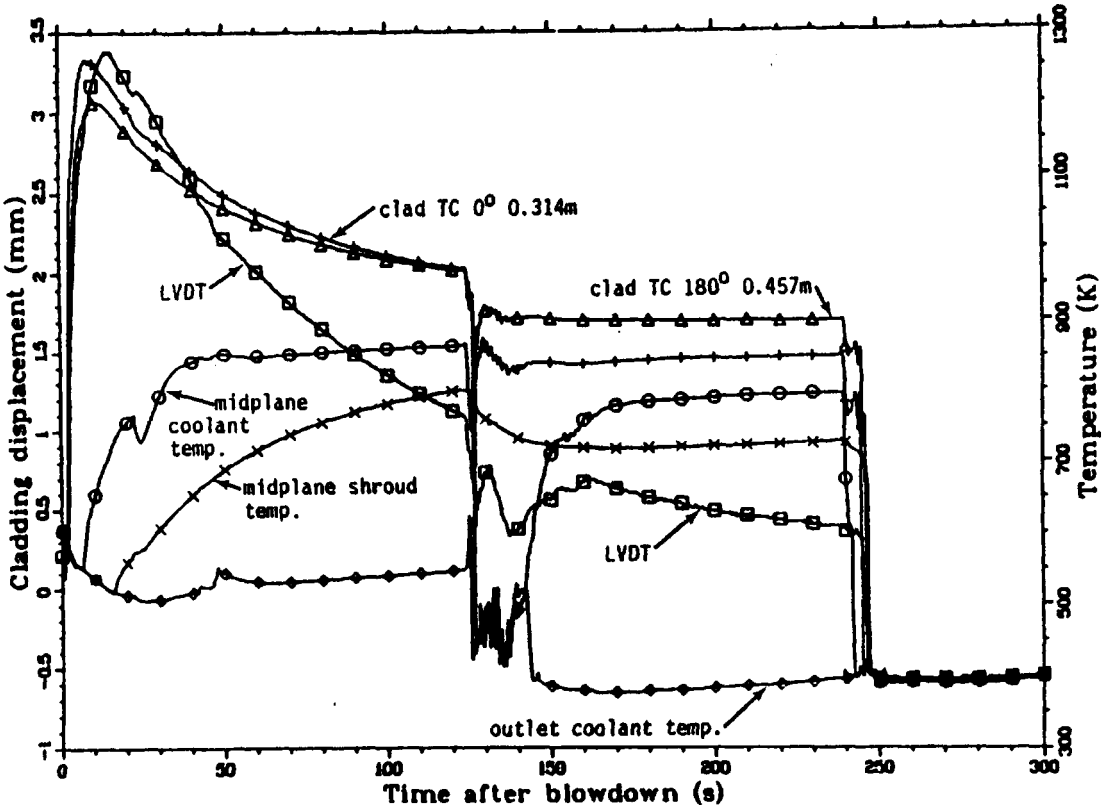

Fig. 45A Comparison of the thermal and mechanical response of fuel rod 3992. Test LLR-4A.

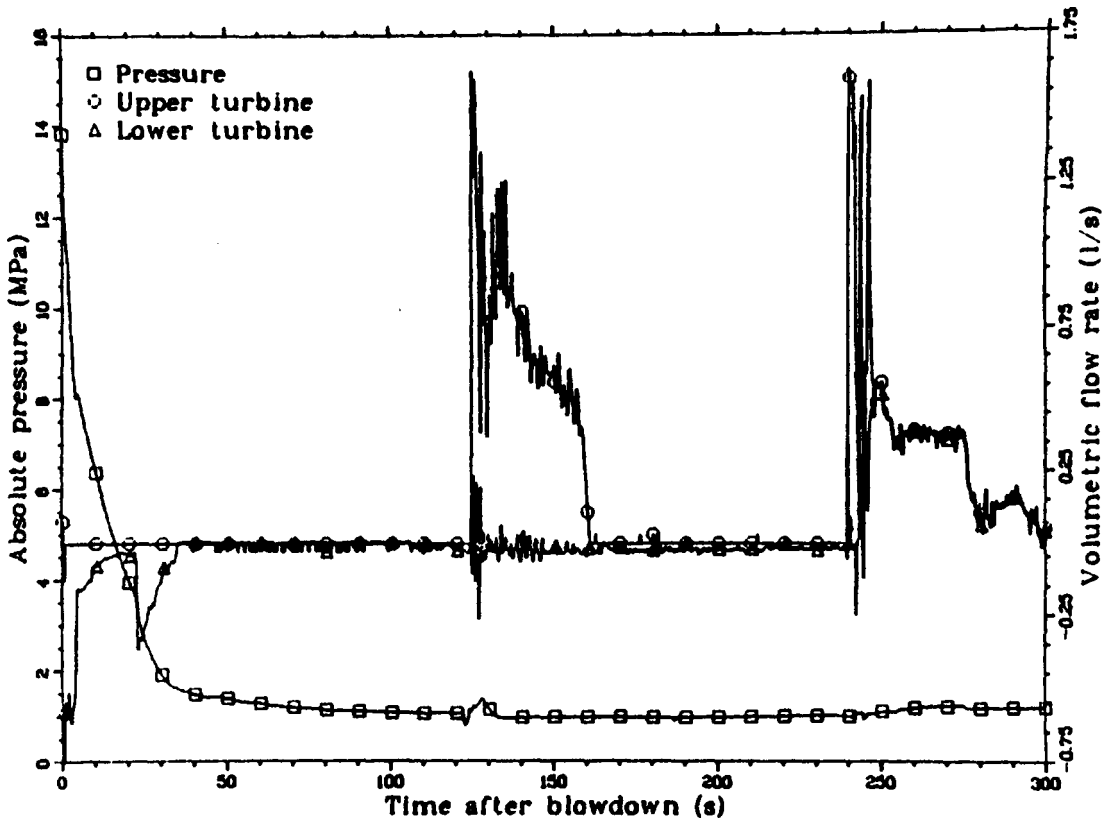

Fig. 45B An overlay showing the system pressure and the upper and lower volumetric flow rates for rod 3992. Test LLR-4A.

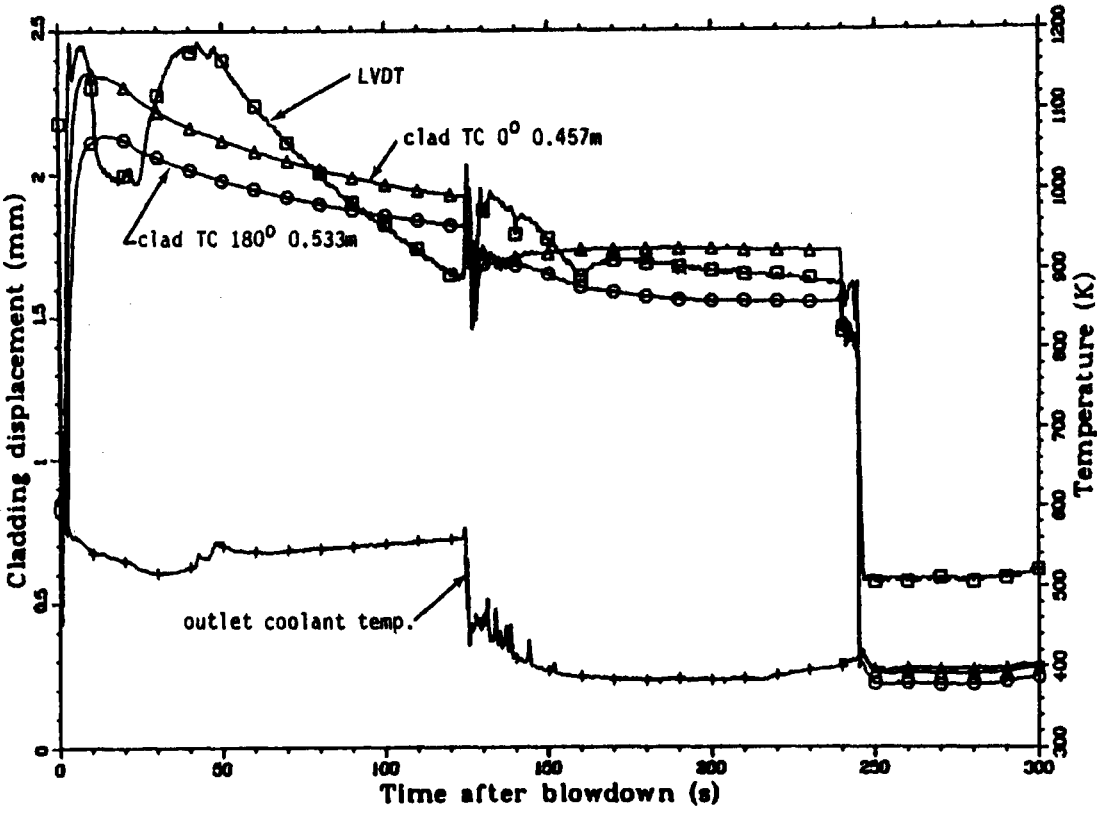

Fig. 46A Comparison of the thermal and mechanical response of fuel rod 3122. Test LLR-4A.

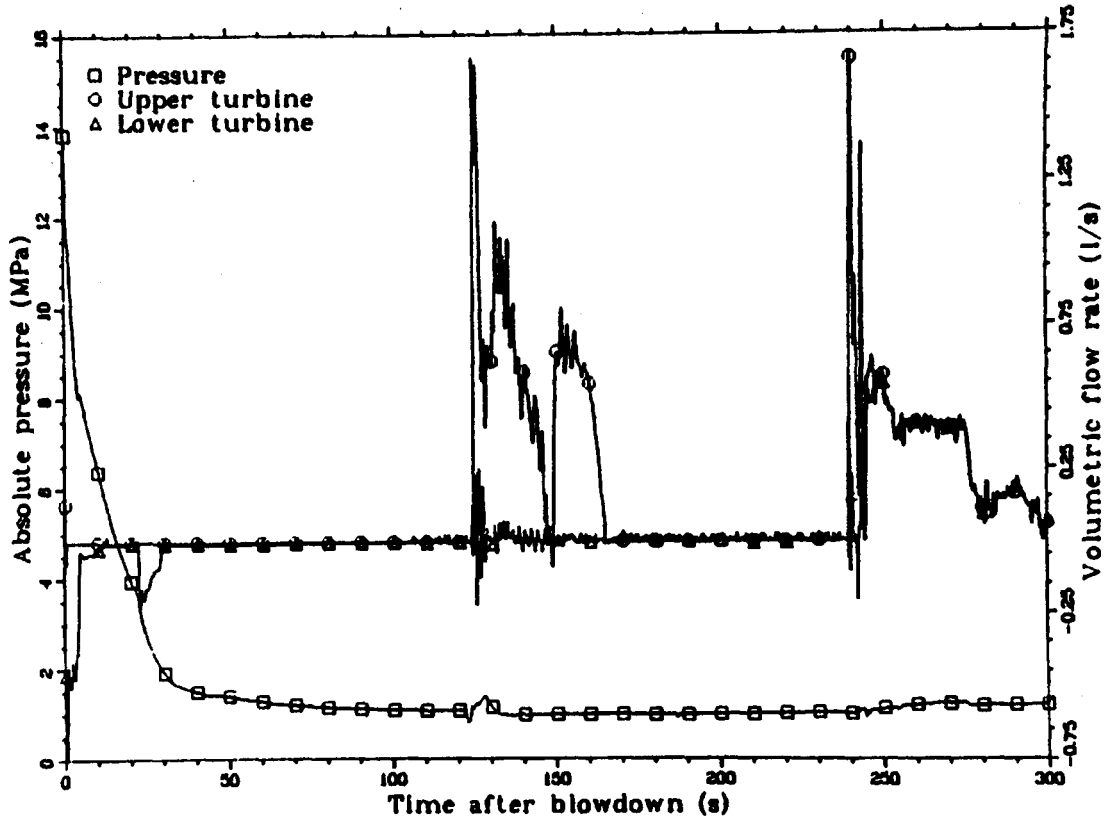

Fig. 46B An overlay showing the system pressure and the upper and lower volumetric flow rates for rod 3122. Test LLR-4A.

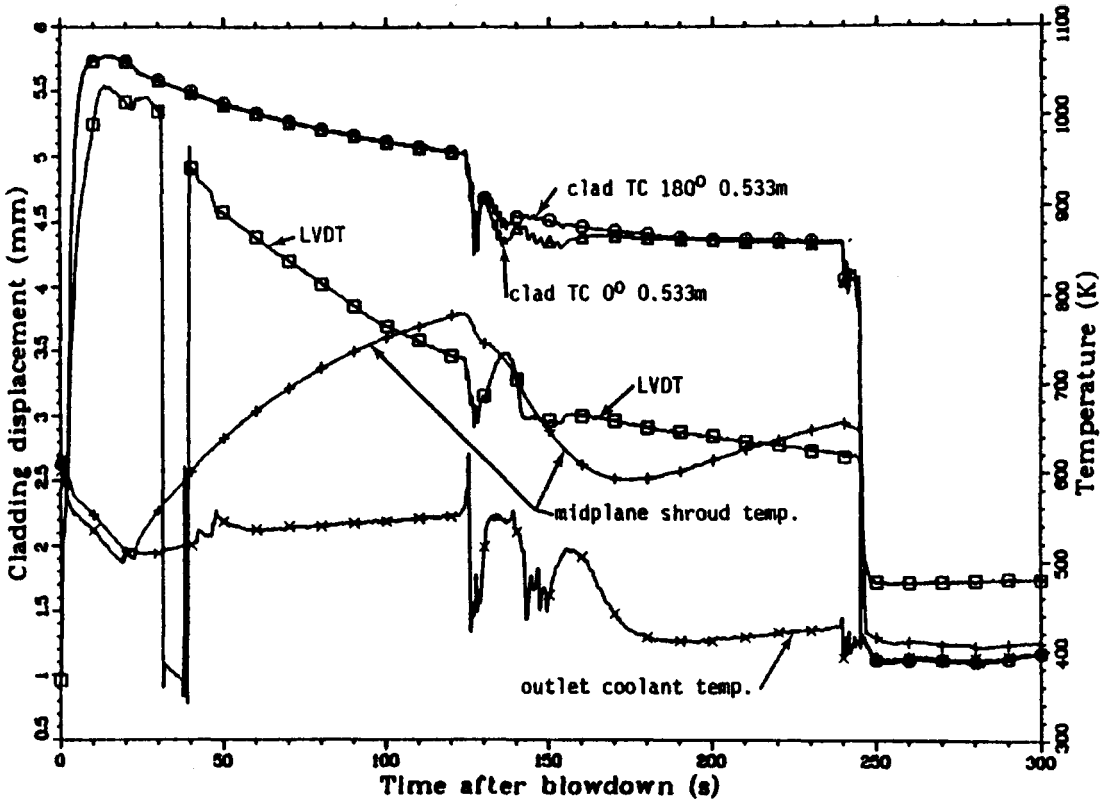

Fig. 47A Comparison of the thermal and mechanical response of fuel rod 3451. Test LLR-4A.

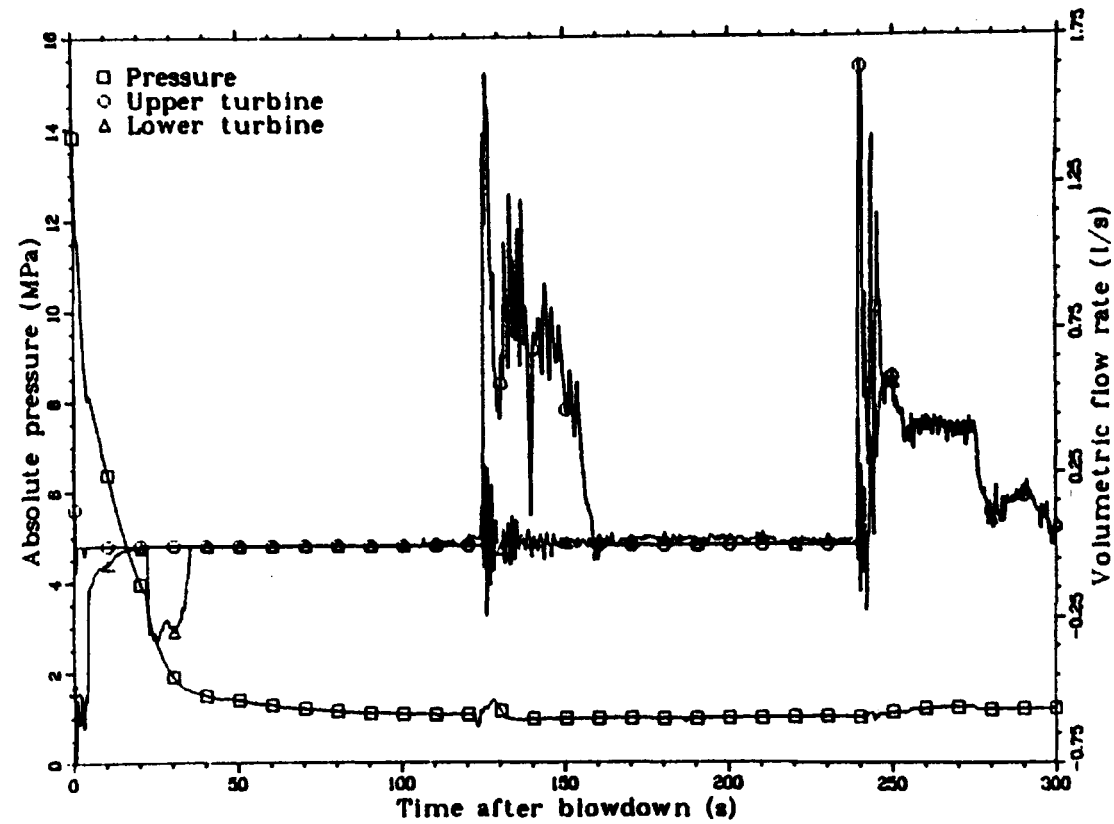

Fig. 47B An overlay showing the system pressure and the upper and lower volumetric flow rates for rod 3451. Test LLR-4A.

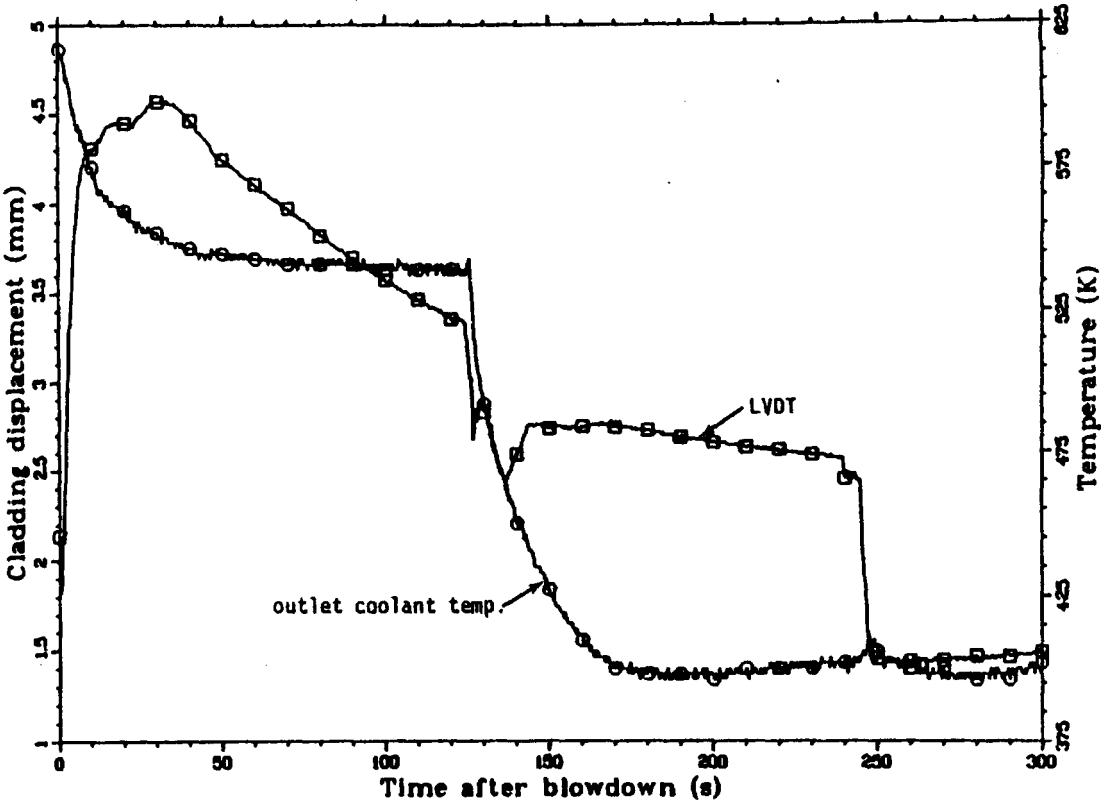

Fig. 48A The mechanical response of fuel rod 3452. Test LLR-4A.

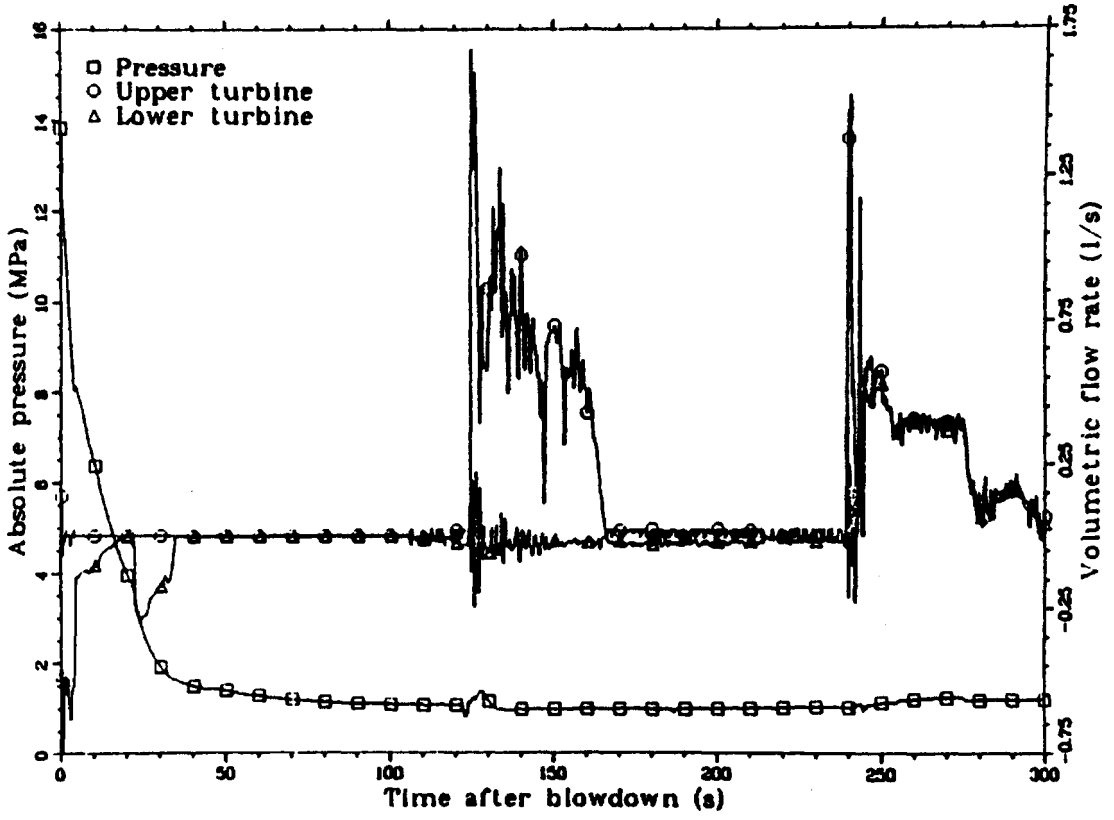

Fig. 48B An overlay showing the system pressure and the upper and lower volumetric flow rates for rod 3452. Test LLR-4A.

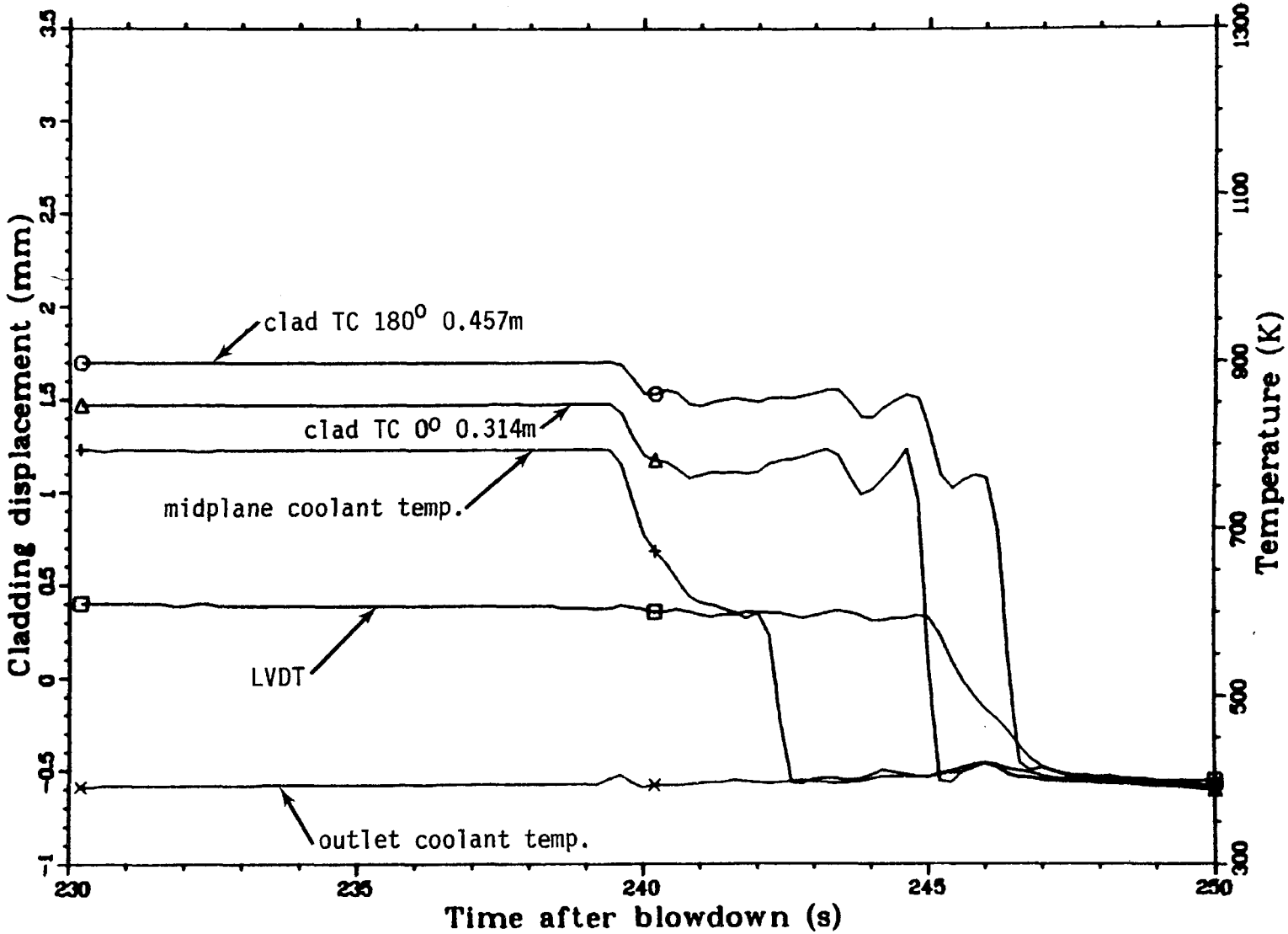

Fig. 49 An overlay showing the thermal and mechanical response of fuel rod 3992. Test LLR-4A.

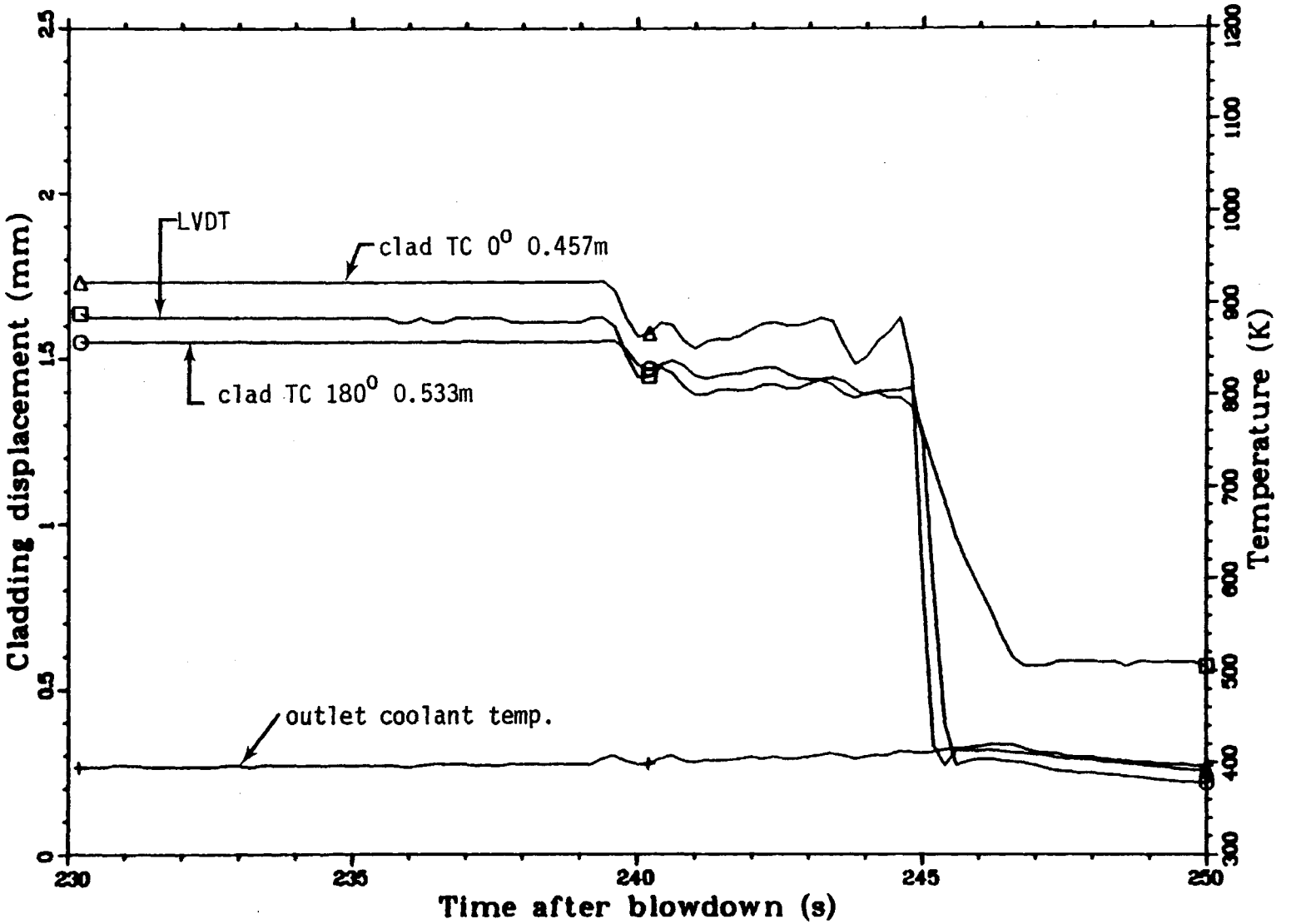

Fig. 50 An overlay showing the thermal and mechanical response of fuel rod 3122. Test LLR-4A.

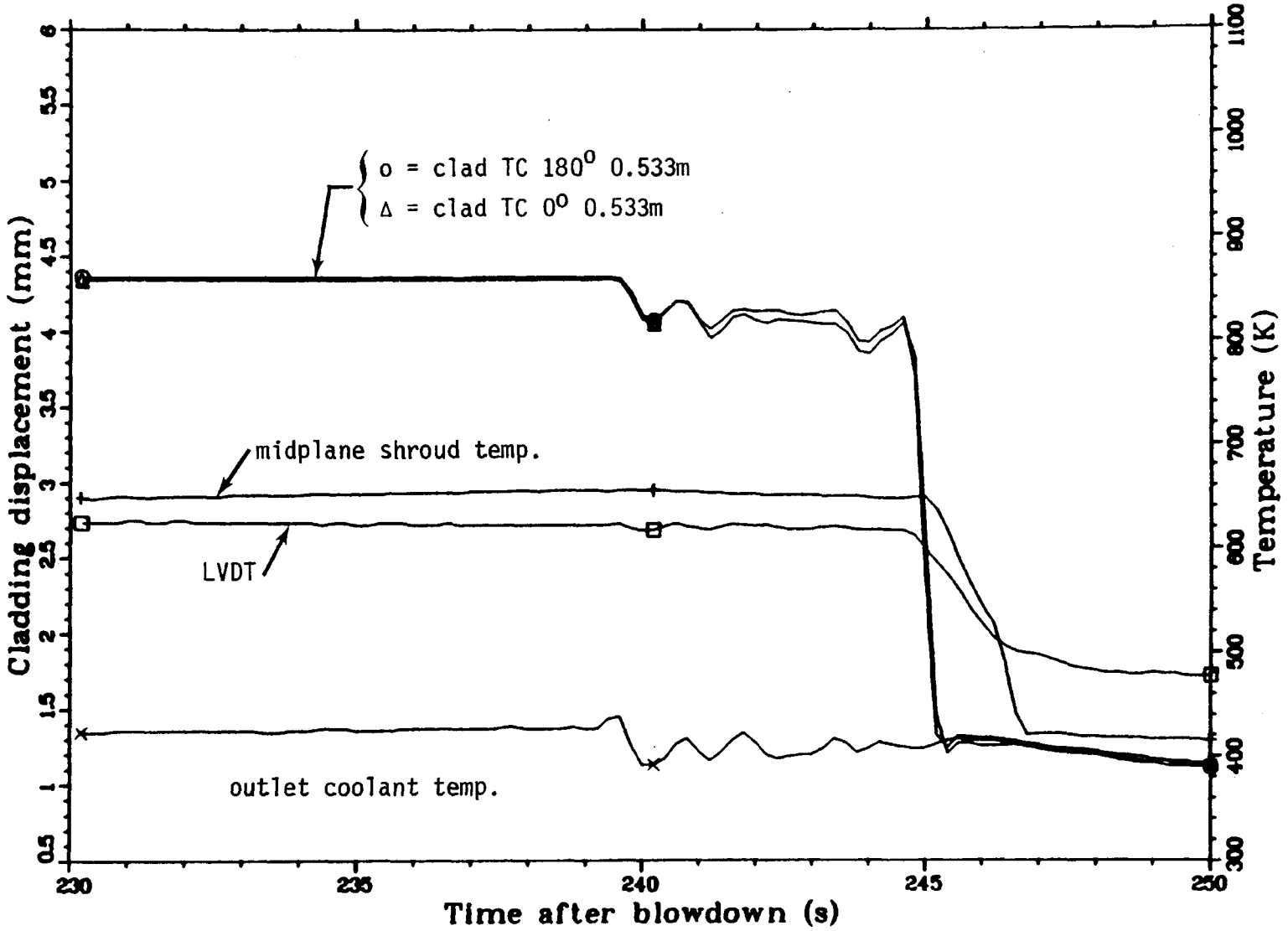

Fig. 51 An overlay showing the thermal and mechanical response of fuel rod 3451. Test LLR-4A.

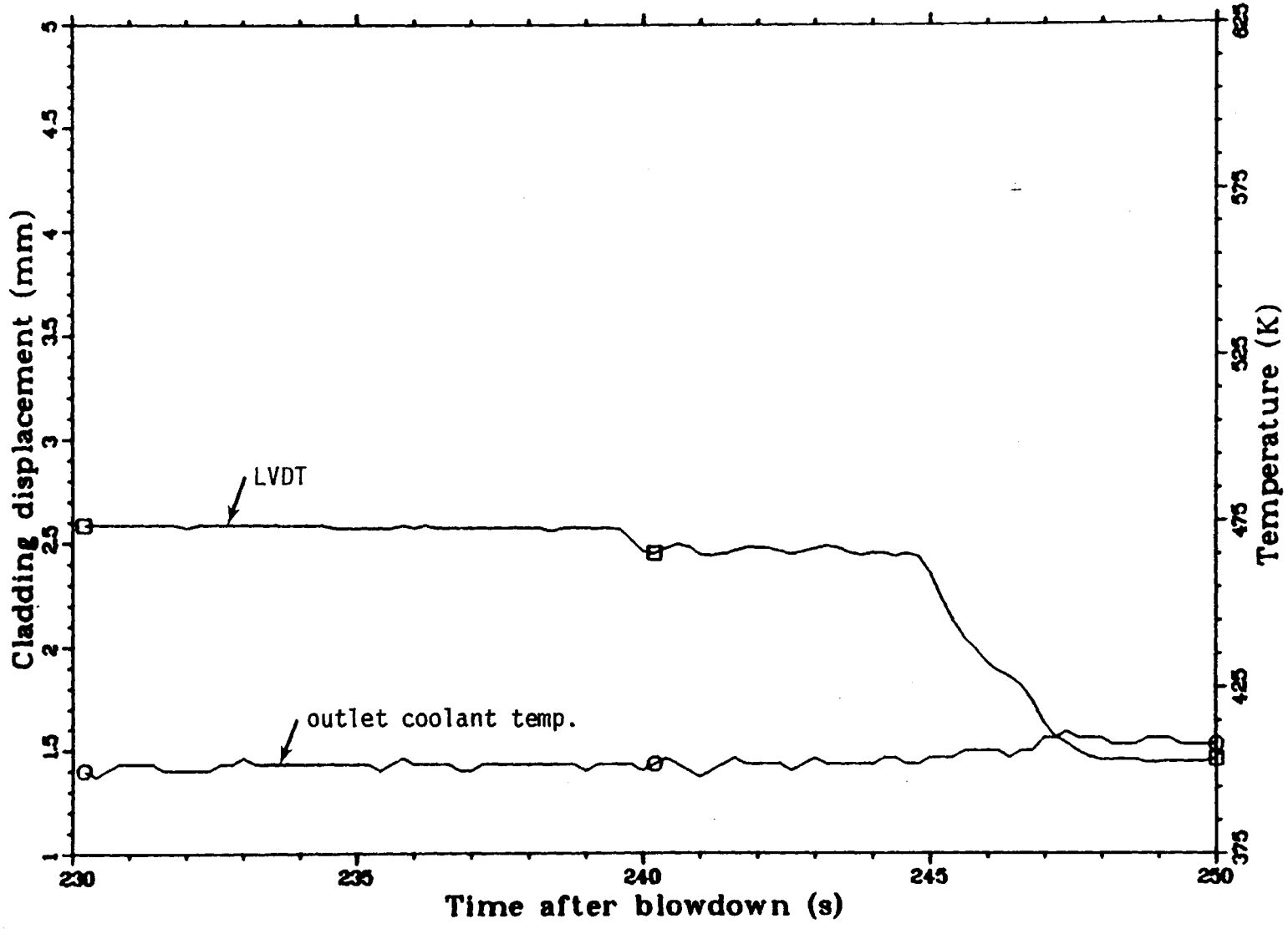

Fig. 52 An overlay showing the mechanical response of fuel rod 3452. Test LLR-4A.

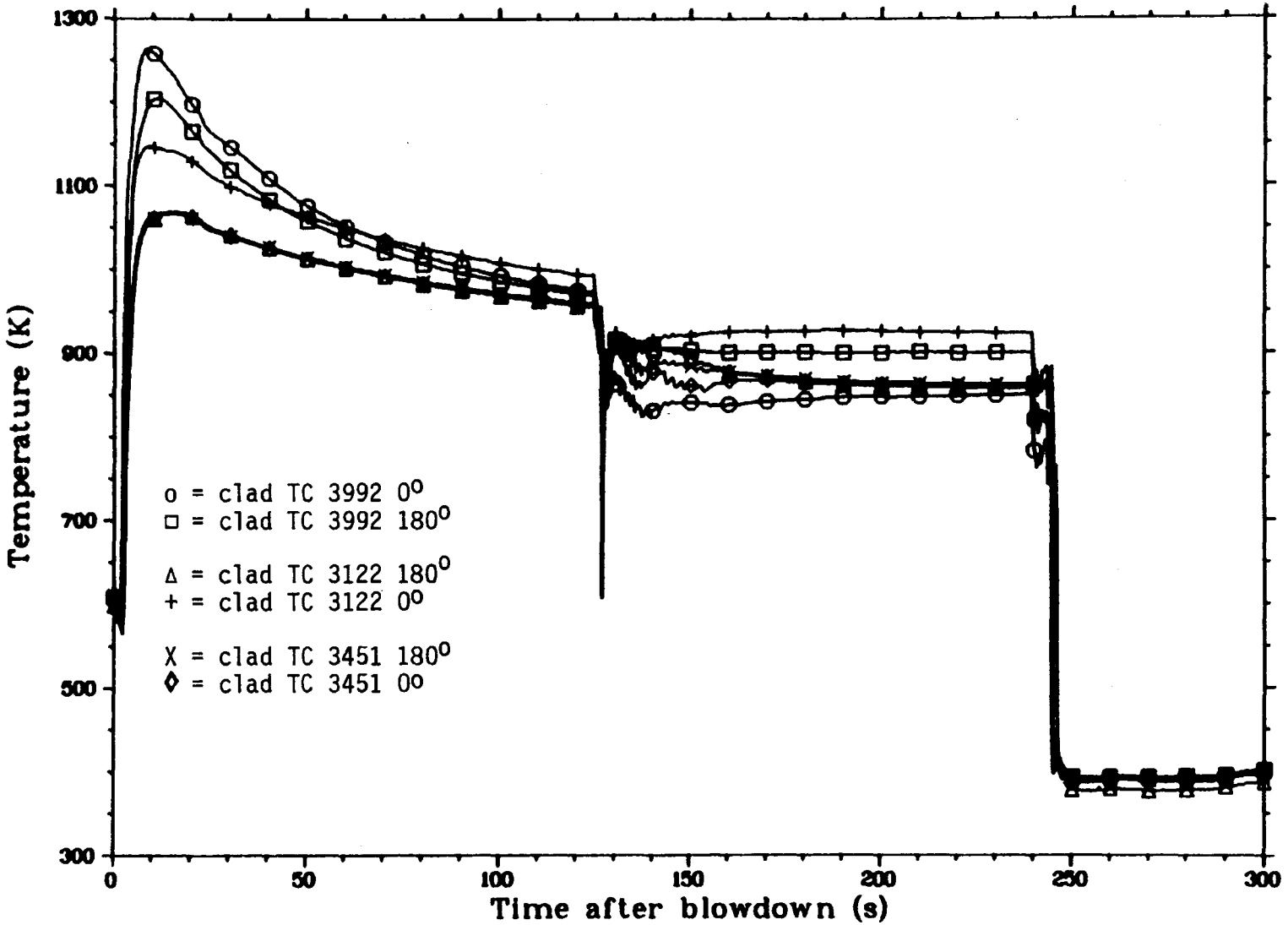

Fig. 53 An overlay showing the thermal response of rods 3992, 3122, and 3451 as determined by all cladding thermocouples. Test LLR-4A.

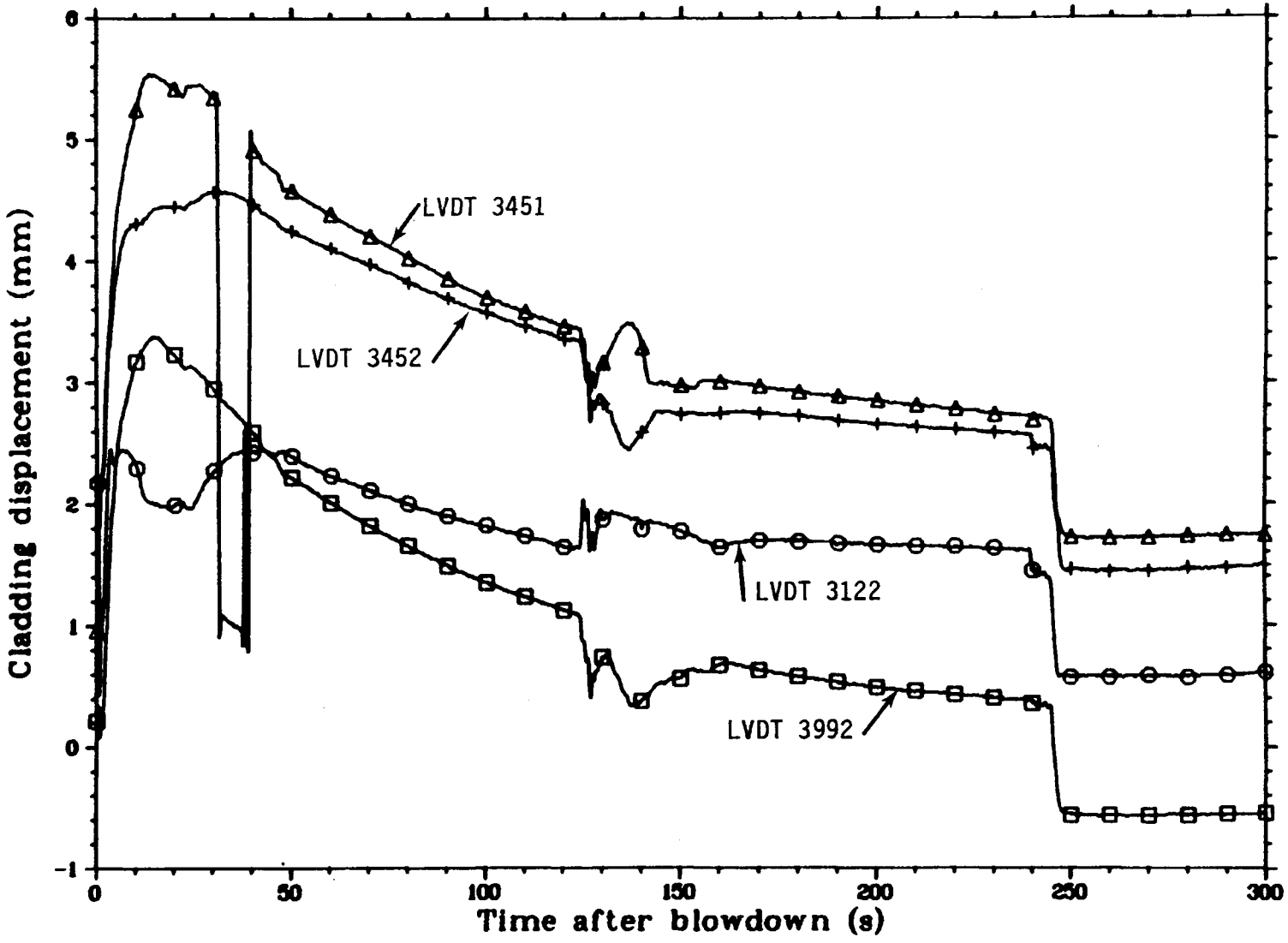

Fig. 54 An overlay showing the mechanical response of rods 3992, 3122, 3451, and 3452 as determined by corresponding LVDTs. Test LLR-4A.

CONCLUSIONS

Comparison of the LOFT Lead Rod thermocouple and LVDT data suggests that there is an axial dependence of the time to DNB condition and that this effect is caused, at least in part, by the surface clad TCs which appear on the top half of the test rods and not on the lower sections. Consequently, it appears that the "fin" type TCs are delaying DNB above the rod midplane by preferentially cooling the upper part of the rod. Nevertheless, since it is possible that other phenomena may also be contributing to this effect, it is not feasible at this time to completely quantify the influence the surface clad TCs had on DNB.

With regard to TC perturbation effects during rod rewet events, the following observations are made:

(1) The data from all tests show that the cladding thermocouples quench before the LVDT indicates rod quench. The time difference appears to be a function of system pressure and reflood rates; however, because of the uncertainty in the fluid quality and mass flow rates, an accurate determination of the flooding rates for the LLR tests could not be made.

(2) Cladding elongation measurements on rods with and without thermocouples, for any given test, are not identical; however, general trends are evident and appear to indicate that the external clad TCs did not significantly affect the overall mechanical response of the rod. The fact that the LVDT responses were not identical may be indicative of (a) non-uniform rod thermal conditions, (b) non-uniform coolant conditions between test rod positions, and/or (c) differences in the LVDT instrumentation.

From observations (1) and (2) it can be concluded that the cladding thermocouples quench somewhat earlier than that indicated by the LVDT measurements; however, the overall mechanical response of rods instrumented with external clad TCs is not significantly affected by the presence of the thermocouples.

Furthermore, the above observations are not particularly conclusive with regard to the cooling effects of external clad TCs during the rapid rewet events observed in the LOFT L2 experiments. Additional experiments are ongoing to resolve these issues for the LOFT system.

APPENDIX A

CORRECTION OF THE LLR LVDT DISPLACEMENT TRANSDUCER DATA FOR SHROUD ELONGATION AND TEMPERATURE EFFECTS

I. INTRODUCTION

To better identify and understand the limiting aspects of the Linear Variable Differential Transformer (LVDT) instrumentation to measure the fuel rod displacement during blowdown conditions, a review of the theory and operation of the LVDT is presented below. In addition, correction of the LVDT data for estimated flow shroud elongation and LVDT temperature effects is made for selected rods. It is believed that the "corrected" LVDT data more closely represents the actual fuel rod displacement and therefore serves as a better indicator of the dynamic response of the fuel rod, than the orginal LVDT data. Unfortunately, due to the additionally required data necessary to "correct" the LVDT data, it is not possible to adjust the LVDT response of each fuel rod in the LLR test series. Therefore, only a small number of cases will be considered.

1.1 LVDT Theory and Operation Information

The Linear Variable Differential Transformer produces a voltage proportional to the displacement of a movable ferromagnetic core relative to the location of three induction coils; a primary and two symmetrically spaced identical secondaries[6]. The LVDT operates on the principal of mutual inductance. When an alternating current is supplied to the primary coil, the subsequent changing magnetic fields produce a voltage, via magnetic coupling, in each of the secondaries;

which is dependent on the position of the ferromagnetic core element. By measuring the induced voltage in each secondary the position of the core element can be deduced from calibration curves. If the core element is centered between the secondary coils, the magnetic coupling between the primary and each secondary is equal, and therefore the voltage induced in each winding is identical in magnitude but 180° out-of-phase with each other. Since the secondaries are connected in series (opposition), the resulting net output voltage is zero. Now, if the core element is displaced from the center or null position, then the mutual inductance of the primary coil with respect to one secondary will be larger than the other secondary, resulting in a net voltage proportional to the given displacement. Figure A1 shows a schematic of the LVDT used in the Power Burst Facility (PBF) experiments.

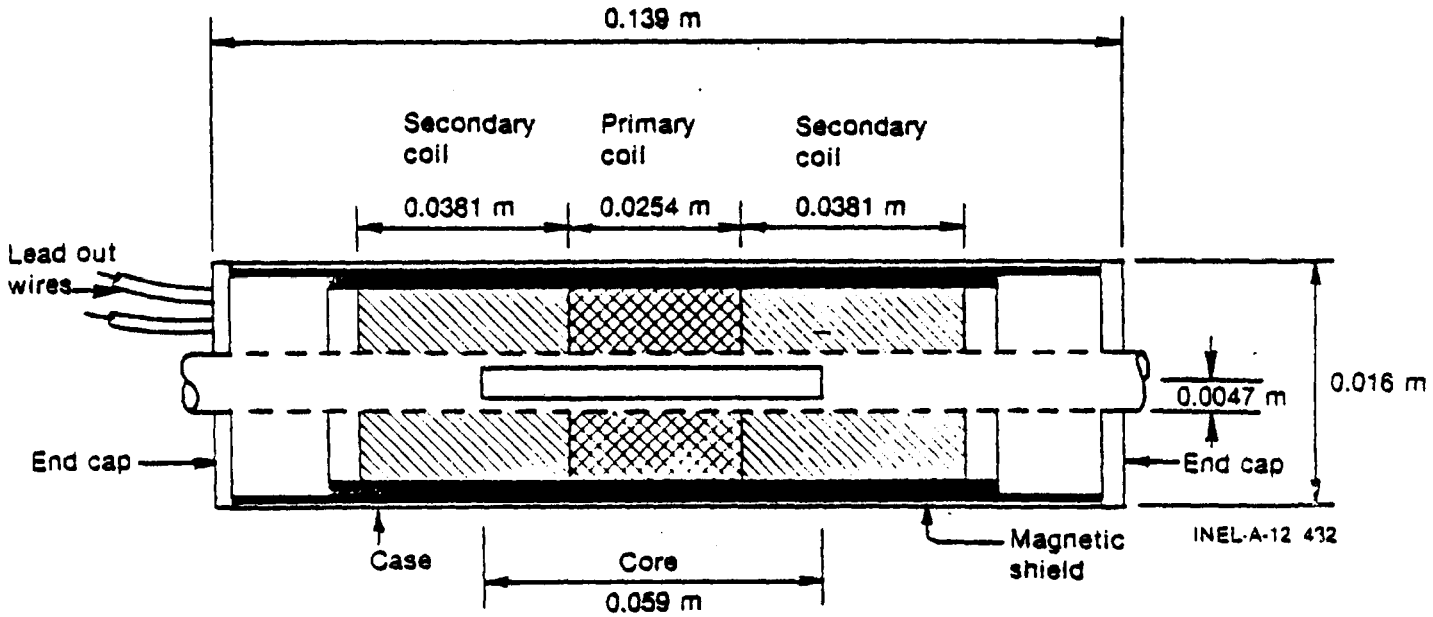

Fig. A1 Schematic of the LVDT used in the Power Burst Facility reactor.

For the PBF LOFT Lead Rod (LLR) tests, the ferromagnetic core element of the LVDT is connected to the bottom of the fuel rod cladding and the case of the LVDT is attached to a stainless steel tube which is connected to the flow shroud. Because of this design characteristic, the LVDT can only measure fuel rod length changes, relative changes in length of the flow shroud and fuel rod. For instance, an increase in the length of the fuel rod produces a proportional increase in output voltage of the LVDT; however, an increase in the flow shroud produces a decrease in the LVDT response. That is, an increase in the length of the flow shroud produces the same LVDT response as if the fuel rod length decreased by a corresponding amount. In particular, a 1 mm increase in the fuel rod length occurring at the same time the flow shroud length increases by 1 mm produces no net change in the LVDT signal.

Besides flow shroud length changes, other factors can also affect the response and limit the accuracy of the LVDT instrumentation. Included among these other factors are: (a) the LVDT temperature, (b) the amount of heated instrument cable residing in the test zone, (c) the total length of cable, (d) the LVDT signal conditioner, and (e) the value of the driving primary voltage. For this investigation only changes in the shroud length and LVDT temperature will be considered. These two factors will be calculated using a one-point or average temperature model and this effect will then be eliminated from the original LLR LVDT data.

1.2 LVDT Calibration Data

The response of each LVDT for given core element displacements at several different parametric temperatures determines a family of calibration curves. Each curve in the family illustrates the functional relationship between the LVDT output (in volts) and the

core element displacement (in mm) for a given temperature. Figure A2 shows a typical family of calibration curves for the LVDT S/N (serial no.) 67725 as determined by the PBF Instrumentation Division.

Although Figure A2 is valid for only one particular LVDT, the following analysis is general enough so as to apply to all LVDT calibration data. First, notice that each calibration curve in Figure A2 can be closely approximated by a straight line. Second, as the temperature of the LVDT is increased the slope of the best fit line also increases. For example, for LVDT S/N 67725 the following equations approximate the measured data:

$$V = 0.079577X + 0.0001942 \quad \text{for} \quad T = 301.4\ K \qquad (A1)$$

$$V = 0.087580X - 0.0011182 \quad \text{for} \quad T = 480.4\ K \qquad (A2)$$

$$V = 0.091097X - 0.0010181 \quad \text{for} \quad T = 561.4\ K \qquad (A3)$$

$$V = 0.093211X - 0.0002955 \quad \text{for} \quad T = 614.8\ K \qquad (A4)$$

where, V is in volts and $-12.7\ mm \leq X \leq 12.7\ mm$.

In general, $V = Mx + b$, where, $M = M(T)$ is the slope of the calibration "line" at the given temperature T. Assuming that M varies linearly with T then $M(T) = \alpha T + \beta$. A least squares analysis of the M versus T data in Equations A2 through A4 indicates that:

$$M = (4.202 \times 10^{-5})\ T + 0.06742 \quad \text{for } 480\ K < T < 615\ K^{*} \qquad (A5)$$

Letting B = the average of the constant terms appearing in equations (A2), (A3), and (A4), then B = -0.0008106. Therefore, for LVDT S/N 67725 (Rod 3122):

---

* The temperature range between 480 and 615 is more representative of expected LVDT temperatures during the LLR blowdown tests than the range between 301 K (room temperature) and 615 K.

$$V(t) = [4.202\times10^{-5}\ T(t) + 0.06742]\ X(t) - 0.0008106 \qquad (A6)$$

where T(t) is the time dependent temperature of the given LVDT and X(t) is the LVDT core element displacement (measured in millimeters).

In general, it is assumed that the response of each LVDT in the PBF LLR tests can be approximated by a function in the following form:

$$V(t) = [\alpha T(t) + \beta]\ X(t) + B \qquad (A7)$$

Values of α, β, and B have been determined for all the LLR LVDTs and are listed in Table A1.

TABLE A1

LLR LVDT TEMPERATURE RESPONSE DATA

Rod No.	LVDT S/N	LLR Tests	α	β	B
3121	47740	3, 5, 4	3.991×10^{-5}	0.06961	-0.002079
3992	47740	4A			
3122	67725	3, 5, 4	4.202×10^{-5}	0.06742	-0.0008106
3122	17836	4A	4.098×10^{-5}	0.06916	-0.001874
3123	67723	3			
3451	67723	4, 5, 4A	4.231×10^{-5}	0.06892	-0.001002
3124	17825	3			
3452	17825	4, 5, 4A	4.790×10^{-5}	0.06448	+0.001992

Besides equation (A7), other relationships have been written for the LVDT output voltage (V) as a function of the LVDT temperature (T) and displacement (X)[7]; however, equation (A7) is simple and directly applicable to the analysis that follows.

II. A MODEL OF THE DYNAMIC RESPONSE OF THE LVDT

For simplicity, the following definitions are made:

(a) $V(t)$ = the output voltage of the LVDT as a function of time.

(b) $H(t)$ = the LVDT data as reported in the previous or main sections of this document.

(c) $X_c(t)$ = the length of the fuel cladding at time t.

(d) $X_s(t)$ = the length of the flow shroud at time t.

(e) $X_{ST}(t)$ = the length of the flow shroud follower, i.e., the length of the support tube between the end of the shroud and the attachment of the LVDT to the stainless steel support tube. The support tube is an extension section of the flow shroud which contains the LVDT instrumentation and the lower flow turbine.

(f) X_b = the length of the LVDT "bar" or shaft which connects the end of the fuel rod to the LVDT core element. This quantity is assumed to be a constant.

(g) $T_s(t)$ = the average temperature of the shroud as a function of time.

(h) $T_L(t)$ = the temperature of the LVDT at time t.

(i) M = $M(T_L)$ the slope of the LVDT calibration line at temperature T_L.

(j) β_s = the thermal expansion coefficient for the shroud.

(k) β_{ST} = the thermal expansion coefficient for the support tube.

Some of the above definitions are illustrated in Figure A3.

From equation (A7), $V = MX+b$ where $X=X(t)$ is the displacement of the LVDT core element. Using the above definitions, $X(t)$ can be written in the following form:

$$X(t) = X_c(t) + X_b - X_s(t) - X_{ST}(t) \qquad (A8)$$

The differential form of equation (A8) is:

$$\Delta X = \Delta X_c - \Delta X_s - \Delta X_{ST} \qquad (A9)$$

Presently, no component of equation (A9) is known; however, since it is the object of this section to determine changes in the fuel rod cladding as a function of time ($X_c(t)$), then the terms ΔX, ΔX_s, and ΔX_{ST} must be computed.

To begin, the term $X(t)$ will first be calculated. In essence, the LVDT data ($H(t)$) has been corrected for temperature effects during steady state conditions, i.e., $t \leq 0$; however, after blowdown ($t > 0$) the LVDT data are still based on the calibration data determined by the steady state temperature ($\simeq 600$ K). Consequently, the relationship between $H(t)$ and the LVDT output $V(t)$ is written as:

$$H(t) = (V(t) - b) / M_o \qquad (A10)$$

Here, M_0 is the slope of the calibration line at the steady state temperature $T_L(0)$. Now, the actual displacement data X(t) can be determined from (A7) as:

$$X(t) = (V(t) - B) / M(t)$$

Since B is approximately equal to b, which depends upon $T_L(0)$, then in order to correct the H-data for the time dependent temperature of the LVDT it is only necessary to multiply H(t) by M_0 and divide by M(t). That is,

$$X(t) = M_0 H(t) / M(t) \qquad (A11)$$

where $M(t) = M(T_L(t))$

Notice that at t=0, $X(0) = M_0 H(0)/M(0) = H(0)$.

Hence, to compute X(t), M(t) must be determined. Since M(t) depends upon $T_L(t)$, then $T_L(t)$ must be known. Since $T_L(t)$ is not measured, an assumed average temperature must be inferred from some measured data. Because the LVDT is contained inside the flow shroud follower it is assumed that the average temperature of the LVDT is approximately equal to the coolant temperature flowing past the LVDT, i.e., the "inlet coolant temperature". With this information X(t) can be calculated.

Next, to correct the X-data for changes in the length of the flow shroud, and the active length of the shroud follower, the length of each must be determined as a function of time. To solve both problems simultaneously let L(t) represent the time dependent length of either item. That is, for the first case let $L(t) = X_S(t)$ and then for the second case let $L(t) = X_{ST}(t)$. In addition, let β represent the thermal expansion coefficient and T the average temperature of the given material. Hence, by the definition of a thermal expansion coefficient:

$$\beta = 1/L(t) \quad dL/dT \tag{A12}$$

But, $dL/dT = dL/dt \quad dt/dT = dL/dt \; / \; dT/dt$

Therefore, $$\beta L(t) \quad dT/dt = dL/dt \tag{A13}$$

With the boundary condition: $L(t=0) = L_o$, the solution of the above differential equation (A13) is:

$$L(t) = L_o \, e^{\beta \, [T(t) - T_o]} \tag{A14}$$

Since $\beta \, [T - T_o]$ is generally small, then the exponential in (A14) can be expanded in a taylor series and evaluated at a limited number of terms to give:

$$L(t) \simeq L_o \, (1 + \beta \, [T(t) - T_o] \,) \tag{A15}$$

Notice that equation (A15) could also have been deduced directly from (A12).

Now, if T(t) is known, then L(t) can be determined from (A14) or (A15). Since T(t) is generally not known, approximations must be made. For example, for the flow shroud it is assumed that the average temperature of the flow shroud thermocouples located at the core midplane and $\pm$ 120 mm above and below the midplane represent a reasonable estimate for the average temperature of the flow shroud. For the support tube (i.e., the shroud follower) an average temperature is assumed to be the average of the inside and outside coolant temperatures. In addition, the following initial length estimates and thermal expansion coefficients are made.

$$X_S(0) = 1051 \text{ mm}$$
$$X_{ST}(0) = 134 \text{ mm}$$
$$\beta_{Zr} = 4.44 \times 10^{-6}/K$$
$$\beta_{Steel} = 18.4 \times 10^{-6}/K$$

Using the above equations, initial values, and listed assumptions, estimates can be made for the fuel rod cladding displacement as a function of time from the original LVDT data. Example calculations have been made for one rod in each of the four LLR tests and displayed in Figures A4, A5, A6, and A7. These figures illustrate the original LVDT data overlayed with the "corrected" or estimated cladding displacement. The "corrected" data has been adjusted for temperature effects and shroud motion.

As can be seen from Figures A4, A5, A6, and A7, the response of the corrected data is generally different from the original data; however, the quench times for both sets of data are in close agreement. Nevertheless, it appears that some of the estimates of the LVDT turnaround time, as reported in the main sections of this document, may be in error if the "corrected" LVDT data is accurately representing the cladding elongation of the fuel rod. Further observations will be pointed out in Appendix B and below.

To illustrate the separate effects of temperature and the influence of the shroud elongation on the LVDT data, separate effects plots have been produced for rod 3451 in test LLR-05 and are shown in Figures A8 through A14.

Figure A8 shows the estimated LVDT temperature correction factor ($M_o/M(t)$) following blowdown, and Figure A9 shows the effect of the temperature correction on the LVDT data. Two fundamental assumptions have been made concerning the calculation of this factor. First, it is assumed that the LVDT data has been correctly adjusted for steady state temperature effects during pre-blowdown operation (i.e., $t \leq 0.0$). Therefore, the LVDT temperature multiplication factor equals 1.0 for times less than or equal to the initiation of blowdown. Second, it is assumed that the LVDT temperature history can be approximated by the temperature of the fluid flowing past the LVDT. Although this last assumption is not completely valid, it is

expected that the temperature corrected LVDT data (based on the inlet coolant thermocouple data) more closely approximates the theoretical response of a temperature dependent LVDT rather than the actual measured LVDT data. Nevertheless, it will be shown that compared to the elongation of the shroud, the LVDT temperature correction effect is rather small.

Now, taking into account the motion of the zircaloy shroud, Figure A10 compares the original LVDT data with the data corrected for temperature changes and shroud elongation. Next, eliminating the elongation of the shroud follower (between the end of the shroud and its connection to the LVDT case) from the previously adjusted data results in an estimate of the fuel cladding displacement. Figure A11 (or A5) compares the orginal LVDT data with the estimated cladding displacement.

Figure A12 shows a separate effects correction of the LVDT data for shroud elongation. LVDT temperature changes and shroud follower elongation corrections have not been made. Notice the similarity between the estimated cladding displacement shown in Figure A11 and the adjusted LVDT data in Figure A12. Clearly, for this particular example the combined effects of temperature and shroud-follower elongation result in only a small vertical offset.

Figure A13 shows an overlay of the LVDT data and the adjusted LVDT data corrected for both shroud and shroud-follower displacement effects. By comparing Figures A11 and A13 it is evident that the LVDT temperature effect is small compared with the other factors. This is somewhat surprising since Figure A8 shows that the temperature correction factor varied up to about 12% over its steady state value of 1.0.

Finally, Figure A14 shows an overlay of the estimated cladding displacement and the average thermocouple data for rod 3451. By comparing Figures A14 and 21A (in the main document) it is evident

that the estimated cladding displacement data more closely correlates with the cladding surface thermocouple data, than the original LVDT data. That is, the estimated cladding displacement data appear to better exemplify the cladding elongation rather than the LVDT data. However, there are still some difficulties that must be explained. For instance, even though general trends seem to correlate between the TC and cladding displacement data in Figure A14, magnitude responses do not correspond. In particular, from 170 to 225 seconds the TC data drops by about 200 K while the cladding displacement falls by approximately 2 mm. In contrast, at quench, the TC data falls by at least 300 K and the cladding displacement changes by less than 1.0 mm. One possible explanation for this behavior is that the core axial node thermocouples do not accurately reflect the average cladding temperature during rod rewet. In spite of this, as shown in Figure A14, the cladding displacement turnaround and time to quench data directly correspond with the thermocouple turnaround and time to quench data. And the near isothermal state existing for the cladding surface thermocouples between 30 and 170 seconds is also evident in the estimated cladding displacement data.

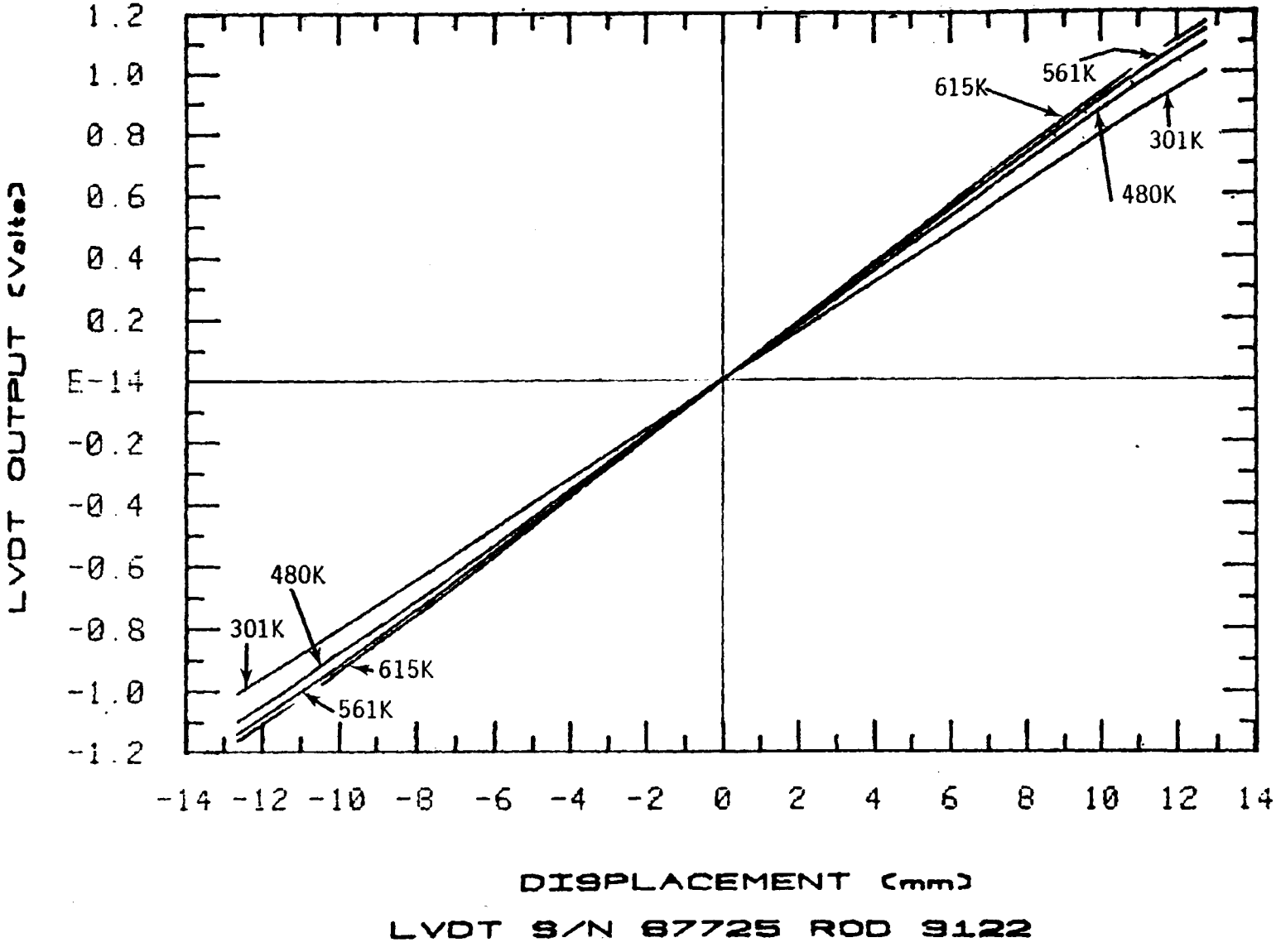

Fig. A2. Family of calibration curves for the LLR fuel rod 3122 LVDT.

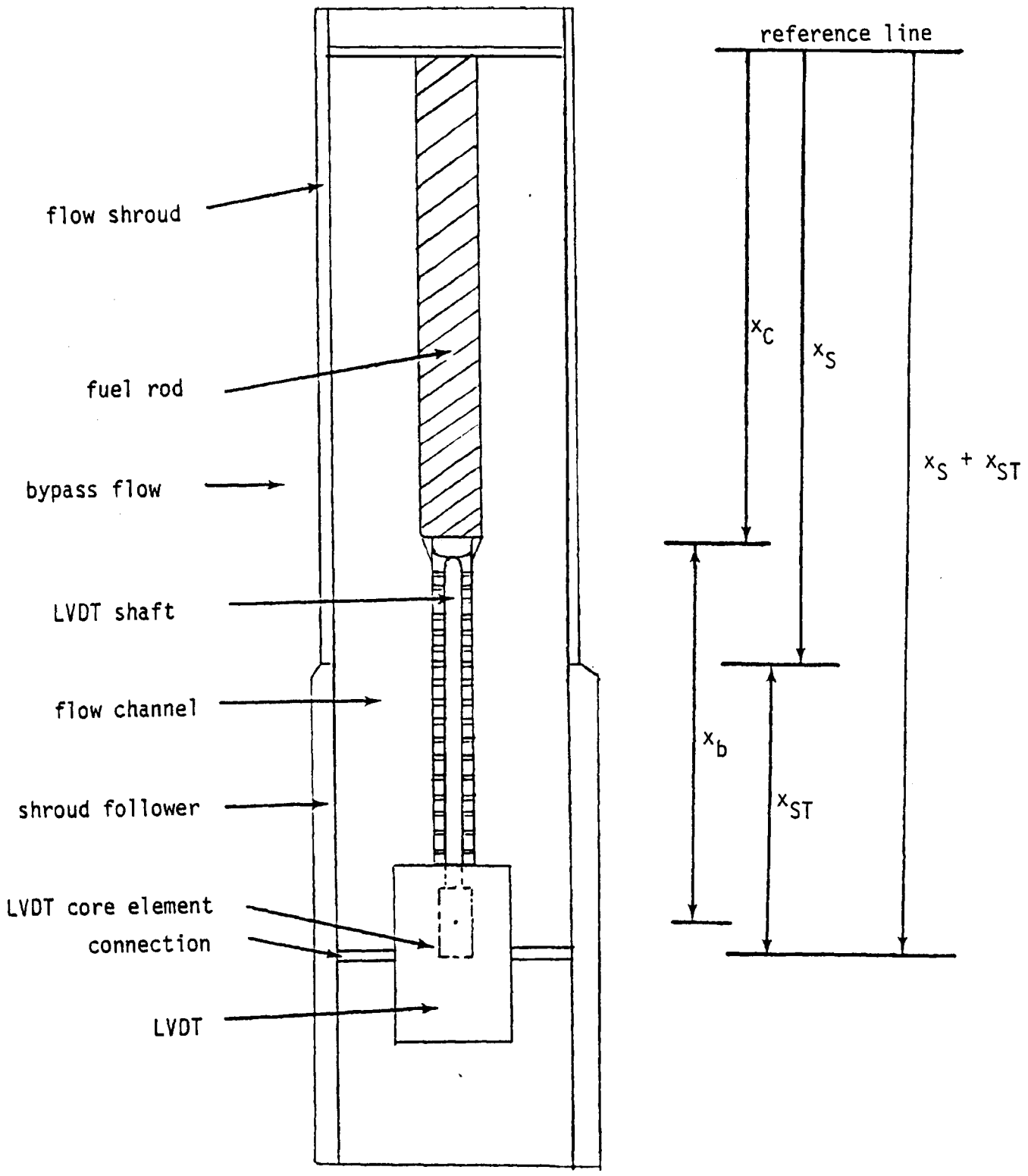

Fig. A3 LVDT model

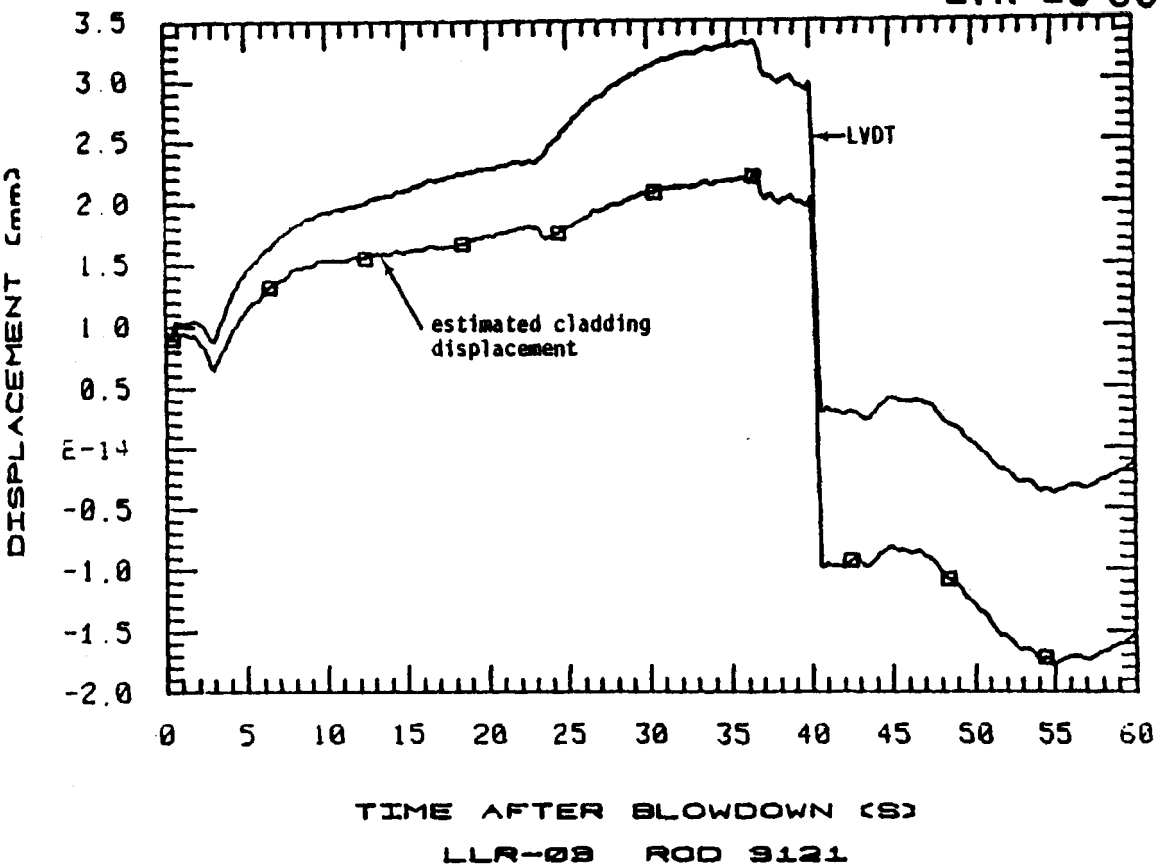

Fig. A4 LVDT response and the estimated cladding displacement for rod 3121. Test LLR-03.

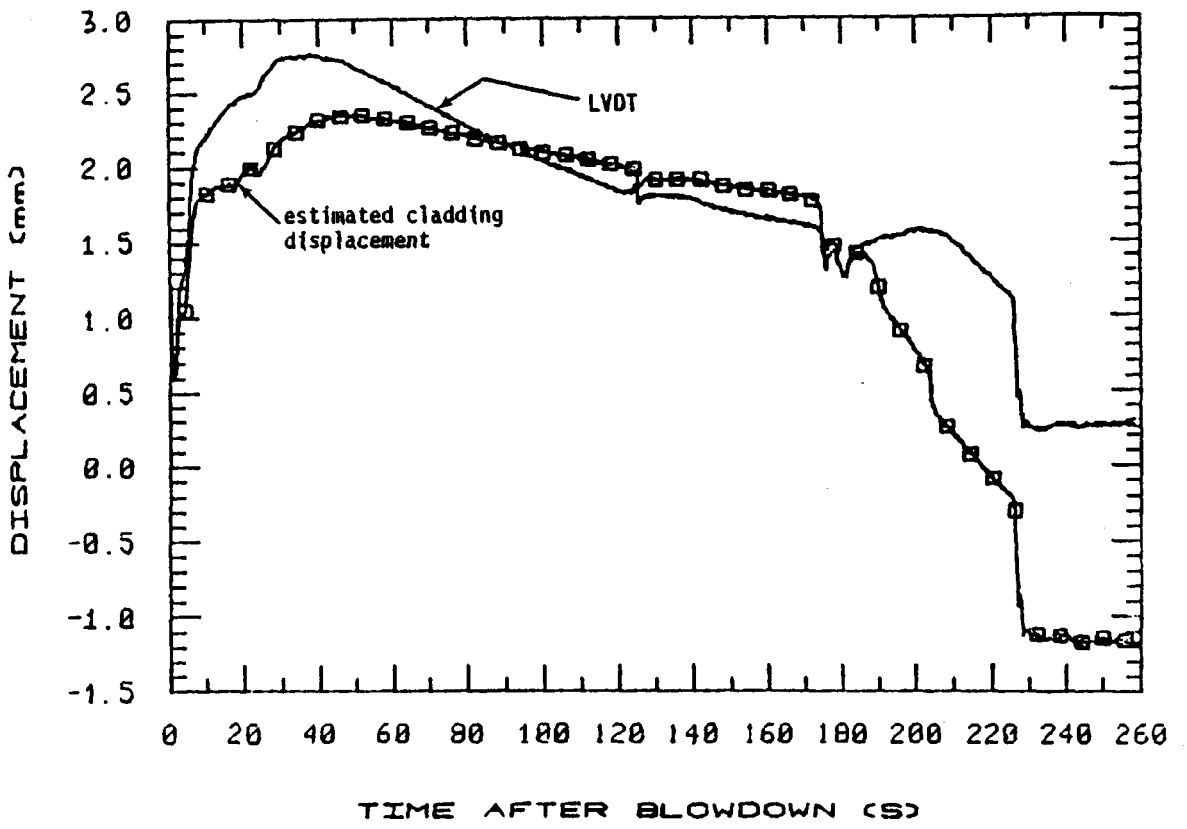

Fig. A5 LVDT response and the estimated cladding displacement for rod 3451. Test LLR-05.

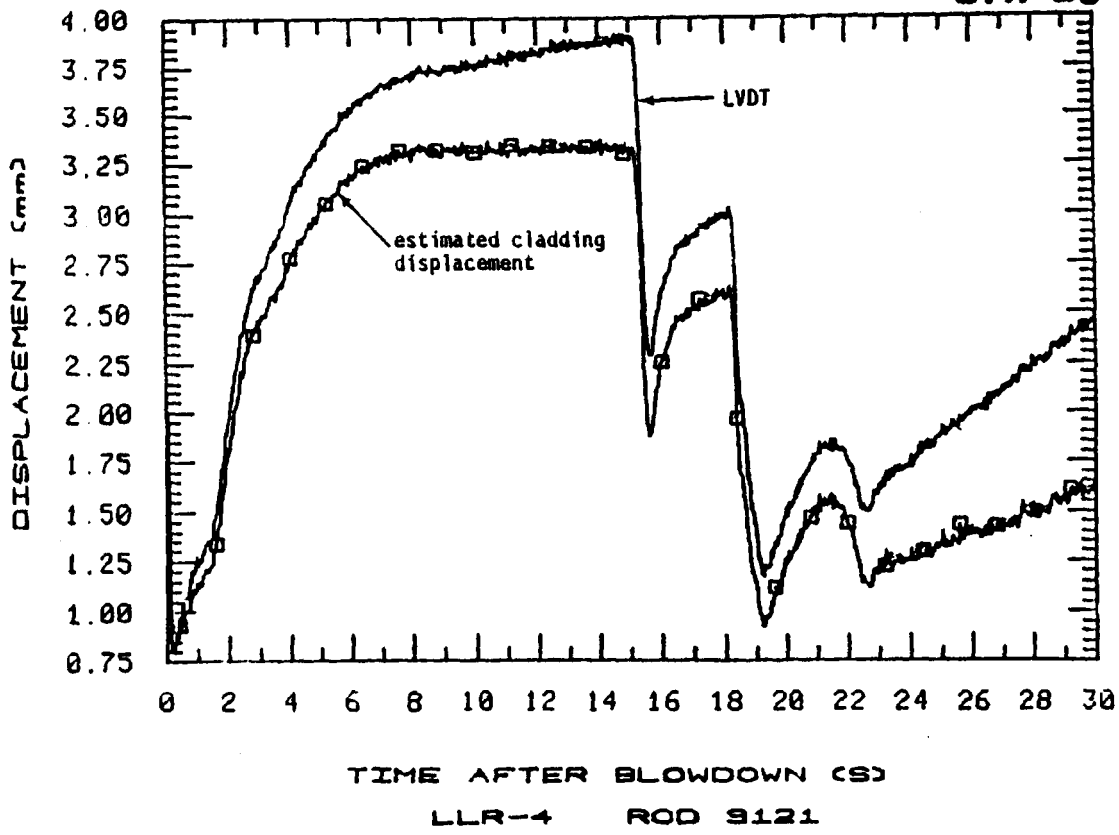

Fig. A6 LVDT response and the estimated cladding displacement for rod 3121. Test LLR-04.

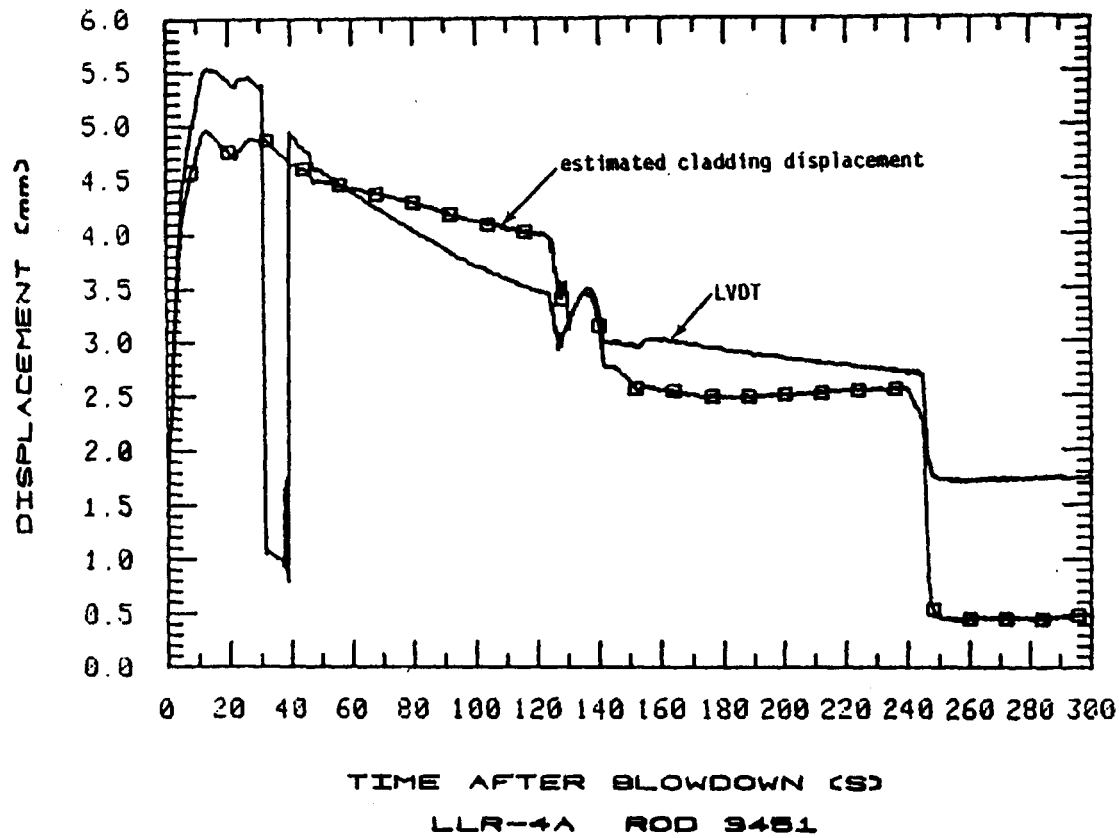

Fig. A7 LVDT response and the estimated cladding displacement for rod 3451. Test LLR-4A

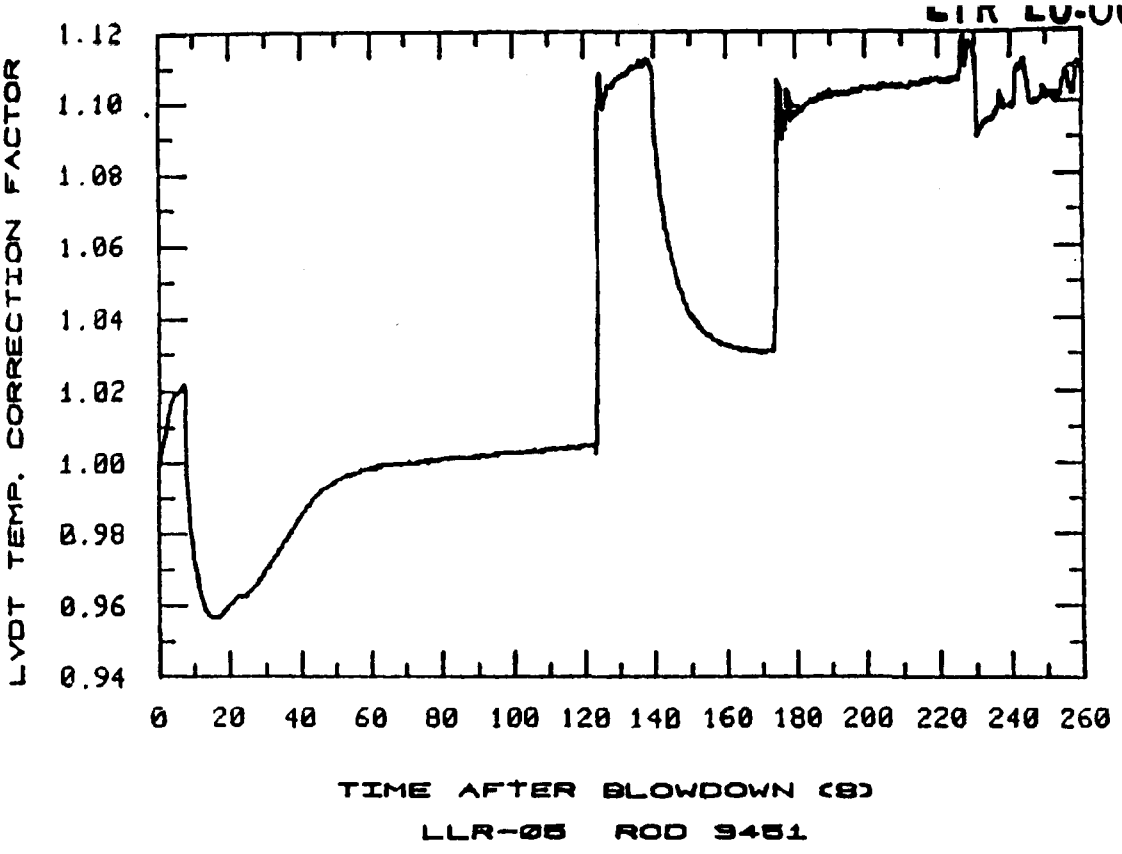

Fig. A8 The estimated LVDT temperature correction factor. Based on the "inlet coolant temperature" for rod 3451. Test LLR-05.

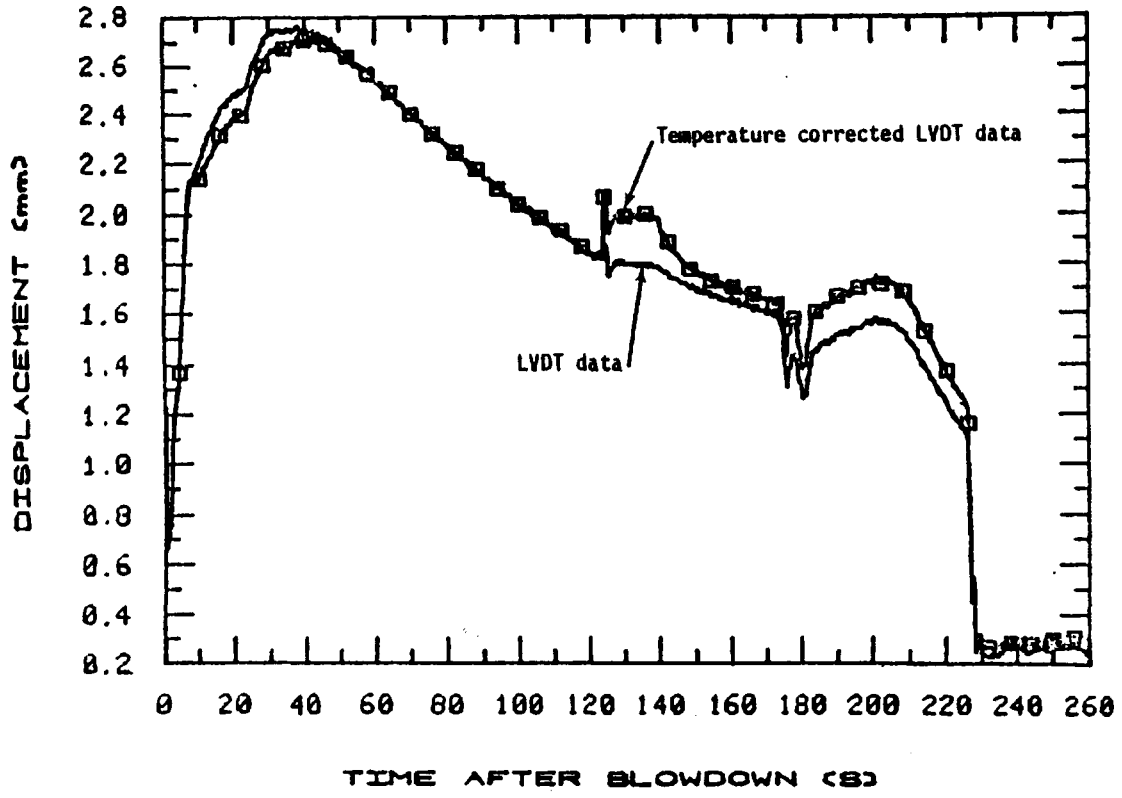

Fig. A9 An overlay of the orginal LVDT data for rod 3451 and the LVDT-temperature-corrected data. Test LLR-05.

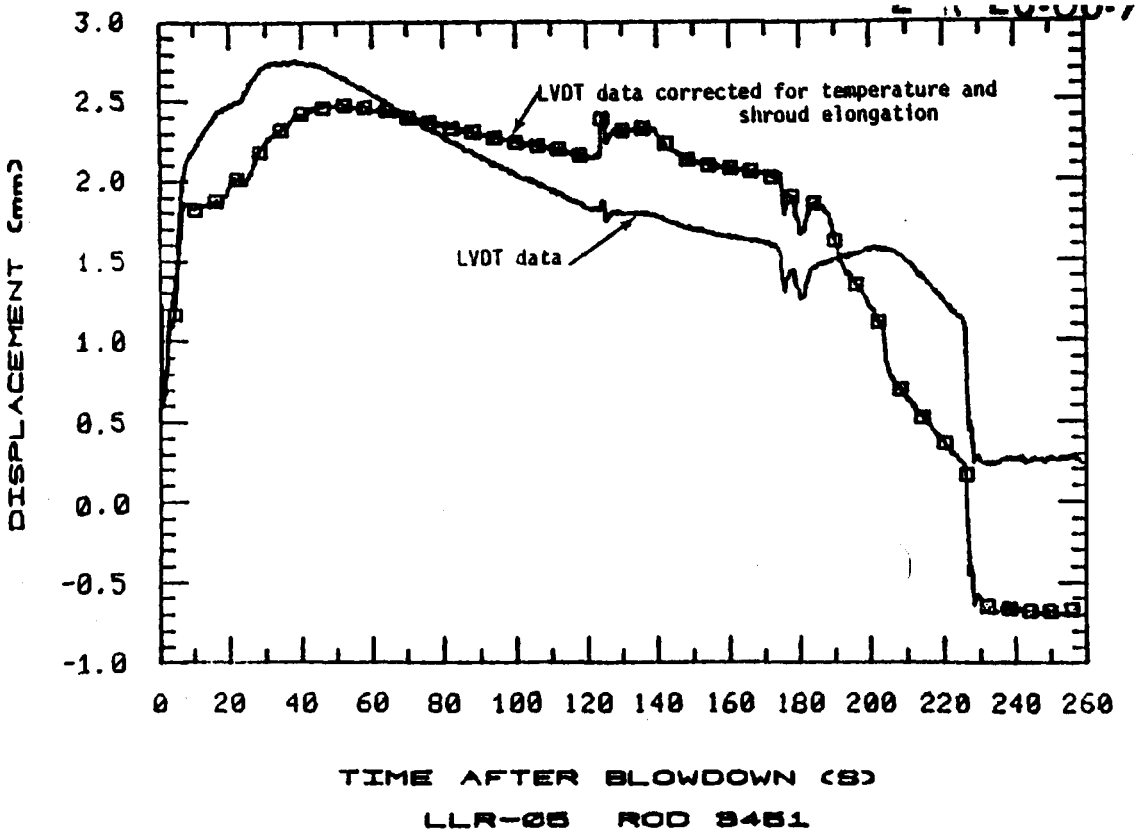

Fig. A10 An overlay showing the LVDT data for rod 3451 and the adjusted LVDT data corrected for temperature effects and shroud elongation. Test LLR-05.

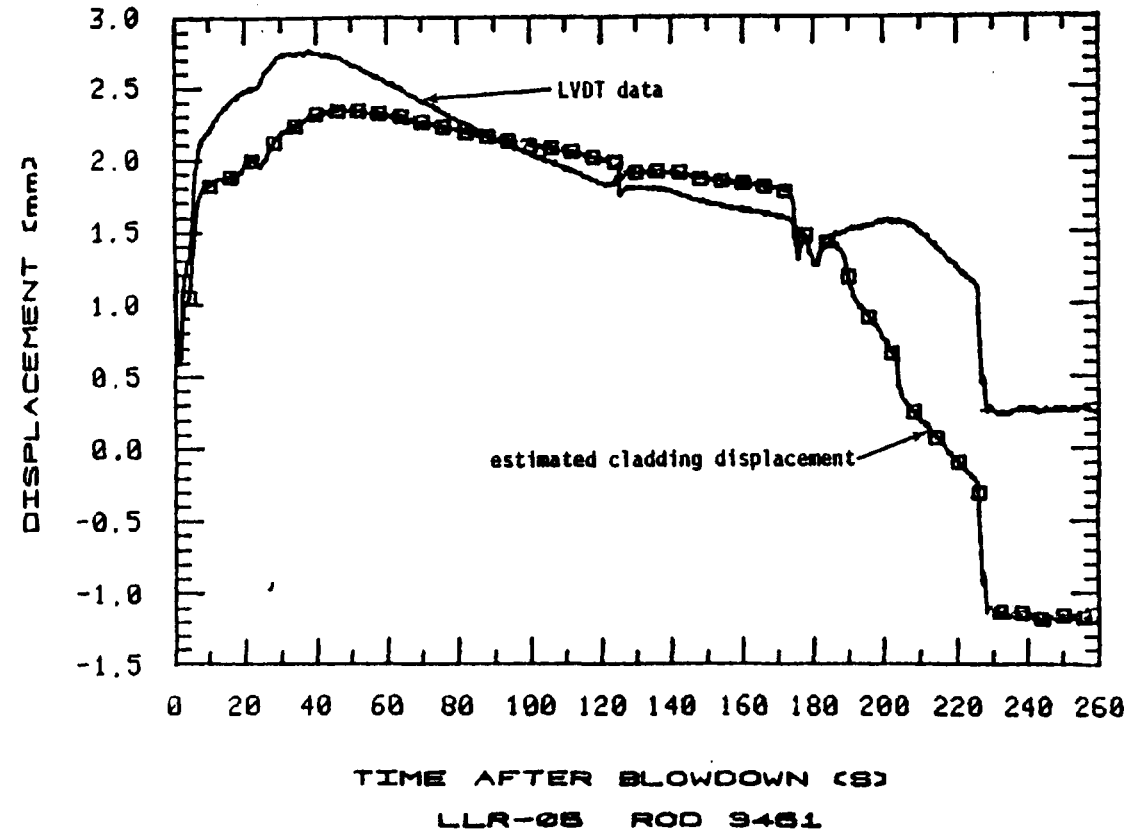

Fig. A11 An overlay showing the LVDT data for rod 3451 and the adjusted LVDT data corrected for temperature effects, shroud elongation, and support tube motion. Test LLR-05.

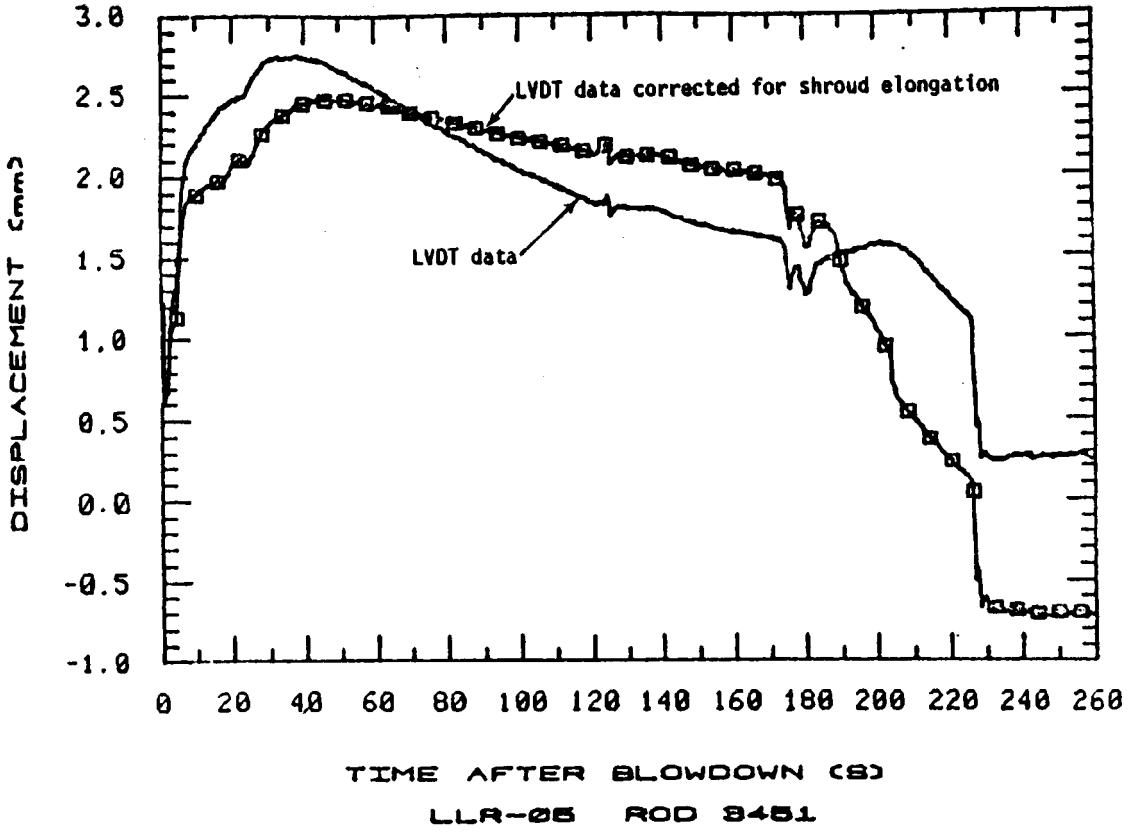

Fig. A12 An overlay showing the LVDT data for rod 3451 and the adjusted LVDT data corrected for shroud elongation. Test LLR-05.

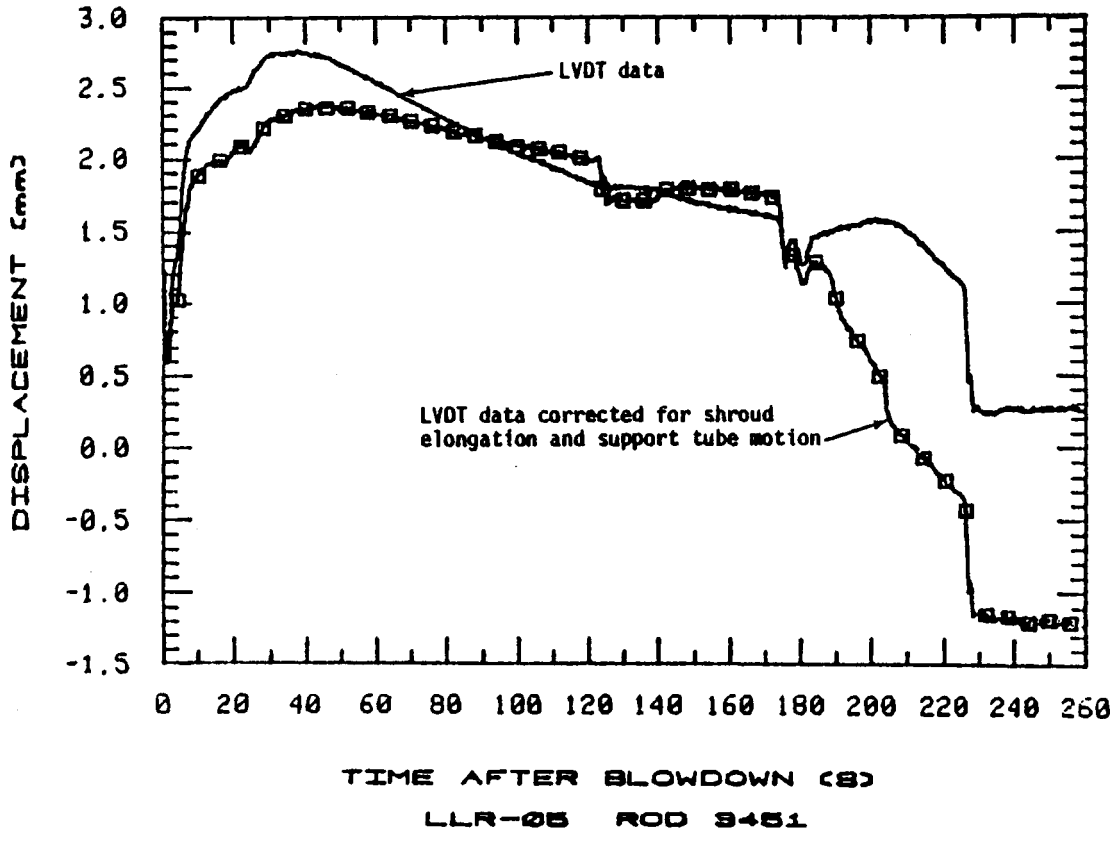

Fig. A13 An overlay showing the LVDT data for rod 3451 and the adjusted LVDT data corrected for shroud elongation and support tube elongation. Test LLR-05.

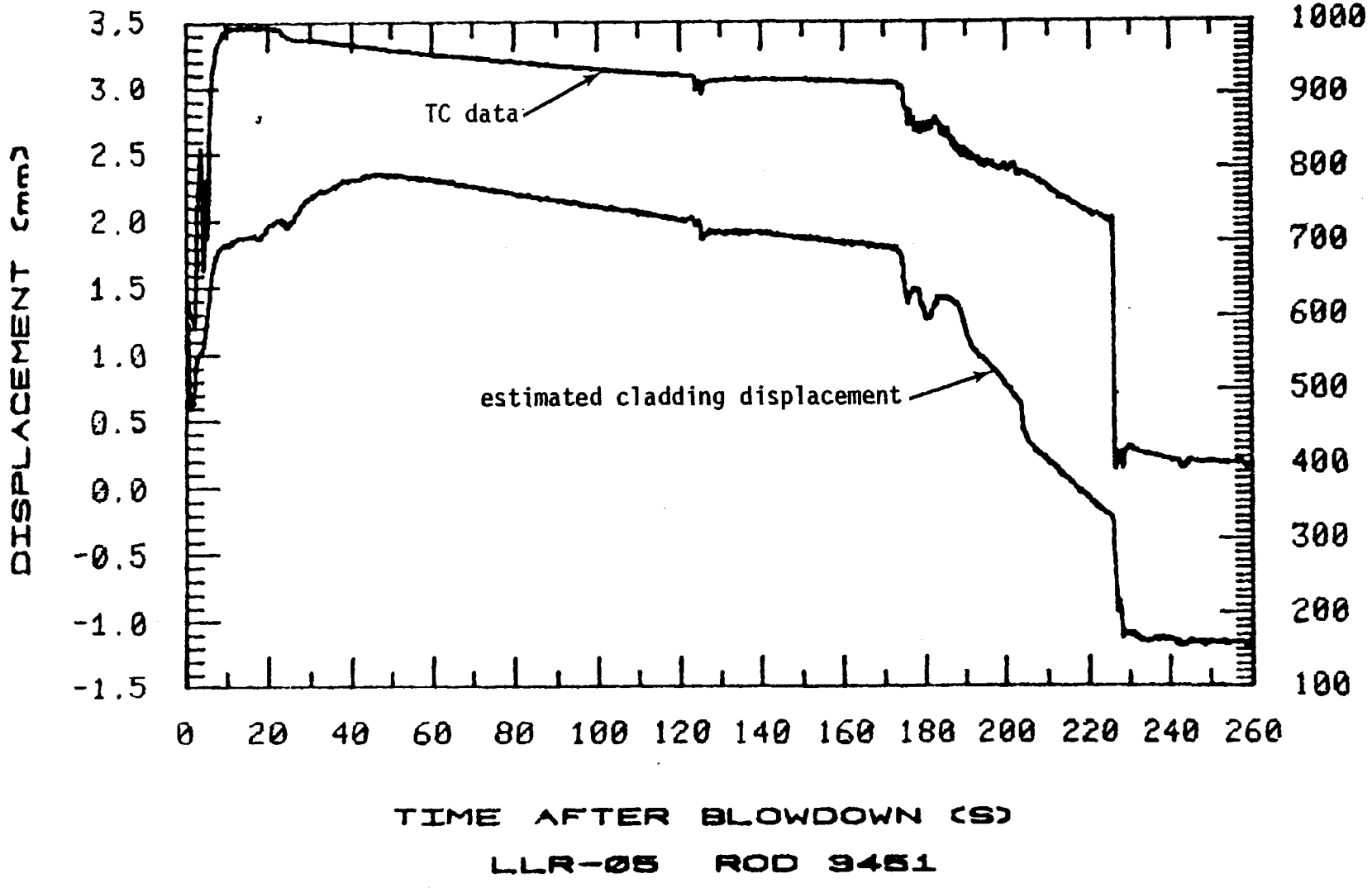

Fig. A14 An overlay of the estimated cladding displacement and the average thermocouple data for rod 3451. Test LLR-05.

APPENDIX B

A REVIEW OF ATYPICAL RESPONSE EVENTS OF THE LVDT INSTRUMENTATION DURING THE LLR EXPERIMENTS

The time to DNB and time to quench estimates made in the main sections of the preceding document utilized the Linear Variable Differential Transformer (LVDT) data as indicators of DNB and rod rewet events. The use of these data were based on the tacit assumption that the LVDTs are accurately measuring the cladding displacement during blowdown. However, as was seen in Appendix A the actual time dependent behavior of a fuel rod may be very much different from the original LVDT data. Therefore, an accurate interpretation of the LVDT data can be difficult without first adjusting the data for shroud motion and LVDT temperature effects. As will be pointed out in this appendix, additional questions still remain unanswered concerning the response of the LVDT instrumentation.

It is the objective of this appendix to discuss some of the important inconsistencies in the LVDT data for the LLR tests and to list a few plausible explanations for these anomalies. It is not possible at this time to present an all-encompassing theory explaining each anomaly. Apparently most atypical LVDT response events are caused by several interdependent factors that are not well understood.

1.1 Example #1

As a first case consider Test LLR-03. In particular, consider the LVDT data shown in Figure B1. Notice that the responses of rods 3122 and 3451 are very similar in shape, start at about the same

value, and remain close together throughout the blowdown. In contrast, the response of rod 3124 is somewhat similar in shape but is vertically translated with respect to the LVDT data for 3121 and 3122. What causes this output shift? The answer to this question probably involves several coupled phenomena. Three most likely factors influencing this behavior will be discussed.

(1) First, in order to assure proper operation of the LVDTs over the linear range of calibration, each LVDT is attached to its corresponding rod so that the position of the LVDT core element is slightly positioned in the negative direction. In this way, when the fuel rod cladding expands the LVDT output rises from a negative value to usually a positive one. Consequently, the position of the LVDT core element at time t=0 is dependent on the original setting prior to testing. Hence, the offset of LVDT 3124 relative to LVDTs 3121 and 3122 at t=0 may be partly due to a small offset at the time the LVDTs were attached to the fuel rods; assuming of course that a zero adjust procedure did not adequately correct for any original small displacements.

(2) Another factor that influences the LVDT output, and could be responsible for a small part of the offset noticed for the LLR-03 LVDTs is the dependency of the LVDT instrumentation on temperature. In addition, each LVDT has a unique set of calibration curves; consequently, the output voltage of each LVDT is slightly different even though the temperature history of each LVDT may be identical. Therefore, by bringing the test section temperature up to steady state conditions ($\sim$ 600 K) from room temperature (ΔT=300 K) could account for a small translation offset; however, it is not likely that the offset noticed for rod 3124 ($\simeq$ 2.6 mm) can be totally explained by this phenomenon. The next hypothesis offers the most likely explanation for the LVDT offset of rod 3124 (and even 3123) relative to rods 3121 and 3122.

(3) A third factor that affects the LVDT output is the motion of the shroud relative to the fuel rod. But why should the motion of the shroud for rod 3124 (and 3123) be significantly different than that of the other two rods? Recall that for LLR-03 rods 3121 and 3122 were encased in zircaloy shrouds while rods 3123 and 3124 had stainless steel shrouds. And since the linear thermal expansion coefficient of stainless steel is approximately 4.1 times larger than zircaloy ($\beta_{SS} = 18.4 \times 10^{-6}$/K and $\beta_{Zr} = 4.44 \times 10^{-6}$/K), then the stainless steel shrouds would expand more than the zircaloy shrouds for a given change in temperature. Also, any increase in the length of the flow shrouds "looks" as if the fuel rod length decreased. Hence, if all four LVDT core elements begin at the same point prior to the start of LLR-03, and the system temperature is increased to steady state conditions (a change of about 300 K), then the LVDT output for rods 3124 and 3123 (with stainless steel shrouds) should be less than that for rods 3121 and 3122 (with zircaloy shrouds). As can be seen from Figure B1 this is exactly what happens! Therefore, this explanation not only gives a reason for the translation offset but also a mechanism that explains why the output of LVDT 3124 is less than that of rods 3121 and 3122. It must be admitted, however, that since rods 3121 and 3122 were higher power rods than rod 3124 (because of the shroud material) then this could also account for some of offset and the direction of translation.

1.2 Example #2

The next example that is to be considered occurred between 3 and 12.3 seconds for rod 3123 during test LLR-03. This event is shown in Figure B1. As is clear from Figure B1 the LVDT data indicates a large increase followed by a sudden decrease that is not seen in the LVDT

data for the other rods. The explanation for this atypical response is likely the result of the rod ballooning and failure that occurred. It is believed that the ballooning of rod 3123 and the increase in the rod pressure (due to the water-log condition) occurred during this time interval and that the resultant dynamic forces on the clad caused this behavior. Therefore, the sudden increase and decrease in the LVDT data may be indicative of a pre-fail state for the rod.

1.3 Example #3

As another example consider the relative magnitudes of the LVDT responses for rods 3121, 3451, and 3452 during LLR-04 as shown in Figure B3. Notice that the output of LVDT 3121 is larger than the output of LVDT 3451 which is much greater than the response of LVDT 3452. This order relationship also existed during LLR-05 as shown in Figure B2. What causes this effect? The complete answer to this problem is not understood; however, some pertinent information is known. It seems that rod 3121 is simply hotter than rod 3451 and rod 3451 is hotter than rod 3452 as shown by the centerline thermocouple data in Figure B4. However, the cladding surface thermocouple data are not as consistent as the centerline data, and anyway a simple calculation shows that this cannot explain the magnitudes in the LVDT responses. For instance, the maximum LVDT output for rod 3121 during LLR-04 was about 3.9 mm, and the maximum output for rod 3452 was about 1.15 mm. Using a thermal expansion coefficient for zircaloy of 4.44×10^{-6}/K, then a difference of 2.75 mm (= 3.9-1.15) corresponds to a change in temperature of approximately 675 K, assuming a rod length of 915 mm. It is not likely that rod 3121 is, on the average, 675 degrees hotter than rod 3452. Therefore, some other mechanism must be responsible for most of variation in the LVDT magnitudes noted during the LLR tests. And at this time it is not exactly clear what is responsible for this phenomenon.

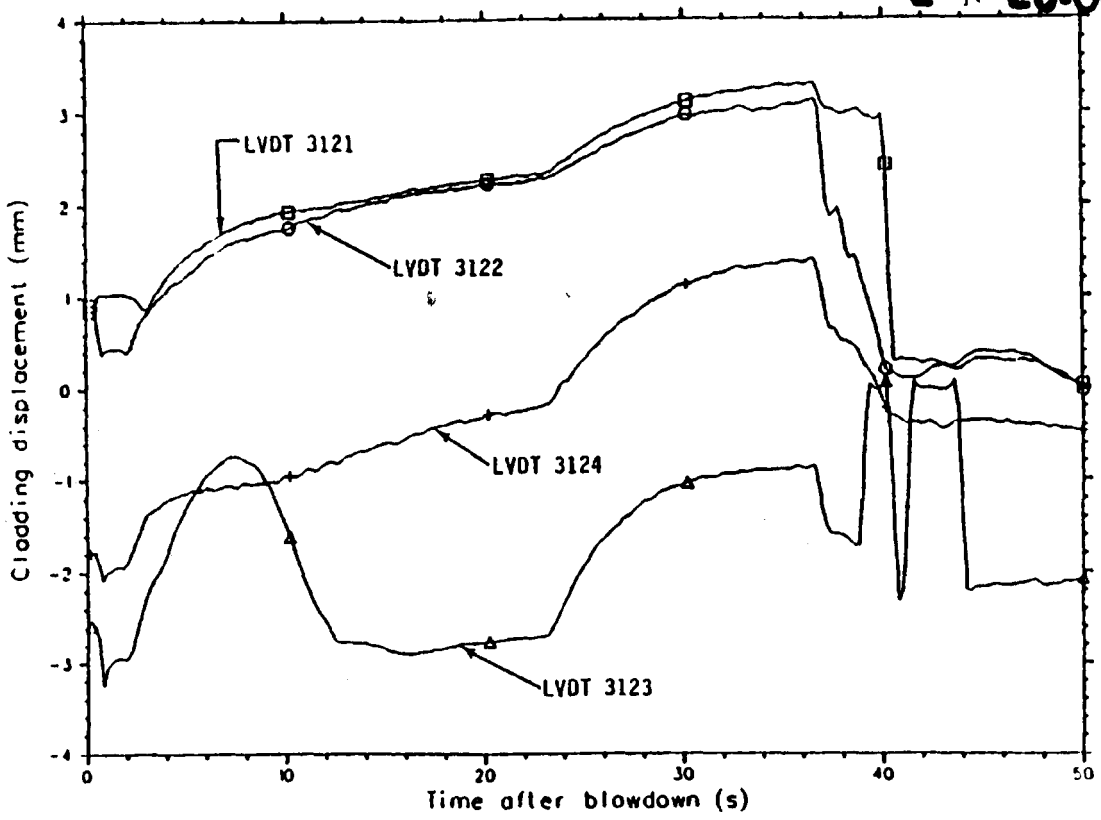

Fig. B1 Overlay of LVDTs for test LLR-03.

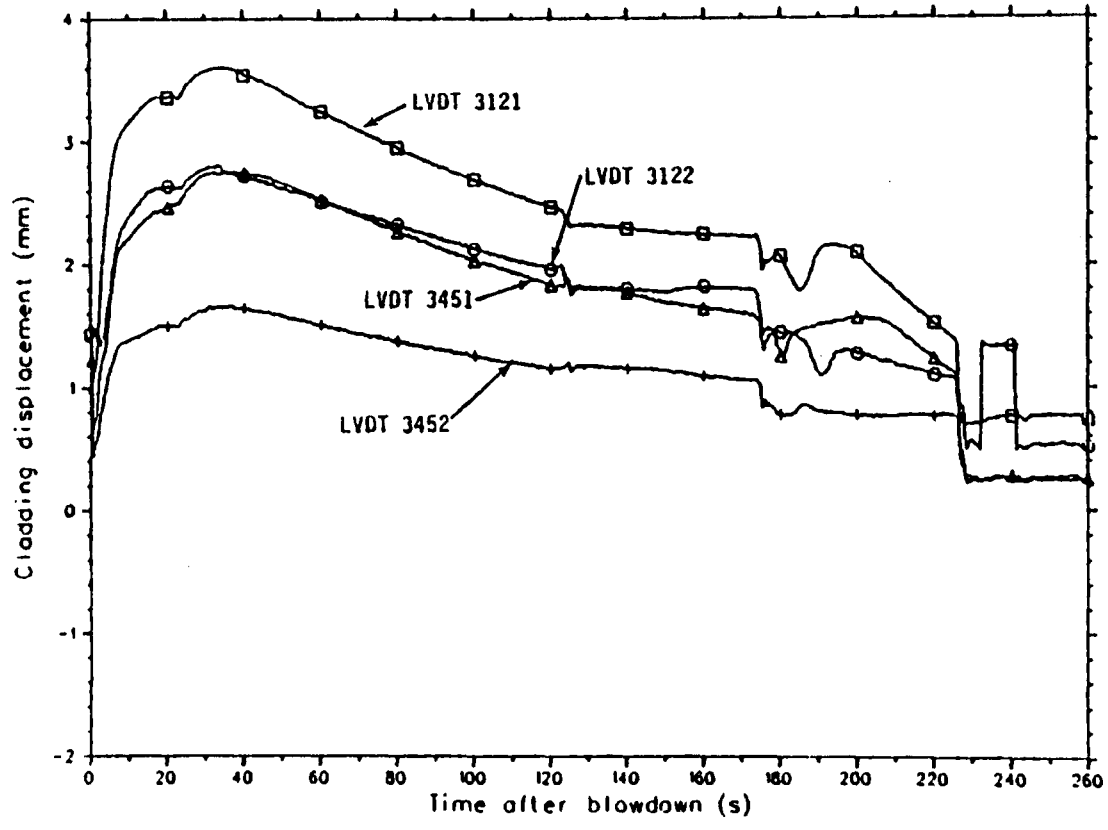

Fig. B2 Overlay of LVDTs for test LLR-05.

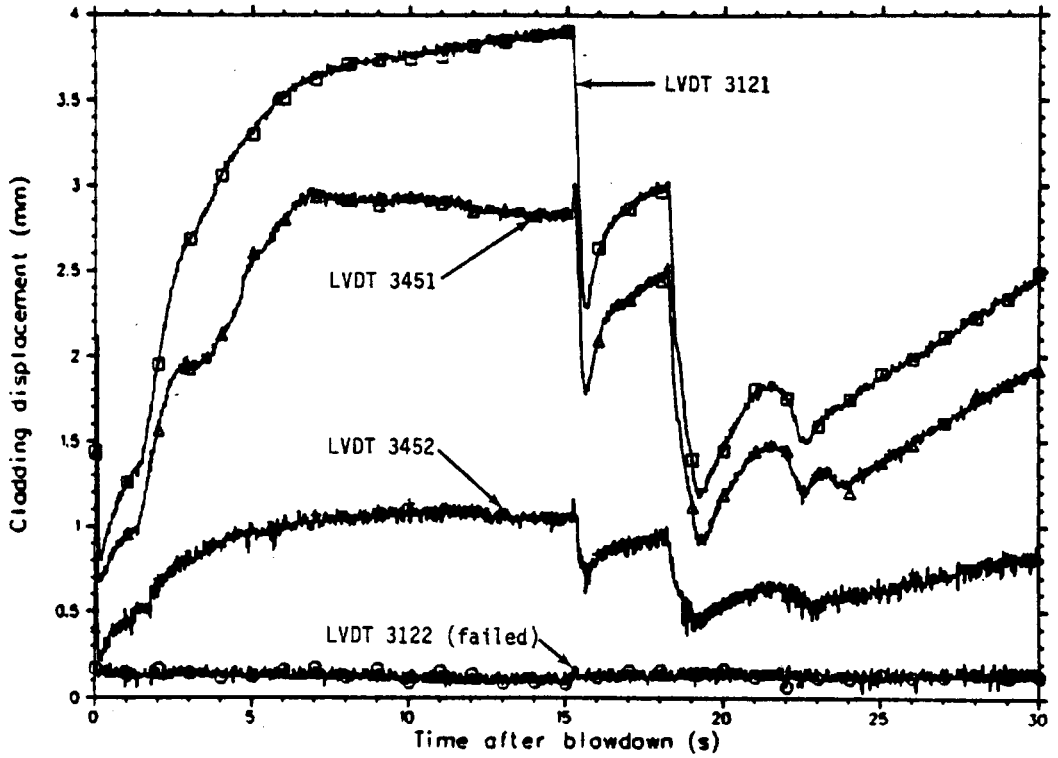

Fig. 83 Overlay of LVDTs for test LLR-04.

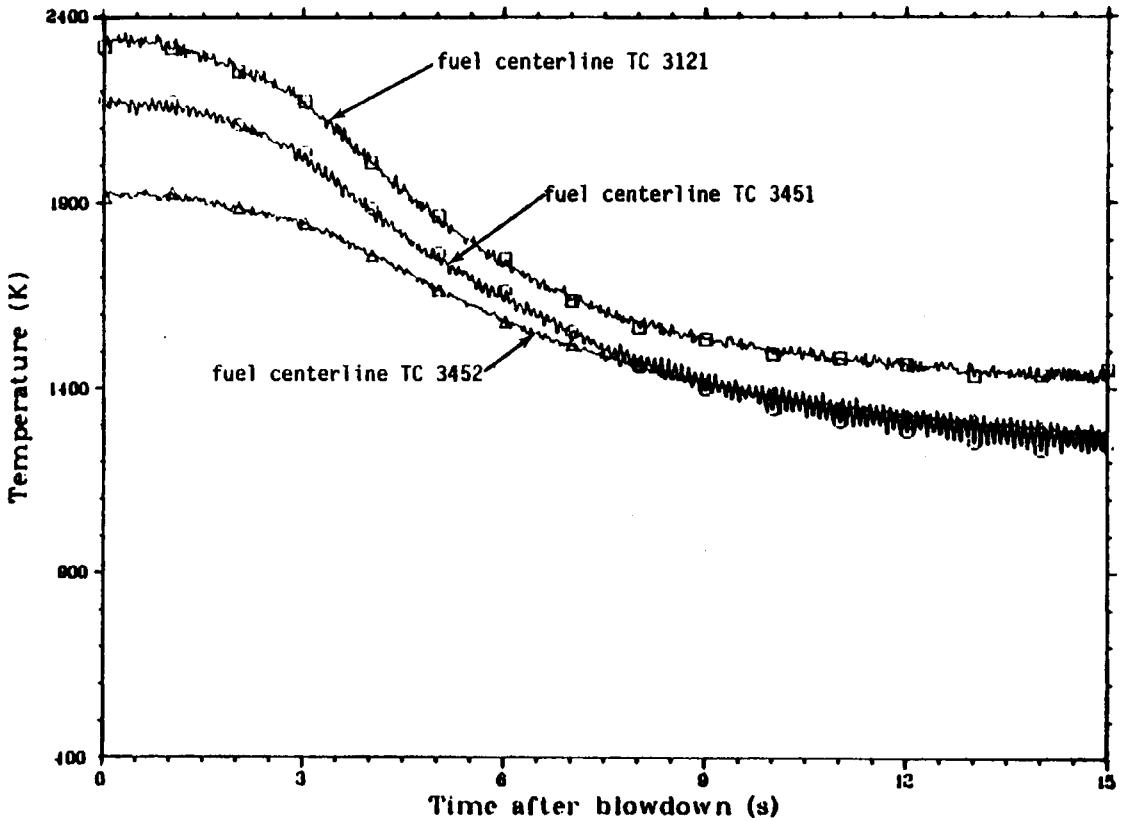

Fig. B4 Fuel centerline thermocouple data for rods 3121, 3451, and 3452. Test LLR-04.

REFERENCES

1. D. J. Varacalle, et al, PBF/LOFT Lead Rod Test Program Experiment Specification Document, TFBP-TR-307, December 1978.

2. D. J. Varacalle Jr., R. W. Garner, PBF/LOFT Lead Rod Program Tests LLR-3, -4, -5 Quick Look Report, TFBP-TR-315, April 1979.

3. D. J. Varacalle Jr., R. W. Garner, PBF/LOFT Lead Rod Program Test LLR-4A Quick Look Report, TFBP-TR-320, June 1979.

4. P. E. MacDonald / D. J. Varcalle Jr., Letter to L. P. Leach, MacD-31-79, "Thermocouple and LVDT Indications of DNB and Quench Times from the LLR-3 Test", March 26, 1979.

5. D. J. Varacalle Jr., Personal Communication Concerning the DNB Data for the LLR Tests.

6. J. R. Wolf, "The Linear Variable Differential Transformer and its uses for in-core Fuel Rod Behavior Measurements," Paper presented at the International Colloquium on Irradiation Tests for Reactor Safety Programmes, Petten Netherlands, June 1979.

7. L. C. Meyer, Personal Communication Concerning the LLR Displacement Transducer Calibration Data, October 1979.